Rauhut *et al. Swiss J Geosci* (2020) 113:8
https://doi.org/10.1186/s00015-020-00360-8

SGG SGS sc | nat
Swiss Journal of Geosciences

ORIGINAL PAPER Open Access

A derived sauropodiform dinosaur and other sauropodomorph material from the Late Triassic of Canton Schaffhausen, witzerland

Oliver W. M. Rauhut[1,2,3*], Femke M. Holwerda[1,4,5,7] and Heinz Furrer[6]

Abstract

Although sauropodomorph dinosaurs have been known for a long time from the Late Triassic of central Europe, sauropodomorph diversity and faunal composition has remained controversial until today. Here we review sauropodomorph material from the Canton Schaffhausen, Switzerland. The material comes from three different but geographically close localities and represents at least three different taxa. Apart from the common genus *Plateosaurus*, the material includes remains of two different large, robustly built sauropodomorphs. One of these is described as a new taxon, *Schleitheimia schutzi* n. gen. et sp., on the basis of an unusual ilium and associated axial and appendicular material. *Schleitheimia* represents a derived basal sauropodiform and possibly the immediate outgroup to Sauropoda, and thus is the most derived sauropodomorph known from the Late Triassic of Europe. These results thus highlight the diversity of sauropodomorphs in the Late Triassic of central Europe and further indicate widespread sauropodomorph survival across the Triassic-Jurassic boundary.

Keywords: Late Triassic, Switzerland, Sauropodomorpha, Sauropod origins

1 Introduction

Sauropod dinosaurs are certainly among the most conspicuous elements of Mesozoic terrestrial vertebrate faunas. They include the largest terrestrial vertebrates and were the dominant herbivores in many Jurassic and Cretaceous ecosystems, probably accounting for a great part of vertebrate body mass in many environments in which they were abundant (e.g. Foster 2003). Their systematics were long thought to be especially problematic (Romer 1966), but research in the past fifteen years has greatly helped to resolve the general interrelationships of sauropods, although the exact placement of several taxa remains enigmatic (see e.g. Upchurch et al. 2004; Carballido and Sander 2014). However, the origin and early evolution of the group is still less well understood, and the interrelationships of non-sauropodan sauropodomorphs and the question of the timing and biogeography of the origin of sauropods are still controversial (see Peyre de Fabrègues et al. 2015; McPhee and Choiniere 2018). The origin of sauropods from more basal sauropodomorphs—the group formerly known as "prosauropods", which is now generally considered to be paraphyletic (see e.g. McPhee et al. 2015; Otero et al. 2015; Apaldetti et al. 2018)—has recently come into focus with the identification of several "prosauropod" taxa as close relatives of sauropods (e.g. Yates 2004, 2007) and the discovery of other Late Triassic and Early Jurassic sauropodomorphs that are close to the origin of this clade (e.g. Buffetaut et al. 2000; Yates and Kitching 2003; Yates et al. 2010; Pol et al. 2011; McPhee et al. 2015, 2018; Otero et al. 2015; Peyre de Fabrègues and Allain 2016; Apaldetti et al. 2018). Together with the

Editorial handling: Daniel Marty

*Correspondence: rauhut@snsb.de
[1] SNSB, Bayerische Staatssammlung für Paläontologie und Geologie, Richard-Wagner-Str. 10, 80333 Munich, Germany
Full list of author information is available at the end of the article

sauropods, these taxa are united in a clade named Sauropodiformes, defined as all sauropodomorphs that are more closely related to *Saltasaurus* than to *Massospondylus* (McPhee et al. 2014).

Sauropodomorph dinosaurs from the Late Triassic of Europe have long been known, ever since the original descriptions of *Thecodontosaurus* (Riley and Stutchbury 1836) and *Plateosaurus* (Meyer 1837), and numerous species have been described since, although the validity of many taxa remains debated (see e.g. Huene 1932; Galton 2001a, b; Yates 2003; Prieto-Marquez and Norell 2011). However, there is general consensus that the vast majority of European Triassic sauropodomorphs represents basal, non-sauropodiform taxa, including *Thecodontosaurus*, *Pantydraco*, *Efraasia*, *Ruehleia*, and *Plateosaurus* (e.g. Apaldetti et al. 2013; McPhee et al. 2015; Otero et al. 2015; Wang et al. 2017). The only European Triassic sauropodomorph that probably represents a basal sauropodiform is the poorly known *Camelotia borealis* from the Rhaetian of England (Galton 1985, 1998). Sauropodiforms seem to be generally rare, although widely distributed in the Late Triassic. Apart from the European *Camelotia*, taxa described so far include *Lessemsaurus* and *Ingentia* from the Norian/Rhaetian Los Colorados Formation of Argentina (Bonaparte 1999; Pol and Powell 2007a; Apaldetti et al. 2018), and *Blikanasaurus*, *Melanorosaurus* and *Meroktenos* from the Late Triassic Lower Elliot Formation of South Africa and Lesotho (Galton 1985; Galton and Heerden 1985; Yates 2007; Peyre de Fabrègues and Allain 2016). Three further sauropodiform taxa are usually said to be Late Triassic in age, the Argentinean *Mussaurus* (Bonaparte and Vince 1979; Pol and Powell 2007b; Otero and Pol 2013), the South African *Antetonitrus* (Yates and Kitching 2003; McPhee et al. 2014), and the genus *Isanosaurus* from Thailand (Buffetaut et al. 2000). However, the Laguna Colorada Formation that yielded *Mussaurus* has recently been dated as Early Jurassic (D. Pol, pers. com. to OR, 2016), and recent fieldwork in the area where *Antetonitrus* was found indicates that the type locality is placed in the Upper Elliot Formation and thus also Early Jurassic in age (McPhee et al. 2017). Likewise, the Upper Nam Phong Formation that has yielded *Isanosaurus* has recently been dated as Early Jurassic (Racey and Goodall 2009).

Triassic sauropodomorph dinosaurs from Switzerland were long only known from the fragmentary type material of *Gresslyosaurus ingens*, which was found in 1856 by geologist A. Gressly in sediments of the Keuper at Niederschönthal near Basel. The species was named by Rütimeyer in the same year (Rütimeyer 1856a, b) and more fully described a year later (Rütimeyer 1857). This animal was subsequently regarded as a teratosaurid (a supposedly carnivorous family of prosauropods) by Huene (1907-8, 1932), but has recently usually been regarded as belonging to *Plateosaurus*, either within the species *Plateosaurus engelhardti* (e.g. Galton 1986, 2001b), or as a separate species, *Plateosaurus ingens* (e.g. Yates 2007; Yates et al. 2010; McPhee et al. 2015; Otero et al. 2015).

The most important sauropodomorph locality in the Triassic of Switzerland is certainly the Gruhalde Quarry at Frick, which has yielded a mass accumulation of *Plateosaurus* from the Norian Upper Variegated Marls (Sander 1992; Hofmann and Sander 2014). Sauropodomorph fossils from this locality were first excavated by Urs Oberli in the late 1970s and scientifically described by Galton (1986), and since then, many partial to complete articulated skeletons have been found in at least three levels (Pabst, pers. com. in Hofmann and Sander 2014).

Further sauropodomorph remains were found in the Norian/Rhaetian beds of the Canton Schaffhausen, but these have only received a preliminary description so far. First remains were reported from the locality of Hallau by Peyer (1943a), who referred a dorsal vertebra to the genus *Gresslyosaurus*. This material, plus additional specimens collected in the vicinity of Schleitheim, were subsequently briefly described and referred to *Plateosaurus engelhardti* by Galton (1986). The aim of the current paper is a revision of materials found at Schleitheim, including the remains described by Galton (1986) and so far undescribed elements in the collections of the Museum zu Allerheiligen in Schaffhausen, as well as remains from a recent excavation led by one of us (HF).

2 Materials and methods

The material described here comes from the Upper Triassic (probably upper Norian) of Canton Schaffhausen, northern Switzerland. Remains referred to basal sauropodomorph dinosaurs in the collection of the Palaeontological Institute and Museum, University of Zurich (PIMUZ) came from two localities, Hallau and Schleitheim, both in the Canton Schaffhausen (Fig. 1). In Hallau (locality Bratelen), two separate excavation campaigns, one in 1915 by F. Schalch (Schaffhausen), and a second in 1942 by B. Peyer (University of Zurich), exposed the Jurassic-Triassic boundary, and numerous vertebrate remains were collected from the "Rhät-Bonebed" between the Lower Hettangian "Psilonotenschichten" and the underlying "Zanclodonmergel" (an equivalent of the Knollenmergel of south-western Germany; see Schalch and Peyer 1919; Peyer 1943a, b, 1956). The material from Schleitheim (locality Santierge) was collected by E. Schutz (Neunkirch) in 1952–1954 and donated to the University of Zurich in 1955. Some of these remains were briefly described and figured by Galton (1986), who referred all of this material to *Plateosaurus engelhardti*.

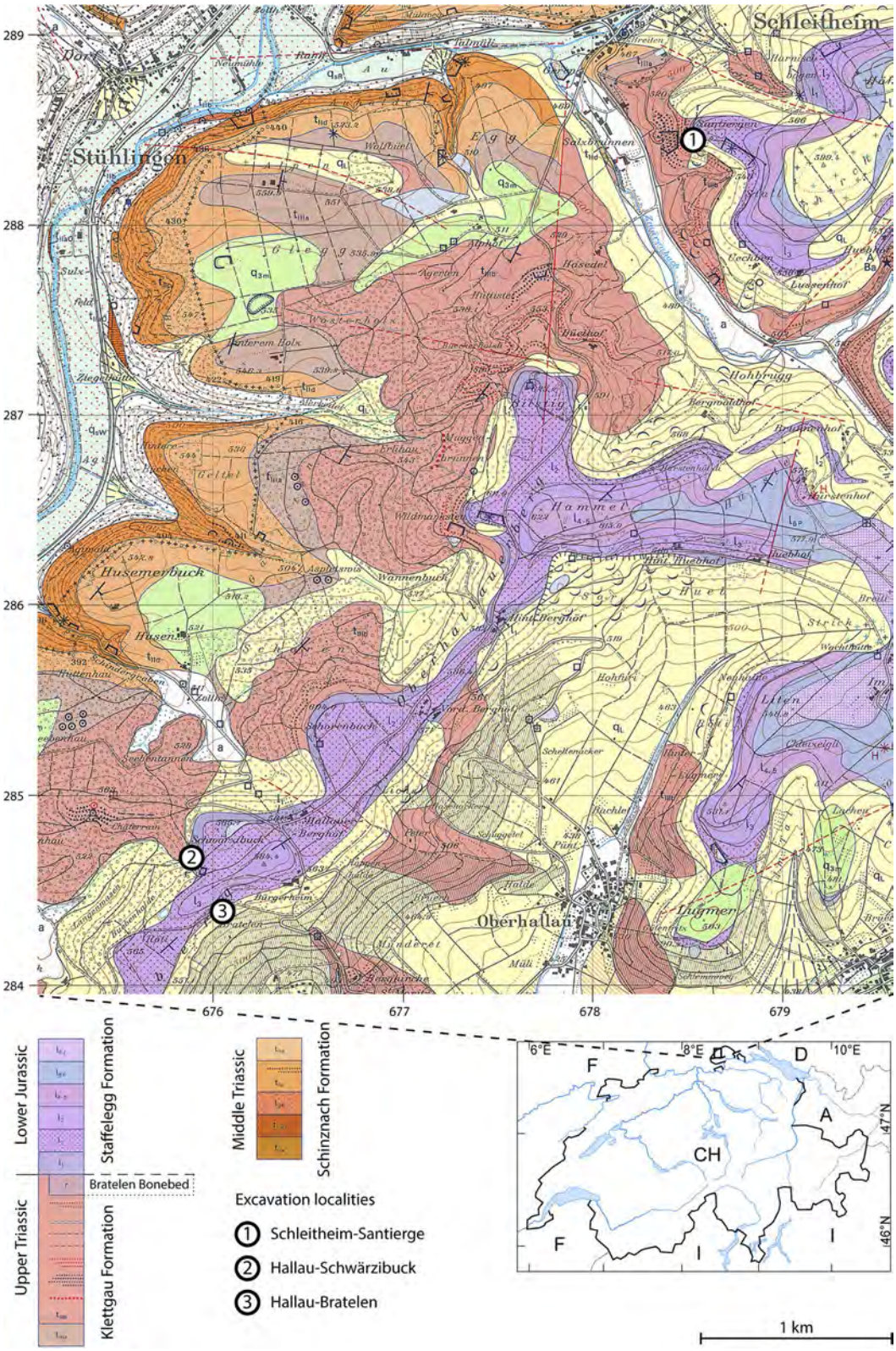

Fig. 1 Geological map with the localities Schleitheim-Santierge, Hallau-Bratelen and Hallau-Schwärzibuck in the western part of Canton Schaffhausen, Switzerland (license for reproduction of the geological map by swisstopo, December 11, 2019)

Galton (1986: Fig. 5) identified a distal end of a femur and one dorsal vertebral centrum as coming from Hallau, and a distal part of a humerus and a proximal ulna (Galton 1986: pl. 1, Figs. 21, 22 and 23) as being derived from Schleitheim. He noticed that the provenance of the rest of material was unclear, as Peyer (1943b) did not specify the material found at Hallau, apart from one dorsal vertebra, and the material from Schleitheim had never been described.

During a recent re-examination of the material, we noticed that several of the bones were marked with the letter "J", which Schutz used to identify material coming from Schleitheim-Santierge, including the distal end of the femur. Furthermore, several fragments marked with this letter were found to belong to a single, large right ilium, on which also the element described as ulna by Galton (1986) fitted, representing the pubic peduncle. This element clearly represents a new taxon and is made the holotype of a new species below. Two of the caudal vertebrae showed the mark mentioned above, and one of the dorsal vertebrae was identified as being derived from the same locality on an old, hand-written label, whereas an anterior dorsal could be united with its neural arch that also showed the mark. As the remaining posterior cervical and two dorsal vertebral centra fit in size, morphology and preservation with the two vertebrae positively identified as coming from Schleitheim, we interpret them as also coming from this locality and probably representing the same individual. A distorted anterior caudal vertebra without locality information fits in size with the last preserved dorsal vertebra and is therefore also tentatively referred to the same animal. A small distal caudal vertebra fits in preservation and, probably, size, but cannot be positively identified as coming from Schleitheim. The element is described below, but a possible referral to the same taxon should be seen as tentative. Likewise, a pedal ungual differs from vertebrate remains of Hallau in colour and preservation and thus might also represent the specimen from Schleitheim. Unfortunately, Schutz (unpublished notes, MzA) noted the stratigraphic position of the remains he excavated, but did not record their spatial distribution, so the association of the remains cannot be established. As all of the material [including the humerus already noted to be derived from Schleitheim by Galton (1986)] is of fitting size to represent a single individual, and there is no duplication of elements, we interpret all of these remains as representing a single animal. This interpretation is supported by the presence of the pubic peduncle of the left ilium, which fits exactly in size and morphology with the pubic peduncle of the right ilium. However, it might be noted that there is at least one sauropodomorph element from the excavation of Schutz that does not fit in size with the rest of the material, an isolated right astragalus (see below).

A number of additional specimens from the same locality, but collected much later (mainly in the 1980s), are present in the collections of the Museum zu Allerheiligen in Schaffhausen. These specimens include seven vertebrae and a partial right humerus. They are comparable in size and morphology to the material described above. Especially the humerus is noteworthy in this respect, as it represents the other (right) side than the humerus in the collections in Zurich (left humerus), is of the same size, and coincides in all comparable characters with this specimen. Thus, this material probably represents the same taxon or, at least partially, even the same individual as the material collected by Schutz, although at least some of the remains were collected from the surface some 20–30 m away from the original excavation site.

Finally, one of us (HF) led an excavation in the Upper Triassic sediments of Schleitheim-Santierge in autumn of 2016, at the approximate locality where the right humerus mentioned above was found, some 20–30 m away from the original excavation site of Schutz. In this excavation, bones were found in a thin (ca. 30 cm) series of partially conglomeratic carbonate sandstones to fine conglomerates intercalated as lenticular layers in brownish mud (Fig. 2), just on top of the yellow-violet marls of the Gruhalde Member of the Klettgau Formation (former "Zanclodonmergel" or "Knollenmergel"). Most of the larger skeletal elements represent sauropodomorphs remains, and at least some of them fit in size with the material collected by Schutz. Although it seems possible that all of these remains belong to a single, partially reworked skeleton, any referral of this material to the same taxon as the remains collected by Schutz is tentative at best. However, this material will also be documented briefly.

Further basal sauropodomorph material was collected by E. Schutz in the area of Hallau, at the locality Hallau-Schwärzibuck (Fig. 1) in 1954 from a correlating "Rhät-Bonebed". Here, Schutz collected a scapula, a distal end of a femur, and two phalanges of a large, basal sauropodomorph. This material cannot be referred to the same taxon as the one identified from Schleitheim, but will be documented briefly, as will be a vertebra from the excavation by Schalch and Peyer at Hallau-Bratelen. A list of specimens and their current identification can be found in Table 1.

In order to test the phylogenetic position of the sauropodomorph from Schleitheim, we included the new taxon in the matrix of Apaldetti et al. (2018), with several changes added based on McPhee et al. (2015), an addition of several new characters and changes in some codings based on own observations. One character [absence or presence of a tibiofibular crest in the femur; c. 360 of

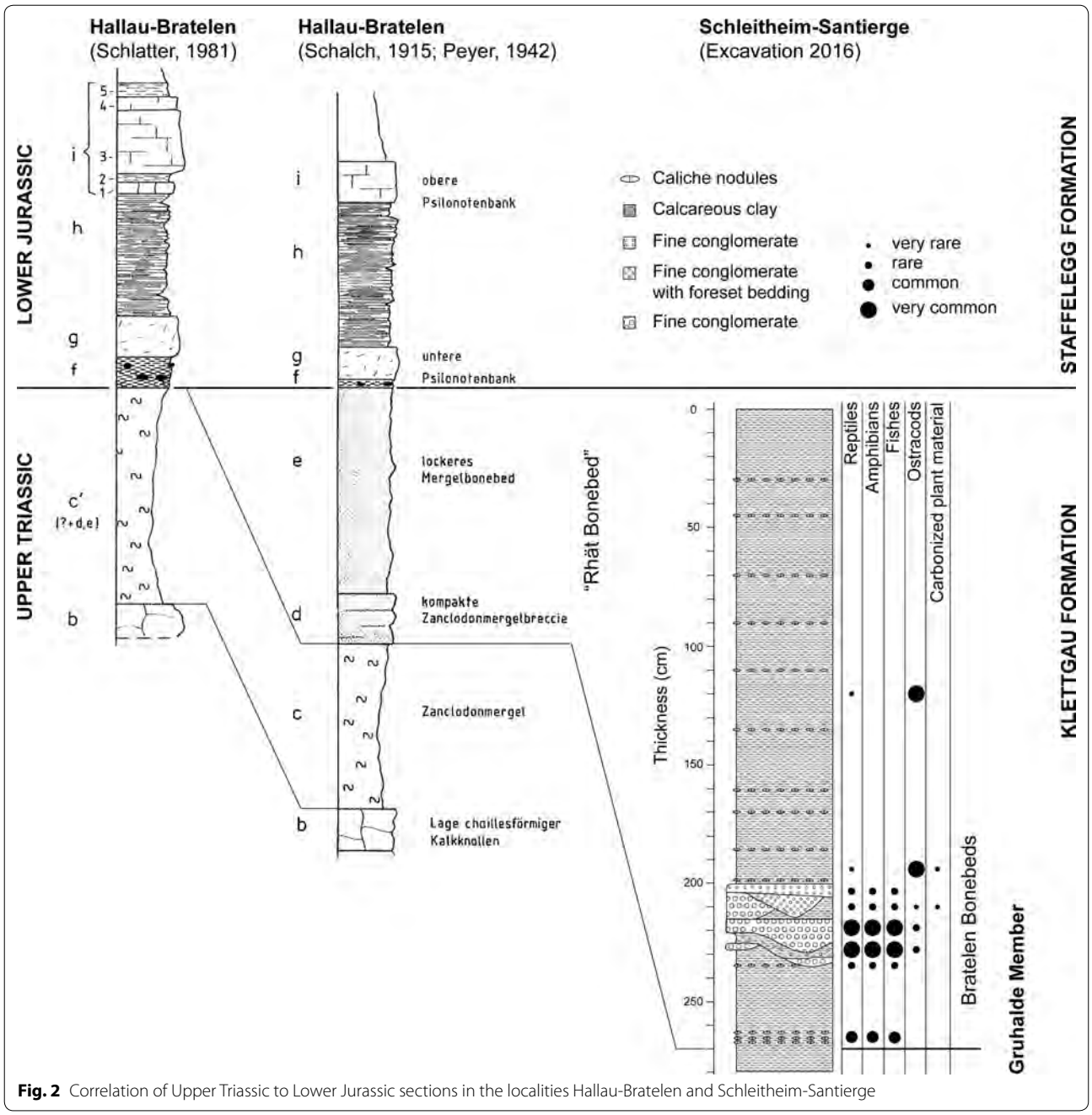

Fig. 2 Correlation of Upper Triassic to Lower Jurassic sections in the localities Hallau-Bratelen and Schleitheim-Santierge

Apaldetti et al. (2018)] was excluded, as it was found to be invariable in the ingroup after recoding, and character 366 of Apaldetti et al. (2018) was subsumed in their character 305, as modified by McPhee et al. (2015: c. 310). The morphology of one other character [Buttress between preacetabular process and the supraacetabular crest of the ilium: present (0); absent (1); c. 250 of Apaldetti et al. (2018)] was unclear as defined, and thus we modified its wording to "Supraacetabular crest on the anterodorsal margin of the acetabulum: absent (0), present (1)" in order to better reflect the original character of Gauthier (1986), the source for this character identified by Otero et al. (2015). All taxa were recoded accordingly. We furthermore added four additional basal sauropod taxa from the Early or early Middle Jurassic, including *Ohmdenosaurus* (Wild 1978), *Amygdalodon* (Cabrera 1947; Casamiquela 1963; Rauhut 2003a), *Spinophorosaurus* (Remes et al. 2009; codings mainly based on McPhee et al. 2015), and *Volkheimeria* (Bonaparte 1979, 1986). On the other hand, the very incomplete and poorly preserved *Gresslyosaurus*

Table 1 List of materials detailing provenance and identifi ation proposed here

Specimen	Element	Provenance	Identific tion
PIMUZ A/III 538	Cervical vertebra	Schleitheim; excavation Schutz	*Schleitheimia schutzi*; probably type indivdual
PIMUZ A/III 540	Dorsal vertebra	Schleitheim; excavation Schutz	*Schleitheimia schutzi*; probably type indivdual
PIMUZ A/III 539	Dorsal vertebra	Schleitheim; excavation Schutz	*Schleitheimia schutzi*; probably type indivdual
PIMUZ A/III 541	Dorsal vertebra	Schleitheim; excavation Schutz	*Schleitheimia schutzi*; probably type indivdual
PIMUZ A/III 545	Dorsal vertebra	Schleitheim; excavation Schutz	*Schleitheimia schutzi*; probably type indivdual
PIMUZ A/III 542	Caudal vertebra	Schleitheim; excavation Schutz	*Schleitheimia schutzi*; probably type indivdual
PIMUZ A/III 543	Caudal vertebra	Schleitheim; excavation Schutz	*Schleitheimia schutzi*; probably type indivdual
PIMUZ A/III 549	Left humerus	Schleitheim; excavation Schutz	*Schleitheimia schutzi*; probably type indivdual
PIMUZ A/III 550	Right ilium	Schleitheim; excavation Schutz	*Schleitheimia schutzi*; holotype
PIMUZ A/III 4390	Pubic peduncle	Schleitheim; excavation Schutz	*Schleitheimia schutzi*; probably type indivdual
PIMUZ A/III 4398	Pubis fragment	Schleitheim; excavation Schutz	*Schleitheimia schutzi*; probably type indivdual
PIMUZ A/III 551	Partial left femur	Schleitheim; excavation Schutz	*Schleitheimia schutzi*; probably type indivdual
PIMUZ A/III 549	Caudal vertebra	Probably Schleitheim; excavation Schutz	*Schleitheimia schutzi*; referred specimen
PIMUZ A/III 544	Caudal vertebra	Probably Schleitheim; excavation Schutz	*Schleitheimia schutzi*; referred specimen
PIMUZ A/III 547	Pedal ungual	Probably Schleitheim; excavation Schutz	*Schleitheimia schutzi*; referred specimen
MzA NAT15051	Dorsal vertebra	Schleitheim; surface collection	(?)*Schleitheimia schutzi*; referred specimen
MzA NAT15052	Dorsal vertebra	Schleitheim; surface collection	(?)*Schleitheimia schutzi*; referred specimen
MzA NAT15058	Dorsal vertebra	Schleitheim; surface collection	(?)*Schleitheimia schutzi*; referred specimen
MzA NAT15050	Sacral vertebra	Schleitheim; surface collection	(?)*Schleitheimia schutzi*; referred specimen
MzA NAT15049	Caudal vertebra	Schleitheim; surface collection	(?)*Schleitheimia schutzi*; referred specimen
MzA NAT15047	Caudal vertebra	Schleitheim; surface collection	(?)*Schleitheimia schutzi*; referred specimen
MzA NAT15048	Caudal vertebra	Schleitheim; surface collection	(?)*Schleitheimia schutzi*; referred specimen
MzA NAT15046	Right humerus	Schleitheim; surface collection	(?)*Schleitheimia schutzi*; referred specimen
PIMUZ A/III 4391	Right astragalus	Schleitheim; excavation Schutz	*Plateosaurus* sp.
MzA NAT15104	Dorsal neural arch	Schleitheim; excavation Furrer	Sauropodomorpha indet.
MzA NAT15059	Dorsal neural arch	Schleitheim; excavation Furrer	Sauropodomorpha indet
MzA NAT15090	Dorsal vertebra	Schleitheim; excavation Furrer	Sauropodomorpha indet
MzA NAT15095	Dorsal vertebra	Schleitheim; excavation Furrer	Sauropodomorpha indet
MzA NAT15100	Dorsal vertebra	Schleitheim; excavation Furrer	Sauropodomorpha indet
MzA NAT15058	Dorsal vertebra	Schleitheim; surface collection	Sauropodomorpha indet
MzA NAT15091	Caudal vertebra	Schleitheim; excavation Furrer	Sauropodomorpha indet
MzA NAT15089	Caudal vertebra	Schleitheim; excavation Furrer	Sauropodomorpha indet
MzA NAT15098	Caudal vertebra	Schleitheim; excavation Furrer	Sauropodomorpha indet
MzA NAT15097	Caudal vertebra	Schleitheim; excavation Furrer	Sauropodomorpha indet
MzA NAT15105	Dorsal rib	Schleitheim; excavation Furrer	Sauropodomorpha indet
MzA NAT15106	Gastral rib	Schleitheim; excavation Furrer	Sauropodomorpha indet
MzA NAT15081	Chevron	Schleitheim; excavation Furrer	Sauropodomorpha indet
MzA NAT15082	Metacarpal one	Schleitheim; excavation Furrer	Sauropodomorpha indet
MzA NAT15075	Dorsal vertebra	Hallau-Bratelen	Sauropodomorpha indet
MzA NAT15067	Left scapula	Hallau-Schwärzibuck	Sauropodomorpha indet
MzA NAT15065	Distal left femur	Hallau-Schwärzibuck	Sauropodomorpha indet
MzA NAT15068	Pedal phalanx	Hallau-Schwärzibuck	Sauropodomorpha indet
MzA NAT15069	Pedal phalanx	Hallau-Schwärzibuck	Sauropodomorpha indet

ingens (*Plateosaurus ingens* in the source matrices) was excluded, as the material is currently being re-prepared and is in need of revision (Meyer et al. 2003); any codings for this taxon in previous matrices should therefore be regarded as tentative. The resulting matrix thus had 66 taxa scored for 382 characters. The matrix was analysed using TNT 1.1 (Goloboff et al. 2008), using heuristic tree search starting from 1000 replicates of Wagner trees

(with random addition sequence of taxa) followed by TBR branch swapping (saving 10 trees per replicate). Given the somewhat uncertain association of the remains of the original excavation of Schutz, we ran three analyses, one including all of the material of the original excavation of Schutz that we interpret as probably belonging to a single individual (though not the material collected later that we tentatively refer to the same taxon), and further analyses with character codings restricted to the type ilium and the referred material, respectively. Furthermore, in a further analysis we reanalysed the dataset including all of the material using implied weights with a k = 12, as outlined by Goloboff et al. (2018). Character support for the different nodes and character transformations were analysed in Mesquite 3.51 (Maddison and Maddison 2018). The character list can be found in the appendix, and the matrices are deposited at Morphobank (http://www.morphobank.org) under project 2320.

Concerning the definition of Sauropoda, we follow the emerging consensus to use the node-based definition originally proposed by Salgado et al. (1997), who defined the clade as *Vulcanodon* and *Saltasaurus* and all descendants of their most recent common ancestor (see Peyre de Fabrègues et al. 2015; McPhee and Choiniere 2018).

Institutional abbreviations BSPG, Bayerische Staatssammmlung für Paläontologie und Geologie, Munich, Germany; MB, Museum für Naturkunde, Berlin, Germany; MCP, Museu de Ciências e Tecnologia PUCRS, Porto Alegre, Brazil; MzA, Museum zu Allerheiligen, Schaffhausen, Switzerland; PIMUZ, Palaeontological Institute and Museum of the University of Zurich, Switzerland; PVL, Paleontolgía de Vertebrados, Instituto Muíguel Lillo, Tucumán, Argentina; PVSJ, Paleontología de Vertebrados, Universidad Nacional de San Juan, San Juan, Argentina; SAM, Iziko South African Museum, Cape Town, South Africa; SMNS, Staatliches Museum für Naturkunde Stuttgart, Germany; UFSM, Universidade Federal de Santa Maria, Brazil.

3 Geology and stratigraphy

Hallau and Schleitheim are municipalities of the Klettgau, about 10 km east of the city of Schaffhausen, forming the boundary region of Canton Schaffhausen (Switzerland) to Baden-Württemberg (Germany) in the Wutach valley. Its hills and valleys expose sections of Upper Triassic to Lower Jurassic sediments, which allow good stratigraphic correlations from south-western Germany to the Tabular and Folded Jura in northern and western Switzerland (Figs. 1, 2). The Upper Triassic (Mittelkeuper) documents a continental environment with the sandy "Schilfsandstein" and "Stubensandstein" and the overlying marls of the "Zanclodonmergel" or "Knollenmergel", renamed as Stuttgart, Steigerwald, Löwenstein and Trossingen Formations in south-western Germany (Etzold and Schweitzer 2005), and as new members of the Klettgau Formation in northern Switzerland (Jordan et al. 2016). Peyer (1943b) noted several bones of *Gresslyosaurus* sp. (vertebrae, fragments of limb bones, and a tooth) at the top of his unit c (see Fig. 2; "Zanclodonmergel", now Gruhalde Member, Jordan et al. 2016) at Hallau (locality Bratelen), but the material could not be identified in the collections. Achilles and Schlatter (1986) dated the upper part of the "Zanclodonmergel" at Hallau (locality Bratelen) using palynostratigraphy as upper Middle Keuper (= upper Norian).

The overlying "Rhät-Bonebed" at Hallau was described by Schalch and Peyer (1919) and Peyer (1943b) as a compact conglomerate with cemented dolomitic clasts (unit d, thickness 0.25 m) and a loose marly bonebed (unit e, thickness 1.00 m). More than eight tons of material were washed in 1915 and 1942, and numerous isolated teeth, scales and bones of fish, reptiles and early mammaliaforms were separated. Schalch and Peyer (1919) published a short list of vertebrate remains (*Gresslyosaurus* sp., *Termatosaurus alberti*, *Megalosaurus* sp., other not yet identified reptiles, labyrinthodont amphibians, *Hybodus* sp., *Hybodoconchus*, ganoid scales), and figured several teeth of the dipnoan *Ceratodus parvus* and the actinopterygian *Sargodon tomicus*, both used as their main criteria to presume a Rhaetian age of the bonebed. Peyer (1943a, p. 261) notes again the dinosaur bones and the tooth found in 1915 and 1942, as belonging to *Gresslyosaurus ingens*, and added, that these dinosaur remains could be reworked from the underlying "Zanclodonmergel". Peyer (1956) described 71 teeth of mammals and mammal-like reptiles from the "Rhät-Bonebed", which were later revised by Clemens (1980). This author discussed the presumed Rhaetian age of the bonebed and wrote: "… the Hallau bonebed local fauna might be of Rhaetian age. It is probably not older than Middle Keuper (Norian) and no younger than the *Psiloceras johnstoni* Zone, early, but not earliest Hettangian". Tatarinov (1985) identified another supposed dinosaur tooth in Peyer's material as representing a heterodontosaurid, but this identification was challenged by Butler et al. (2006), who could only identify this tooth as an undetermined archosaur. A new genus and species of rhynchocephalian lepidosaur from Peyer's vertebrate material was published by Whiteside et al. (2017) who also introduced the new lithostratigraphic name Bratelen Bonebeds.

Further vertebrate material was collected by E. Schutz in 1954 from a 2.10 m thick "Rhät-Bonebed" from an outcrop in a forest near Schwärzibuck, 350 m NNW of the locality Hallau-Bratelen. He donated the sieved material, some hundred fish teeth and small lepidosaurs in 1955

to the University of Zurich (Whiteside et al. 2017). Some larger dinosaur bones were deposited in a local museum at Neunkirch; these fossils are described below and are now in the inventory of the Museum zu Allerheiligen, Schaffhausen.

As noted above, the dinosaur material from Schleitheim (locality Santierge) was collected in 1952–1954. According to the unpublished notes of E. Schutz, deposited at the MzA, the big bones came from a hard conglomeratic layer in grey greenish to reddish marls with a thickness of c. 30 cm, together with teeth of *Ceratodus* and ostracods. The remains were recovered in situ in a small excavation "c. 50 m in front of the quarry in the Liassic, c. 20 m below the highest road at the margin of a recently created field" (translated from the notes of E. Schutz).

Hofmann (1981) mapped the area of Hallau and Schleitheim in detail and noted a larger bone fragment that he identified as *Gresslyosaurus ingens*, found as isolated fossil in a field, covering the "Rhät-Tone, Bonebed usw." (Hofmann 1981, p. 11) at the locality Harnischbogen, only 600 m ENE of the locality Schleitheim-Santierge.

Achilles and Schlatter (1986), who studied a new section about 200 m east of Peyer's 1942 excavation at Hallau-Bratelen, did not find any bonebed. They identified a typical Liassic palynomorph assemblage from bed f (Planorbis to Liasicus Zone; Fig. 2) overlying directly bed c ("Knollenmergel") with palynomorphs from the upper Middle Keuper (= upper Norian). They also studied samples from the "Rhät-Bonebed" from other sections at Hallau and Schleitheim, but could not find any palynomorphs. They suggest that the "Rhät-Bonebed" represents probably a bonebed of the upper Middle Keuper (= Upper Norian).

In 2016, one of us (HF) led a small excavation in the Upper Triassic sediments of Schleitheim-Santierge (Fig. 2), some 20–30 m away from the original excavation site of Schutz. The unpublished sketch of the section made by Schutz in 1954 could be confirmed, studying a 15 m long and 3 m deep trench in a gently sloping, just harvested field. The bedding was nearly horizontal, but slightly deformed by a landslide. Above the yellow to violet dolomitic marls of the Gruhalde Member with calcrete nodules (former "Zanclodonmergel" or "Knollenmergel"), disarticulated dinosaur bones were found together with vertebrae, teeth and scales of phytosaurs, amphibians, osteichthyan and chondrichthyan fishes (Bratelen Bonebeds, Fig. 2). Ostracods were the only invertebrate fossils; indeterminable coaly plant remains were rare. The often fragmentary and abraded fossils were embedded in pebbly mudstones and carbonate sandstones to fine conglomerates intercalated as three, up to 15 cm thick lenticular cemented layers in brownish marl. The carbonate sandstones to fine conglomerates never include quartz, feldspar nor mica grains, but well rounded clasts of limestone and dolomite with diameters from 1 to 10 mm. Up to 5 cm large intraclasts of red marl and calcrete nodules must be eroded from the underlying Gruhalde Member. The in total 35 cm thick Bratelen Bonebeds were overlain by more than 2 m of green-grey calcareous clay with several layers of white calcrete nodules of probably late Triassic age. A tooth and a bone fragment of a phytosaur were the only vertebrate fossils, but ostracods are very common. Test samples on palynomorphs were negative (E. Schneebeli-Hermann, pers. comm.). The section in the 3 m deep trench was deeply weathered and the base of the Lower Jurassic was not reached. Calcareous clay together with bonebeds were also mapped and described from Santierge and a few other natural and artificial outcrops in the Klettgau by Hofmann (1981: p. 10/11, "Rhät-Tone, Bonebed usw."). However, the Rhaetian age was not proved.

The "Rhät-Bonebed" or Bratelen Bonebeds (Whiteside et al. 2017) from Hallau and Schleitheim are directly overlain by black marls and limestone of the "Psilonotenschichten" (Fig. 2; Hallau Bed of the Schambelen Member, Staffelegg Formation; Reisdorf et al. 2011). Schalch and Peyer (1919) and also Achilles and Schlatter (1986) found ammonites of the Lower Hettangian in the Hallau section (unit f); however, the lowermost subzone of the *planorbis* zone could not be identified. This lowermost subzone was found near Beggingen, 4 km northeast of Schleitheim (Schlatter 1983). As a consequence, a hiatus of some million years at the Triassic-Jurassic boundary is typical for the area, spanning the whole Rhaetian and locally also the earliest Hettangian. It could have been a long time of non-deposition during the Rhaetian or important erosion in the latest Rhaetian and earliest Hettangian.

Extensive fieldwork by one of us (HF) documents that the Bratelen Bonebeds (former "Rhät-Bonebeds") in the Klettgau form a characteristic lithostratigraphic bed on top of the Gruhalde Member, where all the studied sauropodomorph material from Hallau and Schleitheim was found (Fig. 2). Variable in composition and thickness, and even locally missing, the Bratelen Bonebeds records an important erosional event at the end or after the deposition of the Gruhalde Member (late Norian?). Rhaetian sediments have never been proved by litho-, bio- or chronostratigraphy in the Canton Schaffhausen. The Bratelen Bonebeds, without any siliciclastic sand grains, clearly differ from the dark mud-, silt- and sandstones with sandy bonebeds, dated by palynostratigraphy to lower, middle and upper Rhaetian in south-western Germany (Exter Formation; Etzold and Schweitzer 2005) and also in the Tabular and Folded Jura of northern

Switzerland (Belchen Member of the Klettgau Formation in Canton Baselland and Solothurn; Jordan et al. 2016; Schneebeli-Hermann et al. 2018; Looser et al. 2018).

4 Systematic palaeontology

Dinosauria OWEN, 1842.

Sauropodomorpha HUENE, 1932.

Sauropodiformes SERENO 2007 (sensu McPhee et al. 2014).

Schleitheimia n. gen.

Type species. Schleitheimia schutzi sp. nov.

Etymology. Genus name refers to the type locality at Schleitheim, Canton Schaffhausen, Switzerland.

Diagnosis. As for type and only known species.

Schleitheimia schutzi sp. nov.

Etymology. Species epithet honours the collector of the type material, Emil Schutz (1916–1974).

Holotype. PIMUZ A/III 550, partial right ilium.

Referred material. Centrum of posterior cervical vertebra (PIMUZ A/III 538), anterior dorsal vertebra (PIMUZ A/III 540), centra of two mid-dorsal vertebrae (PIMUZ A/III 539 and 541), centrum of posterior dorsal vertebra (PIMUZ A/III 545), centrum of anterior caudal vertebra (PIMUZ A/III 548), two centra of posterior mid-caudal vertebrae (PIMUZ A/III 542, 543), posterior caudal vertebra (PIMUZ A/III 544; referral tentative), distal end of left humerus (PIMUZ A/III 549), pubic peduncle of left ilium (PIMUZ A/III 4390), possible pubic fragment (PIMUZ A/III 4398), partial left femur (PIMUZ A/III 551), ungual of right pedal digit I (PIMUZ A/III 547; referral tentative). Further tentatively referred specimens were collected considerably later and include three fragmentary dorsal vertebral centra (MzA NAT15051, NAT15052 and NAT15058), a sacral centrum (MzA NAT15050), three caudal vertebrae (MzA NAT15047, NAT15048, NAT15049), and a partial right humerus (MzA NAT15046). As discussed above, all of these remains come from the same general locality, are consistent in morphology, and probably represent the same taxon and at least partially the same individual as the holotype.

Type locality and horizon. The type locality is Santierge (Fig. 1), a hill situated 900 m south of the church of Schleitheim in the Swiss Canton Schaffhausen (47° 44′ 30″ N, 8° 29′ 13″ S). The material, collected in the Bratelen Bonebed ("Rhät-Bonebed"), was most probably derived from the uppermost part of the ‚Zanclodonmergel'(= Knollenmergel), now called Gruhalde Member of the Klettgau Formation, uppermost Norian (Jordan et al. 2016).

Diagnosis. The new taxon can be diagnosed by the following autapomorphies: medial brevis shelf of ilium developed as dorsoventrally broad, rounded ridge just below the mid-height of the iliac blade on the medial side that ends in a large, round expansion at the posterior end of the ilium; fourth trochanter of the femur very robust and arises gradually out of the posterior surface of the bone at about its mid-width towards its apex at the posteromedial margin; crista tibiofibularis of the femur exceptionally broad and only very slightly offset medially from the lateral margin of the shaft, so that no posteriorly facing shelf is present lateral to the crista.

5 Description

5.1 Original material of Schutz

5.1.1 Axial skeleton

A total of nine vertebrae are present in the original material of Schutz, representing cervical, dorsal and caudal vertebrae. Five presacral vertebral centra are present, representing one posterior cervical and four dorsal elements, based on the absence/presence and the position of the parapophysis on the centrum. The specimen PIMUZ A/III 538 is the poorly preserved centrum of a posterior cervical vertebra (Fig. 3). Due to the rather poor preservation, its exact position in the vertebral column cannot be established, but, assuming that *Schleitheimia* had ten cervicals, as other non-sauropodan sauropodomorphs, it probably represents one of cervicals eight to ten. The centrum was rather short (ratio of centrum length to anterior centrum height approximately 1.3) and amphicoelous, as in other basal sauropodomorphs. The anterior articular surface is almost round, being very slightly wider than high; the posterior surface is largely broken. The centrum is strongly constricted between the articular ends, its minimal width (35 mm) being only 37% of the width of the anterior articular surface (94 mm). The parapophyses are placed at the anteroventral end of the centrum and are slightly offset posteriorly from the rim of the anterior articular end. They form lateroventral projections and have concave articular surfaces that are teardrop-shaped in outline, with the pointed end pointing posteriorly. Their ventral and dorsal surfaces are anteroposteriorly convex, unlike the recessed dorsal surface of the parapophyses in

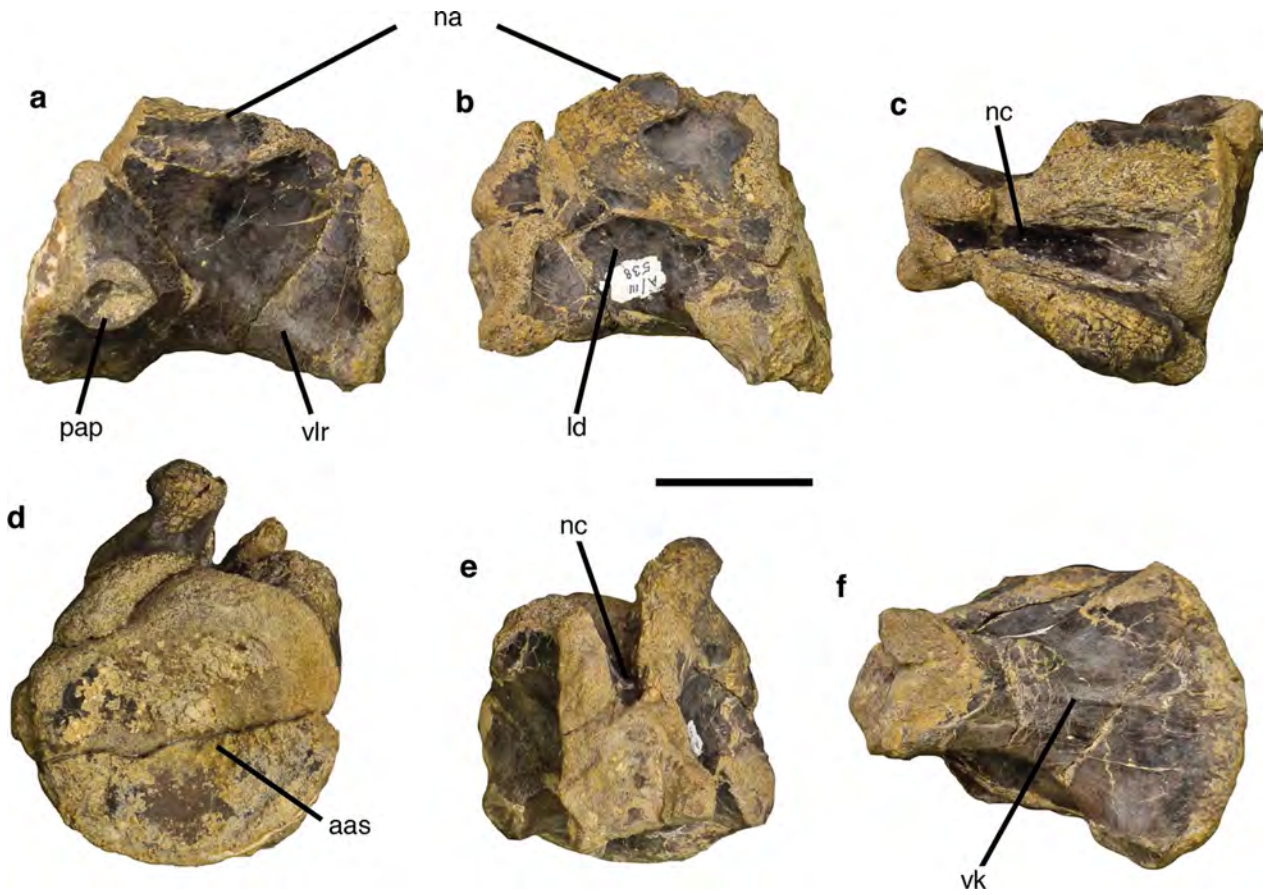

Fig. 3 Posterior cervical vertebra of *Schleitheimia schutzi* n. gen., n. sp., PIMUZ A/III 538. **a**, **b** left and right lateral views; **c** dorsal view; **d** anterior view; **e** posterior view; **f** ventral view. aas, anterior articular surface; na, neural arch; ld, lateral depression; nc, neural canal; pap, parapophysis; vk, ventral keel; vlr, ventrolateral ridge. Scale bar equals 5 cm

eusauropods. A stout, rounded edge extends posteriorly from the posterior end of the parapophysis and separates the lateral side of the centrum from its ventral side; this edge corresponds to the ventrolateral ridge of Wilson (2012). The ventral surface of the centrum forms two flat surfaces that converge medially towards a low, transversely rounded midline keel that becomes slightly more conspicuous anteriorly (Fig. 3f). At the anterior end, the ventral surfaces lateral to the keel are slightly concave between the latter and the projection of the parapophyses, but a marked depression, as it is present in some sauropods, is absent. A large, but shallow depression is present on the lateral side of the centrum.

Not much can be said about the morphology of the neural arch, as it is mostly broken away. A small portion of the neurocentral suture is visible on the left side of the vertebra; the rest of suture cannot be made out, probably due to preservation. It separates the neural arch pedicle from the lateral side of the centrum and extends ventrally to approximately 1/3 of the centrum height anteriorly. Only the bases of the anterior and posterior centrodiapophyseal laminae are preserved. These laminae were obviously stout and extended obliquely towards the transverse process in the central part of the vertebra, the ventral end of the anterior centrodiapophyseal lamina being offset posteriorly from the anterior end of the neural arch pedicle. The neural canal is narrow and was obviously high, indicating a dorsoventrally high neural arch. It becomes narrower in its central part, where it is also deeply incised into the dorsal side of the centrum.

Specimen PIMUZ A/III 540 is a rather poorly preserved anterior dorsal vertebra, including parts of the neural arch and spine (Fig. 4). The centrum is amphicoelous, being more deeply concave posteriorly than anteriorly. In ventral view, it is strongly constricted, but the minimal width is reached approximately 1/3 of the length posterior to the anterior end; from this point the centrum strongly expands posteriorly. A rather sharply defined, but low midline keel extends anteriorly from the minimal width of the centrum. The posterior part of the

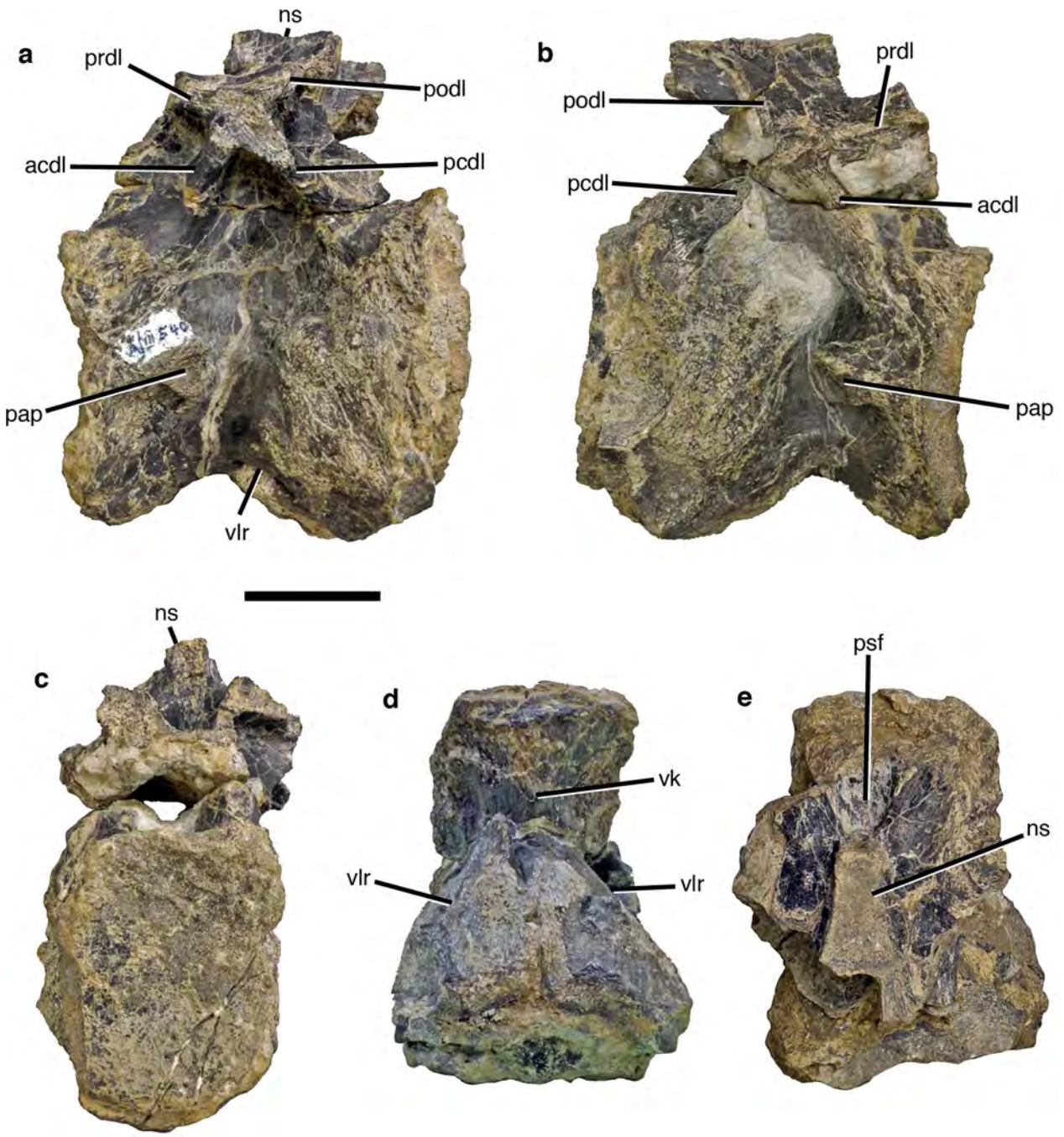

Fig. 4 Anterior dorsal vertebra of *Schleitheimia schutzi* n. gen., n. sp., PIMUZ A/III 540. **a**, **b** left and right lateral views; **c** anterior view; **d** ventral view; **e** dorsal view. acdl, anterior centrodiapophyseal lamina; nc, neural canal; pap, prapophysis; pcdl, posterior centrodiapophyseal lamina; podl, postzygapophyseal diapophyseal lamina; prdl, prezygodiapophyseal lamina; psf, prespinal fossa; spdl, spinodiapophyseal lamina; vk, ventral keel; vlr, ventrolateral ridge. Scale bar equals 5 cm

ventral side is broad, with apparently a small, but poorly preserved midline ridge towards the posterior end and marked, but also poorly preserved lateroventral ridges on either side (Fig. 4d).

The lateral side of the centrum is poorly preserved. The parapophysis is placed at about the half height of the centrum. It is relatively small, oval in outline, and notably displaced posteriorly from the anterior end, its posterior

rim lying at approximately one-third of the length of the centrum. The anterior rim of the parapophysis is connected to the rim of the anterior articular surface by a low, rounded ridge. The articular surface of the parapophysis faces posterolateroventrally. A deep and marked centrodiapophyseal fossa is present posterodorsal to the parapophysis, but there is no pleurocoel posterior or posterodorsal to the parapophysis, nor is the dorsal part of the centrodiapophyseal fossa deepened, as it is the case in some basal sauropods (e.g. Bonaparte 1986). The neural arch is low, the height from the centrum to the dorsal surface of the transverse process being approximately two-thirds of the height of the centrum. The base of the broken transverse process is placed slightly anterior to the mid-length of the centrum on the neural arch. It is connected to the centrum by relatively short and stout anterior and posterior centrodiapophyseal laminae that meet at an angle of slightly less than 90°. The anterior centrodiapophyseal lamina is slightly more steeply inclined than the posterior centrodiapophyseal lamina and the ventral bases of both lamina are notably offset from the respective rim of the centrum. Short, but robust prezygodiapophyseal and postzygodiapophyseal laminae extend from the transverse process anteriorly and posterodorsally, respectively, but the zygapophyses are missing. This well-developed neural arch lamination results in the presence of large prezygapophyseal-centrodiapophyseal, centrodiapophyseal and postzygapophyseal-centrodiapophyseal fossae, of which the latter two are slightly larger and deeper than the former. On the right side of the neural arch, the postzygodiapophyseal lamina is partially complete and shows that this lamina formed a laterally extensive and stout roof over the postzygapophyseal-centrodiapophyseal fossa. The slightly dorsally protruding stalks for the prezygapophyses diverge slightly anteriorly and define a wide and deep prespinal fossa. The roof of the neural arch ascends towards the missing postzygapophyses posteriorly. The neural spine was anteroposteriorly short, placed approximately above the mid-length of the centrum and robust. Anteriorly, a broad, roughened surface for the attachment of the interspinal ligaments is present. The neural spine expands transversely towards its posterior end and was obviously connected to the postzygapophyses by stout spinodiapophyseal laminae that define a large postspinal fossa, although this region is poorly preserved. The dorsal part of the neural spine is missing, so nothing can be said about its height. In anterior view, the spine expands slightly and gradually dorsally. As in the cervical vertebra, the neural canal is narrow, round in outline anteriorly and deeply incised into the dorsal side of the centrum in its central part.

PIMUZ A/III 539 (Fig. 5a–d) and 541 (Fig. 5e, f) are mid-dorsal vertebral centra. The centra are amphicoelous, with slightly more deeply concave anterior than posterior articular surfaces. The centra are only moderately constricted between the articular ends and the ventral sides are broadly transversely rounded. A notable elongate lateral depression is present on the dorsal part of the lateral surface on either side, but these depressions have no sharply defined rims and thus cannot be considered to be true pleurocoels (sensu Carballido and Sander 2014). As in the anterior dorsal, the base of the broken posterior centrodiapophyseal lamina is very stout and the neural canal is narrow, high and deeply incised into the dorsal side of the centrum.

Specimen PIMUZ A/III 545 is a posterior dorsal centrum, probably of one of the most posterior dorsals (Fig. 5g–i). The centrum is notably short (ratio of length to posterior width about 0.8) and massive, being broad and rounded ventrally. The centrum is amphicoelous, with a more deeply concave posterior than anterior side. As in the mid-dorsal centra, a marked lateral depression is present in the dorsal half of the lateral side; this depression is somewhat smaller, but more clearly defined than in the mid-dorsal vertebrae, without, however, having sharply defined borders. The base of the broken posterior centrodiapophyseal lamina is massive. The neural canal is relatively wider than in the mid-dorsal vertebrae, but is very deeply and abruptly incised into the dorsal side of the centrum, its deepest part being placed more than 30 mm below the rim of the articular surfaces.

A large and strongly distorted anterior caudal vertebral centrum without precise locality information (PIMUZ A/III 548; Fig. 6) fits in size with the posterior dorsal vertebra and thus might also represent the same animal. The centrum is amphicoelous, being more strongly concave anteriorly than posteriorly. It is notably short, its anteroposterior length (c. 90 mm) being only about 60% of its anterior height (c. 150 mm), although both of these measurements should be seen with caution due to the distortion. The ventral rim of both the anterior and posterior articular surface flexes slightly ventrally. The centrum is constricted in the middle, and there seems to have been a broad, flattened to very slightly transversely concave surface on the ventral side, ending in a short groove posteriorly between the chevron facets. The lateral side of the centrum is smooth and does not show any notable depression below the transverse processs. The base of the broken transverse process is placed on the neurocentral suture. It is massive and extends over almost the entire length of the centrum. Anteriorly, the base of the process is slightly higher than posteriorly, and a short, stout ridge connects its anteroventral edge with the anterodorsal end of the centrum. The neural canal is narrow and somewhat incised into the dorsal surface of the centrum, but most of the neural arch is missing.

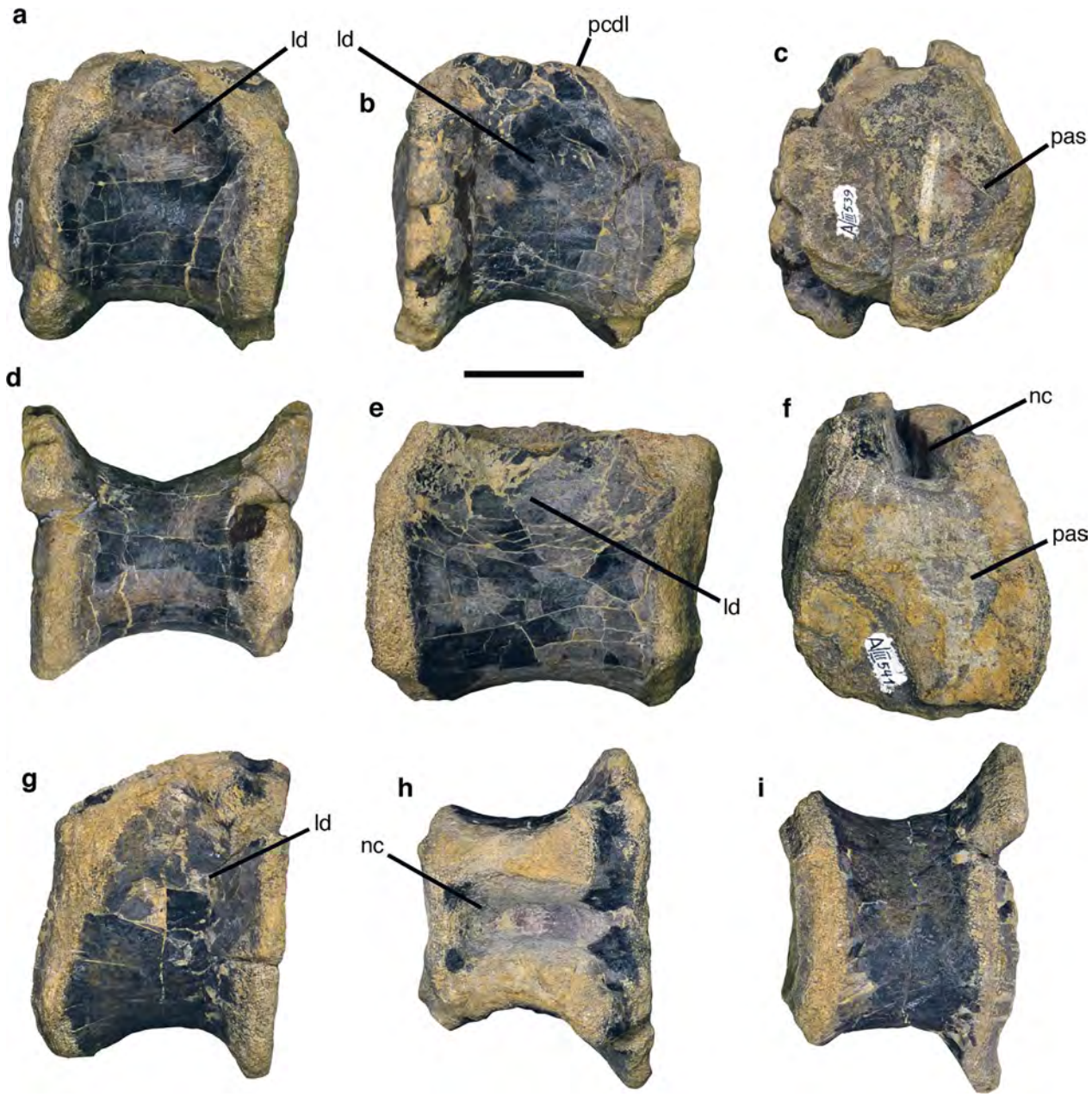

Fig. 5 Mid and posterior dorsal vertebrae of *Schleitheimia schutzi* n. gen., n. sp. **a**–**d** Mid dorsal vertebral centrum, PIMUZ A/III 539, in right (**a**) and left (**b**) lateral, anterior (**c**), and ventral (**d**) views; **e, f** mid dorsal vertebral centrum, PIMUZ A/III 541, in lateral (**e**) and posterior (**f**) views; **g**–**i** posterior dorsal vertebral centrum, PIMUZ A/III 545, in lateral (**g**), dorsal (**h**) and ventral (**i**) views. ld, lateral depression; nc, neural canal; pas, posterior articular surface; pcdl, posterior centrdiapophyseal lamina. Scale bar is 5 cm

Three posterior mid- to distal caudals are present in the collections of the PIMUZ (Fig. 7). While two of them can positively identified as coming from the locality of Schleitheim (PIMUZ A/III 542 and 543; Fig. 7a–d), the provenance of the third vertebra (PIMUZ A/III 544; Fig. 7e, f) is uncertain. However, its preservation is consistent with the other material from this locality, and we tentatively refer it to the same animal. All of them are poorly preserved and miss most of the neural arch. The caudal centra are amphicoelous and rather massive. They are rounded ventrally and do not show any ventral groove or ridge. The articular ends are only complete in the smallest vertebra (PIMUZ A/III 544; Fig. 7e, f) and show no signs of chevron facets. No transverse process

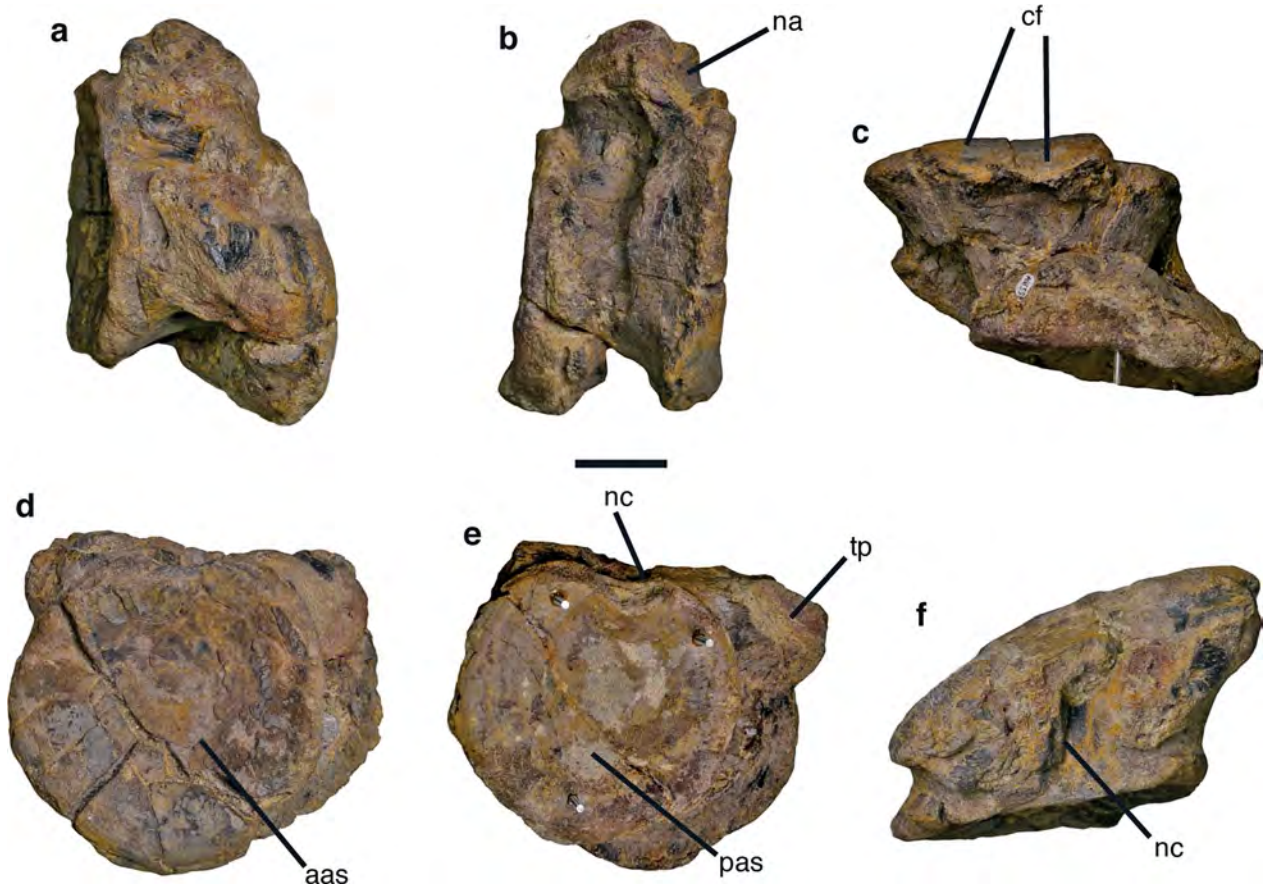

Fig. 6 Anterior caudal vertebra of *Schleitheimia schutzi* n. gen., n. sp., PIMUZ A/III 538. **a**, **b** right and left lateral view; **c** ventral view; **d** anterior view; **e** posterior view; **f** dorsal view. Abbreviations: aas, anterior articular surface; cf, chevron facet; na, neural arch; nc, neural canal; pas, posterior articular surface; tp, transverse process. Scale bar equals 5 cm

is present in any of the elements, although it cannot be ruled out that this process was present on the missing neural arch of the most anterior specimen, PIMUZ A/III 542. The specimen PIMUZ A/III 543 has a dorsoventrally somewhat flattened centrum and a stout longitudinal ridge on the lateral side, resulting in a longitudinal depression on this side between the ridge and the attachment of the neural arch (Fig. 7d). PIMUZ A/III 544 has parts of the neural arch preserved. The pedicles of the arch do not extend over the entire length of the centrum, but are offset from the posterior end. The neural arch is rather low, with a transversely rounded dorsal roof anterior to the broken neural spine. The prezygapophyses obviously overhung the centrum anteriorly, but are broken away. The neural canal is round in outline. Measurements of the axial elements can be found in Table 2.

5.1.2 Appendicular skeleton

Appendicular elements preserved include a partial humerus, ilium, a pubis fragment, a partial femur, and a pedal ungual. The only element of the forelimb recovered is the distal third or fourth of a large and massive left humerus (PIMUZ A/III 549; Fig. 8). The other element mentioned and figured by Galton (1986: 175; pl. 1, Fig. 23) as the proximal part of the right ulna is the pubic peduncle of the right ilium (see below). The distal end of the humerus is notably expanded, from a minimal transverse width of the shaft at the proximal break of 92 mm to a maximal distal width of c. 175 mm. The shaft is anteroposteriorly flattened, with a maximal anteroposterior depth of c. 46 mm at the proximal break. The posterior side of the bone is occupied by a large, shallow depression, as in most basal saurischians. On the anterior side, a large, rounded and rather deep flexor fossa is present towards the distal end between the distal condyles. The fossa is well defined proximally by stout, distally diverging, broadly rounded ridges. On the lateral side of the lateral of these ridges, the side of the bone forms a flat, anterolaterally facing surface that meets the slightly curved posterolateral side in a well-defined

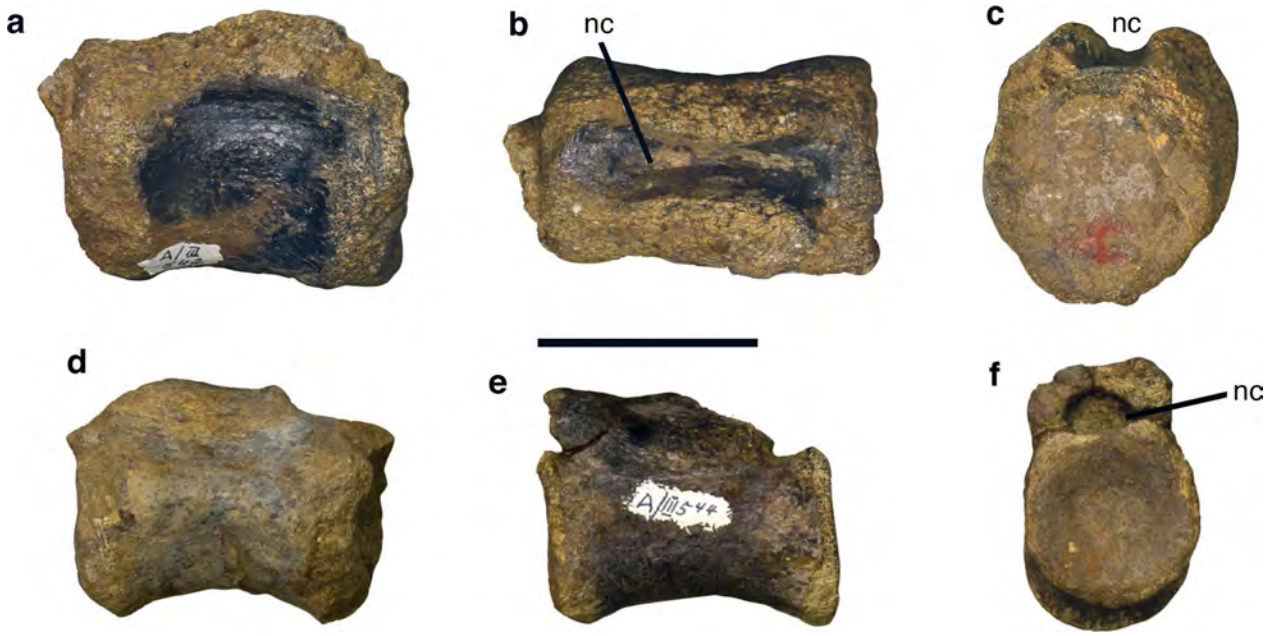

Fig. 7 Middle and distal caudal vertebrae of *Schleitheimia schutzi* n. gen., n. sp. **a**–**c** Middle caudal vertebral centrum, PIMUZ A/III 542, in right lateral (**a**), dorsal (**b**) and anterior (**c**) views; **d** posterior mid-caudal vertebra, PIMUZ A/III 543, in left lateral view; **e**, **f** distal caudal vertebra, PIMUZ A/III 544 in left lateral (**e**) and anterior (**f**) views. nc, neural canal. Scale bar equals 5 cm

Table 2 Measurements of vertebrae of the original Schutz excavation; probably belonging to type individual of *Schleitheimia*

Specimen	Centrum length	Anterior height	Anterior width	Posterior height	Posterior width	Minimal width
PIMUZ A/III 538	c. 120	92	94	–	–	c. 35
PIMUZ A/III 540	c. 119	88	–	91	88	c. 30
PIMUZ A/III 539	117	100	102	107	97	59
PIMUZ A/III 541	100	85 +	80 +	85 +	90	60
PIMUZ A/III 545	c. 89	–	–	111	110	c. 70
PIMUZ A/III 542	90	52 +	53	61	52	43
PIMUZ A/III 543	72	42 +	51	41 +	45 +	36
PIMUZ A/III 544	64	36	35	35	36	30

Measurements are in mm

+ indicates minimal estimates

ridge at about the anteroposterior mid-width of the lateral side. This lateral ridge becomes less conspicuous towards the proximal break, but is well-marked on the lateral side of the distal condyles. The anteromedial surface is less steeply inclined and gradually curves into the posterior side on the posterior edge of the medial side of the bone.

The distal articular surface is more or less hourglass-shaped in distal view (Fig. 8e). The radial condyle is slightly more massive and more strongly expanded anteriorly than the ulnar condyle. Both condyles are well separated by anterior and posterior indentations, but more or less continuous in anterior or posterior view distally. The anteromedial edge of the ulnar condyle is broken, but the condyle seems to have curved gradually proximomedially on the medial side, unlike in many basal sauropodomorphs, where there is a marked, mediodistally inclined flat area on the medial side of the ulnar condyle. The distal surface is not smoothly convex, but has several marked pits and grooves. One groove traverses the distal side of the radial condyle obliquely from anterolateral to posteromedial; in its medial part, this groove opens anteriorly onto a large, mediolaterally concave facet that separates the humeral condyles on the anterodistal side.

Fig. 8 Distal end of left humerus of *Schleitheimia schutzi* n. gen., n. sp., PIMUZ A/III 549. **a** anterior view; **b** lateral view; **c** posterior view; **d** medial view; **e** distal view; **f**, proximal view of proximal break. dp, posterior depression; ff, flexor fossa; lr, lateral ridge; rc, radial condyle; uc, ulnar condyle. Scale bar equals 5 cm

At least two oblique grooves are also present on the ulnar condyle and extend from anteromedial posterolaterally.

A good part of the right ilium was preserved in numerous fragments (PIMUZ A/III 550; Fig. 9a–f). Several of these fit together to form the entire acetabular margin of the ilium and the iliac peduncles. Other fragments represent much of the postacetabular blade and the dorsal margin of the ilium, which is here designated as the holotype of *Schleitheimia schutzi* gen. et sp. nov.

As in all sauropodomorphs, the pubic peduncle is considerably longer than the ischial peduncle. Whereas the expansion of the latter from the base of the postacetabular process is about 65 mm, the pubic peduncle expands for approximately 210 mm from the base of the preacetabular process. The pubic peduncle is almost straight, and its lateral surface slightly and gradually expands distally. The acetabular rim of the pubic peduncle is notably concave transversely, although this is somewhat exaggerated by compression. The lateral surface is flat proximally but becomes slightly anteroposteriorly convex distally. The anterior margin of the peduncle is much more narrow than the acetabular rim and rounded transversely, whereas the medial surface faces slightly anteromedially and is flattened. The distal articular surface for the pubis is comma-shaped in outline, tapering posteromedially. It is flat to very slightly convex and has a roughened, pitted surface. A stout supraacetabular crest was obviously present, but is only preserved in its dorsal part. The broken base of the crest starts on the lateral acetabular margin at about one-third of the length of the pubic peduncle from the distal end of the latter. The crest seems to have had its greatest extension at the anterodorsal part of the acetabulum, where it overhangs the latter, forming a markedly ventrally concave hood. The crest ends slightly posterior to the mid-length of the acetabulum and does not extend onto the base of the ischial peduncle, although the rim of the acetabulum protrudes slightly laterally almost to the distal end of this peduncle.

The acetabular rim on the ischial peduncle is slightly wider transversely than on the pubic peduncle, and it is slightly convex transversely. The lateral surface of the peduncle is slightly concave anteroposteriorly between the raised acetabular rim and the base of the postacetabular process, but becomes convex towards the distal end. The distal end of the ischial peduncle is considerably wider transversely than long anteroposteriorly and has a strongly anteroposteriorly convex distal articular surface for the ischium. As in the pubic peduncle, this articular surface is rugosely pitted. The distal end of the ischial peduncle is slightly expanded posteriorly, resulting in a

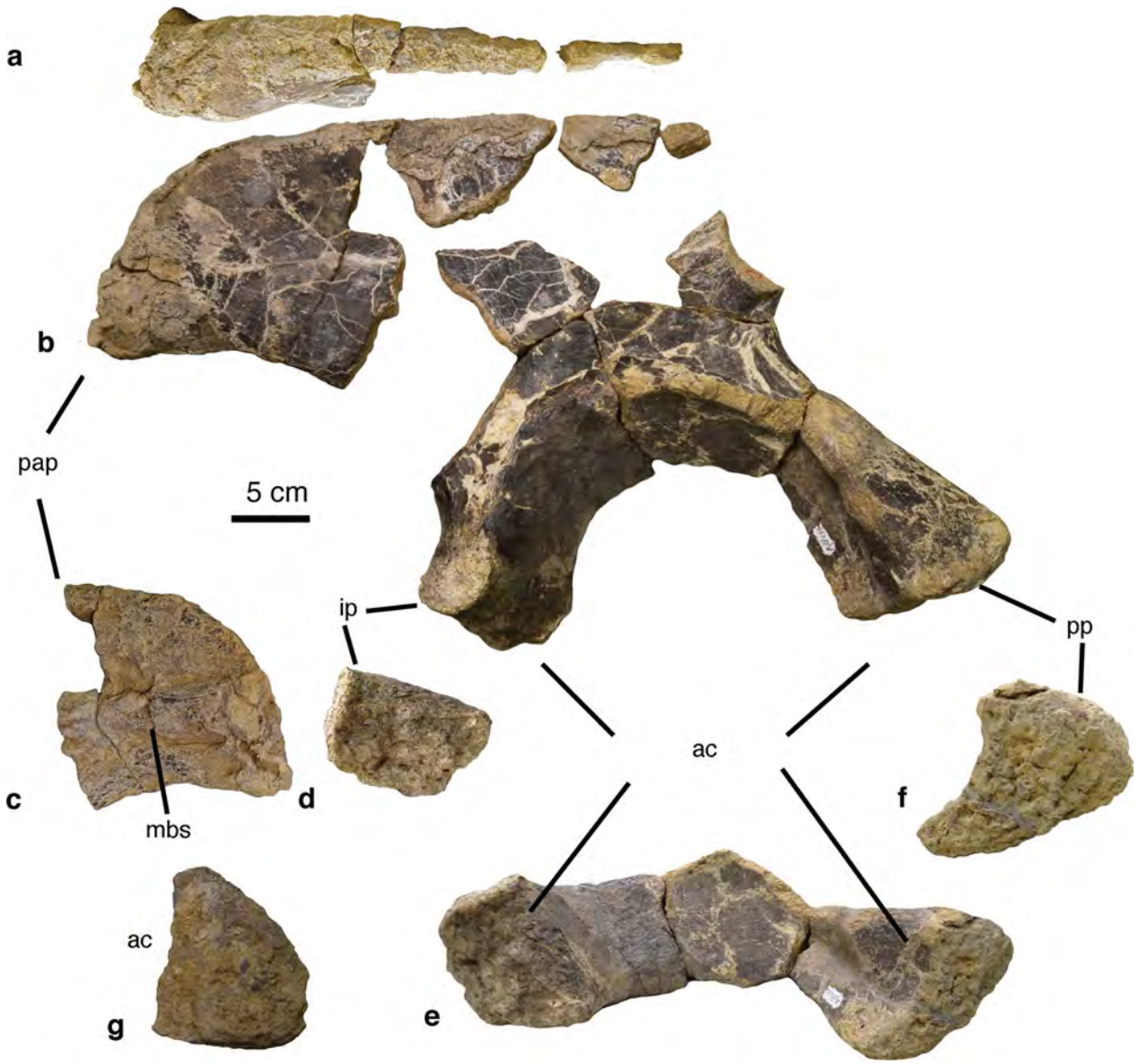

Fig. 9 **a**–**f** Partial right ilium PIMUZ A/III 550, holotype of *Schleitheimia schutzi* n. gen., n. sp., and **g** distal end of left pubic peduncle PIMUZ A/III 4390. **a** dorsal view of preserved parts of iliac blade; **b** preserved parts in approximate original configuration in lateral view; **c** postacetabular process in medial view; **d** ischial peduncle in distal view; **e** acetabular region in ventral view; **f** pubic peduncle in distal view; **g** left pubic peduncle in distal view PIMUZ A/III 4390. ac, acetabulum; ip, ischial peduncle; mbs, medial brevis shelf; pap, postacetabular process; pp, pubic peduncle. Scale bar equals 5 cm

dorsoventrally concave posterior margin of the peduncle. The ischial peduncle seems to have been especially short in respect to the level of the ventral margin of the postacetabular blade: whereas the latter is placed above the level of the dorsal rim of the acetabulum in most non-sauropodan sauropodomorphs (e.g. Galton and Upchurch 2004), it is at this level or below in *Schleitheimia*, as in sauropods (e.g. Bonaparte 1986). Although the direct contact between the ischial peduncle and postacetabular blade is not preserved in PIMUZ A/III 550, any arrangement that places the ventral rim of the blade above the level would result in an anteroventrally sloping dorsal iliac margin, which would be highly unusual.

The base of the broken preacetabular process is transversely widened to form a ventrally facing shelf, whereas the dorsal part of the process forms a thin bony lamina that is dorsoventrally convex laterally. A large, anteroventrally facing nutrient foramen is present proximally in the

lateral side of the ventrally facing shelf. The base of the postacetabular process faces slightly lateroposteriorly, and the lateral surface of the proximal part of this process was obviously slightly concave anteroposteriorly.

The posterior end of the postacetabular process forms a large, lobe-shaped expansion. Its ventral margin is anteroposteriorly concave and meets the posterior margin in a sharp angle of c. 60°. The posterior margin is dorsoventrally notably convex, but the transition into the dorsal margin posterodorsally is marked by a short, slightly concave edge. Anterior to this, the dorsal margin is slightly undulating, with a low, but notable, rounded dorsal expansion towards the supraacetabular region. The lateral surface of the posterior end of the postacetabular blade is markedly convex dorsoventrally. More anteriorly, the dorsal two-thirds of the lateral surface of the iliac blade become slightly dorsoventrally concave. The posterior end is strongly thickened transversely, and the posterior surface of this thickened region is strongly rugose, with the rugosities forming a laterally protruding margin in the posterodorsal part. Dorsally, the dorsal part of the postacetabular blade forms a broad, dorsally and slightly laterally facing surface, which becomes gradually narrower anteriorly and has a slightly rugose texture. In the anteriormost preserved part of the dorsal rim, this surface is still slightly rugose, but not markedly thicker than the iliac blade, the thickness of which decreases from posterior towards the anterior break.

The medial side of the postacetabular process is poorly preserved, but a stout, but rather low medial brevis shelf is clearly visible and extends posteriorly some one-third of the height of the process from the ventral margin and approxmately parallel to the latter. The shelf becomes dorsoventrally wider and more marked towards the posterior margin, where it forms a notable semicircular medial expansion of the posterior surface.

Only the distal end of the pubic peduncle of the left ilium is present (PIMUZ A/III 4390; Fig. 9g). It corresponds to the pubic peduncle of the right ilium in size and shape, but is slightly more massive mediolaterally, confirming the assumption that the latter has suffered from compression.

A poorly preserved bone fragment might represent the distal end of the right pubis (PIMUZ A/III 4389). The bone is anteroposteriorly thickened laterally and becomes gradually more slender medially, indicating that the pubis apex was slightly thickened, as in many large basal sauropodomorphs.

Portions of the left femur are preserved in two parts (PIMUZ A/III 551a and b; Fig. 10). A small piece of the posteromedial side of the shaft preserves the fourth trochanter (Fig. 10a, b). The latter is developed as a large posteromedial expansion. In medial view, it is more or less symmetrical in outline, with sloping proximal and distal margins and a straight posterior margin of the central part. This is unlike the fourth trochanter in many basal sauropodomorphs, which is asymmetrical and shows a marked posterodistal angle. It is notably thick in posterior view, with approximately the medial width of the shaft gradually rising towards the apex of the trochanter, which is placed at the posteromedial edge. Thus, the lateral side of the trochanter is convex in both mediolateral and proximodistal direction. In contrast, the medial side is flat to very slightly proximodistally concave. However, a deep groove or rugose pit for the insertion of the musculus caudofemorlis longus, as it is present in many sauropods, is absent; the medial side of the femoral shaft is smooth and slightly convex anteroposteriorly.

The other part of the femur represents the distal end (Fig. 10c–g). The preserved portion is almost completely straight, with only the proximal part of the preserved shaft showing a very weak curvature. At the proximal break, the shaft is oval in outline and anteroposteriorly flattened, its transverse width (117 mm) being more than 130% of its anteroposterior depth (c. 88 mm). Distally, the bone considerably but gradually expands to a maximal distal width of 227 mm. The anterior side of the shaft and also the distal end is damaged, but there was obviously a shallow longitudinal depression in the central part of the anterior side, slightly displaced medially, which leads to a broad but very shallow extensor groove at the distal end. Lateral and medial to the groove, the anterior side curves gradually into the lateral and medial side, respectively. The posterior condyles are massive and separated by a wide, deep, U-shaped incision. A small posteriorly directed tubercle is present within this intercondylar groove towards the distal end. The intercondylar groove continues a short way proximal from the condyles onto the posterior side of the shaft, where it becomes less deep and wider. The condyles are subequal in transverse width, but the tibial condyle extends slightly further posteriorly than the crista tibiofibularis. In distal view, the posterolateral margin of the tibial condyle is rounded, whereas posteromedially, the posterior margin forms an almost right angle with the medial margin. The massive lateral condyle has a flattened posterior side that faces slightly posteromedially. In distal view, the posterolateral corner of the condyle forms a slightly sharp angle, so that the condyle overhangs a shallow longitudinal depression on the lateral side of the bone. However, in contrast to most other saurischians, the lateral condyle is not offset medially from the lateral side of the shaft, and a posterolaterally facing shelf lateral to the condyle is absent. Proximally, the flattened posteromedial surface of the condyle is offset from the shaft by a notable step.

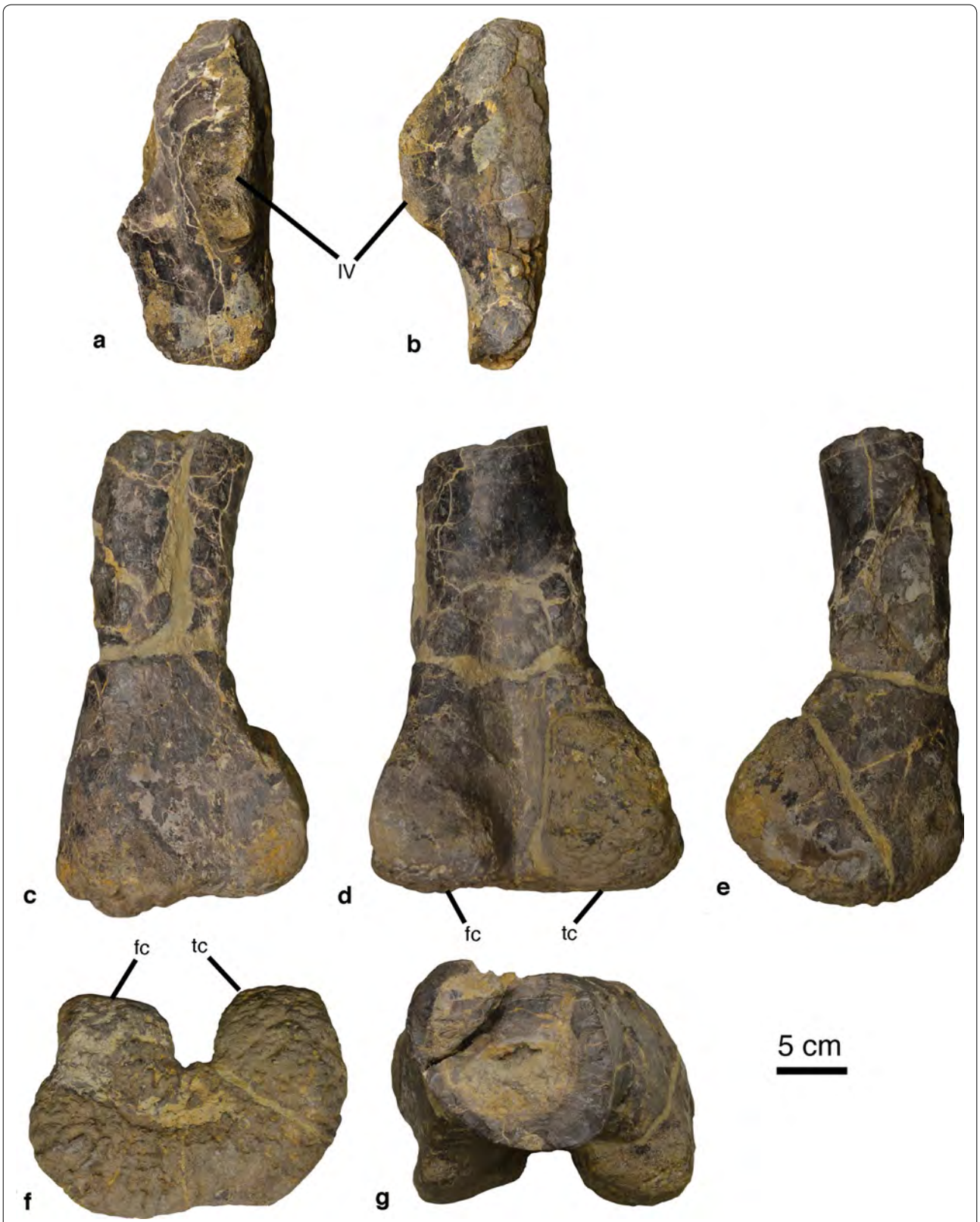

Fig. 10 Partial left femur of *Schleitheimia schutzi* n. gen., n. sp., PIMUZ A/III 551. **a**, **b** Fragment of the mid-shaft in posterior (**a**) and medial (**b**) view; **c**–**g** distal end in lateral (**c**), posterior (**d**), medial (**e**), and distal (**f**) views, and proximal view of proximal break (**g**). Abbreviations: IV, fourth trochanter; fc, fibular condyle; tc, tibial condyle. Scale bar equals 5 cm

The distal surface of the tibial condyle is gently rounded anteroposteriorly, whereas the distal surface of the crista tibiofibularis is flat. While the distal surface of the tibial condyle is continuous with the distal articular surface of the femur, that of the crista tibiofibulris is offset from the anteroposteriorly slightly convex anterior part of the distal articular surface by a shallow transverse indentation. The distal articular surface is covered by irregularly arranged pits and grooves, as in sauropods.

A small ungual (PIMUZ A/III 547; Fig. 11) is present, but it is somewhat uncertain if this element comes from the same locality or might have been found during an excavation of the "Rhaetic bonebed" at Hallau (see Peyer 1943a, b). However, its preservation is consistent with the other material from Schleitheim, whereas other bones from Hallau, including one other sauropodomorph ungual, are usually darker. Thus, we assume that this ungual also comes from the former locality and represents the same animal as the other remains.

In comparison with unguals of *Antetonitrus* (McPhee et al. 2014) and *Lessemsaurus* (Pol and Powell 2007a), this element represents the ungual of the first pedal digit, and it closely resembles the same element in these two taxa. It is dorsoventrally flattened, only little recurved and strongly asymmetrical. The proximal articular end is missing. The ventral side is triangular in outline and flattened, being only very slightly convex transversely. On one side it forms a sharp angle towards the lateral or medial side of the bone, and the edge separating the two sides is offset ventrally from the claw groove. On the other side, the ventral side much more gradually curves into the side of the ungual, and the claw groove is placed directly dorsal to this curve. The dorsal side of the ungual is broad and transversely rounded.

5.2 Tentatively referred material from the MzA Schaffhause

5.2.1 Vertebrae

Seven fragmentary to partial vertebrae from the locality Schleitheim-Santierge are present in the MzA. Three of these vertebrae represent dorsal vertebrae, one seems to be a sacral vertebra and three elements belong to the caudal series. Measurements of the elements can be found in Table 3.

MzA NAT15051 is a dorsal vertebra, possibly one of the anteriormost dorsals. Only the poorly preserved centrum and the basalmost parts of the neural arch pedicles are preserved. The centrum is short and high, its better preserved posterior articular surface being higher than the length of the centrum. The anterior end is largely missing, and the remains are poorly preserved, so that nothing can be said about the possible presence and position of a parapophysis on the centrum. In ventral view, the centrum is strongly waisted and narrow in its central part, with the ventral side forming a narrow, rounded keel. As in the dorsal vertebrae described above, a broad,

Fig. 11 Pedal ungual tentatively referred to *Schleitheimia schutzi* n. gen., n. sp., PIMUZ A/III 547. **a** lateral view; **b** dorsal view; **c** anterior view. Scale bar equals 1 cm

Table 3 Measurements of vertebral remains from Schleitheim Santierge held in the MzA, tentatively referred to *Schleitheimia*

Specimen	Centrum length	Anterior height	Anterior width	Posterior height	Posterior width	Minimal width
MzA NAT15051	90	–	75	–	–	42
MzA NAT15058	–	–	–	95	92	40
MzA NAT15049	92	110	83[a]	100	76	68
MzA NAT15047	114	100	95	90	100	59
MzA NAT15048	97	83	78	82	–	48

Measurements are in mm

[a] Indicates deformation

poorly defined depression is present on the lateral side of the centrum. Of the neural arch, only the basal part of a stout anterior centrodiapophyseal lamina is preserved. This lamina is placed at the anterior end of the centrum and steep, whereas the broken base of the less steeply inclined posterior centrodiapophyseal lamina is slightly offset from the posterior end of the centrum. As in the vertebrae described above, the neural canal is deeply incised into the dorsal side of the vertebral centrum and widens dorsally.

The other two dorsal vertebrae are too poorly preserved to yield much useful information. MzA NAT15052 seems to be generally similar to MzA NAT15051 in that the centrum is short and waisted, being narrow in its central part. MzA NAT15058, the most recently found specimen (in April 2016), seems to be a poorly preserved more posterior dorsal, with a broad, ventrally broadly rounded centrum. Both of these vertebrae share the character of a deeply incised neural canal with the dorsal vertebrae of *Schleitheimia* and MzA NAT15051.

The specimen MzA NAT15050 is a large, deformed and strongly abraded vertebral centrum of presumably the last sacral vertebra. The centrum is massive and shorter than high, with the posterior articular surface being oval, higher than wide, and only slightly concave. The attachments of the transverse process are massive and extend from the dorsal part of the centrum anteriorly over the entire base of the neural arch. The neural canal is widened in its central part, but narrows posteriorly. At about mid-length of the centrum, a narrow, deep groove incises into the dorsal surface of the centrum from the neural arch.

MzA NAT15049 is the poorly preserved centrum of an anterior caudal vertebra. The centrum is massive, shorter than high and amphicoelous, with the anterior articular surface being more deeply concave than the posterior surface, as is often the case in saurischians. The centrum is broadly rounded ventrally, without any ventral keel or groove, and the lateral sides are convex dorsoventrally and lack the lateral depression seen in the dorsal vertebrae. The massive attachment of the transverse process is placed on the posterior part of the neurocentral suture. The neural canal is narrow, but not incised into the dorsal surface of the centrum.

The specimen MzA NAT15047 (Fig. 12a–c) represents a mid-caudal vertebra and is the best preserved vertebral specimen from Schleitheim–Santierge in the collections of the MzA, preserving the entire centrum and the neural arch, but lacking transverse processes, zygapophyses and the neural spine. The centrum is massive and longer than high, with the articular surfaces being subcircular in outline. The articular surfaces are markedly amphicoelous, being considerably concave both anteriorly and posteriorly, both with a slight protuberance just above mid-height. In lateral view, the anterior articular surface is slightly angled anteroventrally, similar to the situation seen in the proximal caudals of a specimen of *Plateosaurus* from Bavaria (Wellnhofer 1993; Moser 2003). The ventral margins of the articular surfaces are flexed ventrally to form the facets for the haemapophyses. Whereas the anterior margin forms a single, undivided and only moderately developed anteroventral facet, the posterior facet is clearly subdivided into two, posteroventrally facing facets. The ventral surface of the centrum is broad and flattened, with two low edges extending from the posterior chevron facets anteriorly and defining a very shallow longitudinal depression on the ventral surface.

The neural arch extends over most of the centrum and is only slightly more displaced from the posterior rim of the centrum than from its anterior rim. Only the broken attachment of the transverse process is present; it extends from the stalk of the prezygapophysis over almost the entire length of the neural canal. The roof of the neural canal adjacent to the base of the neural spine is anteroposteriorly concave. The neural canal is oval in outline and wider than high. The transversely narrow base of the neural spine is placed more over the posterior part of the centrum, but largely broken away. Anteriorly, weakly developed ridges represent the spinoprezygapophyseal laminae and define a very shallow, anteriorly widening prespinal fossa.

The caudal vertebra MzA NAT15048 (Fig. 12d) represents a posterior mid-caudal. Its centrum is generally similar to that of MzA NAT15047, but more slender, being slightly higher than wide. In the neural arch, the transverse process is placed on the posterior end of the neurocentral suture and anteroposteriorly short, but connected to the broken stalks of the prezygapophysis by a broad, stout prezygodiapophyseal lamina, as it was most probably also present in the vertebra described above. As in the former, this lamina is slightly curved, resulting in a similar, anteroposteriorly concave depression adjacent to the base of the neural spine. The base of the broken neural spine is placed slightly more posteriorly than in the vertebra described above, and there are no spinoprezygapophyseal laminae, nor a prespinal fossa.

5.2.2 Humerus

The right humerus, MzA NAT15046 is almost complete, but misses the proximal end and the distal condyles are damaged, especially the lateral condyle (Fig. 12e, f). As preserved, the humerus is 380 mm long, and, based on the position of the distal end of the deltopectoral crest, which ends 240 mm above the distal end, its total length can be estimated to be between 450 and 500 mm. As preserved the distal end is c. 145 mm wide, with

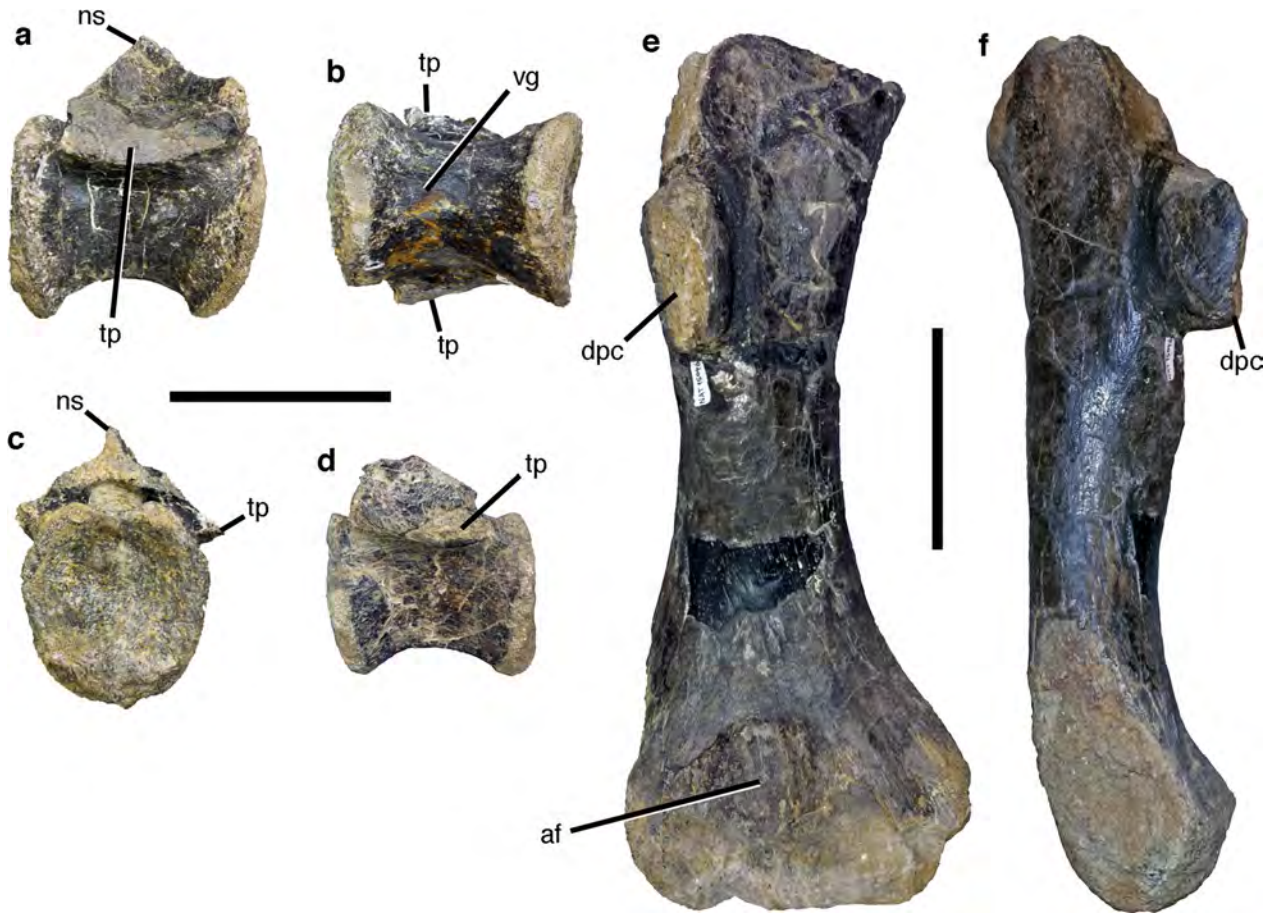

Fig. 12 Material from the locality Schleitheim-Santierge in the MzA, tentatively referred to *Schleitheimia schutzi* n. gen., n. sp. **a-c** Mid-caudal vertebra, MzA NAT15047, in right lateral (**a**), ventral (**b**) and posterior (**c**) view; **d** posterior mid-caudal vertebra, MzA NAT15048, in left lateral view; **e**, **f** partial right humerus, MzA NAT15046, in anterior (**e**) and lateral (**f**) view. af, anterior fossa; dpc, deltopectoral crest; ns, neural spine; tp, transverse process; vg, ventral groove. Scale bars equal 10 cm

30-40 mm missing, and the bone is thus of closely matching size as the distal end of the left humerus referred to *Schleitheimia* and described above.

The shaft of the humerus is stout, and whereas the distal half is more or less straight in medial view, the proximal end curves posteriorly, so that the proximal half of the bone is posteriorly concave. The deltopectoral crest is well-developed, placed on the anterolateral edge of the proximal shaft and directed anteriorly, but its proximal parts and its distal extremity are broken off. Distally, the crest seems to be sharply offset from the shaft at an approximately right angle, with a marked, flat area anterolaterally just distal to it. The minimal width of the shaft, just distal to this area and c. 200 mm from the distal end, is 68 mm; at this level, the shaft is c. 62 mm deep. The minimal depth of c. 48 mm is reached just at the base of the distal transverse expansion of the bone, some 130 mm proximal to the distal end. The cross-section of the shaft distal to the deltopectoral crest is ovoid, with a broader, almost laterally flattened lateral side, and a pointed medial side. Distally, the bone is considerably expanded transversely and has stout medial and lateral condyles, although the lateral condyle is largely broken off. As in the humerus of *Schleitheimia*, the posterior side shows a large, shallow, triangular depression, whereas there is a smaller, but deeper and well-defined fossa between the distal condyles on the anterior side of the bone. This latter fossa has well-defined medial and proximomedial margins, but fades more gradually laterally. Distally it becomes more shallow towards a narrow, but well-defined intercondylar groove.

5.3 Other sauropodomorph material from Canton Schaffhause

5.3.1 Sauropodomorph astragalus of Schutz' excavation at Santierge

The material collected in situ by Schutz includes an isolated right astragalus (PIMUZ A/III 4391; Fig. 13), which closely matches the astragalus of *Plateosaurus* specimen SMNS 13200 in size (Huene 1926), and is thus too small to belong to the same individual as the type and referred material of *Schleitheimia*, in which comparable measurements of the ilium and femur, for example, are approximately 150% of those of this specimen of *Plateosaurus*.

The astragalus is considerably broader transversely (c. 15 cm) than deep anteroposteriorly (max. c. 7.8 cm). The body of the astragalus was placed entirely below the tibia, as indicated by its proximal articular surface, and is c. 5 cm thick proximodistally. In proximal view, the anterior margin is very gently concave, almost straight, whereas the posterior margin is convex and flexes anteriorly towards its medial end. Thus, whereas the lateral margin is straight, the medial margin is strongly convex posteriorly; its anteromedial edge is damaged. The ascending process is placed anteriorly on the lateral two-thirds of the astragalar body and gradually ascends laterally to a moderate height of maximally c. 2 cm. The posterior margin of the anteroposteriorly broad ascending process separates an anterior facet from the medially flat to slightly concave proximal articular surface for the tibia. With increasing height of the ascendings process, this facet faces gradually more anteriorly than proximally towards the lateral side, until it forms an anteroproximally inclined facet that stands at an angle of 50°–60° towards the main articular facet for the tibia. The articular surface for the tibia posterior to the ascending process is slightly concave anteroposteriorly, with only a slightly raised posteromedial margin. The proximal edge of the lateral rim of the astragalus slightly overhangs the facet for the calcaneum so that the latter is slightly concave proximodistally. The distal articular surface is anteroposteriorly convex, though with a notable depression on the anterodistal surface. There are several large pits or foramina on the anterodistal surface, most notably directly below the maximal expansion of the ascending process.

This astragalus very closely resembles the astragalus of *Plateosaurus* (SMNS 13200) in size and shape. Especially the subequal anteroposterior breadth throughout its mediolateral width argues for a referral to this taxon, as the medial side is anteroposteriorly expanded in many other taxa (e.g. Langer et al. 2003; Martínez

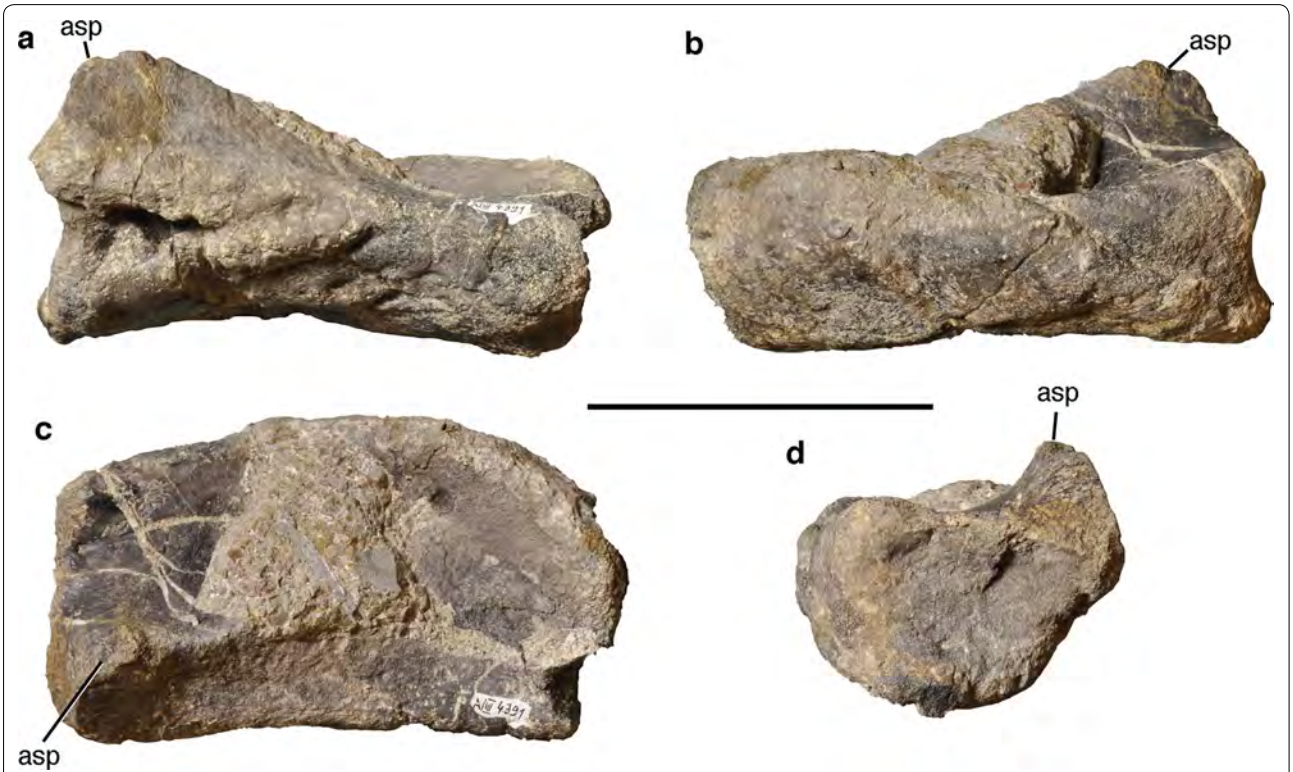

Fig. 13 Right astragalus of *Plateosaurus* sp. from Schleitheim-Santierge, PIMUZ A/III 4391. **a** Anterior view; **b** posterior view; **c** proximal view; **d** lateral view. asp, ascending process. Scale bar equals 10 cm

2009; Apaldetti et al. 2013). Thus, we tentatively identify this astragalus as *Plateosaurus* sp.

5.3.2 Material resulting from new excavation at Santierge

The excavation at Santierge led by one of us (HF) in 2016 resulted in the recovery of numerous vertebrate remains, including remains of six dorsal vertebrae, four caudal vertebrae, a dorsal rib, a gastral rib, and a metacarpal of sauropodomorphs. Although it cannot be excluded that at least some of these elements might represent *Schleitheimia* and could even be derived from the same individual as the holotype (e.g. the metacarpal, which would fit in size with the remains referred to that taxon above), the remains represent animals of different sizes, and thus any referral would be tentative at best. This material can currently only be regarded as Sauropodomorpha indet. and is described here briefly. Measurements of the vertebrae recovred can be found in Table 4.

Dorsal vertebrae Whereas two dorsal vertebrae (MzA NAT15059 and 15104) are only represented by their neural arches and one (MzA NAT15058) by a partial centrum, the other elements (MzA NAT15090, 15095 and 15100) preserve the centrum and at least parts of the neural arch and spine. However, many of these elements are also moderately to strongly deformed, making detailed descriptions difficult.

MzA NAT15104 is a relatively small, strongly anteroposteriorly compressed anterior dorsal neural arch. The relatively short transverse processes are directed laterodorsally and supported ventrally by a stout posterior centrodiapophyseal lamina, whereas the anterior centrodiapophyseal lamina is only indicated by a slight swelling at the anterior rim of the transverse process. Pre- and postzygodiapophyseal lamina are well developed, as is the centroprezygapophyseal lamina. The neural spine is anteroposteriorly short, slightly lower than the height of the neural arch and notably expanded transversely dorsally. The spinoprezygapophyseal laminae are very short, almost absent, whereas the spinopostzygapophyseal laminae strongly diverge towards the postzygapophyses. An incipient hyposphene is present between the postzygapophyses.

MzA NAT15059 is a poorly preserved partial anterior dorsal neural arch (Fig. 14a–c) that was found on the surface close to the excavated area. The neural spine, distal ends of the transverse processes and the posterior end of the neural arch are missing. The presence of a large, high oval parapophysis on the anteroventral end of the neural arch identifies this element as an anterior dorsal. The prezygapophysis is large, approximately as wide as long and flexed ventrally medially to form a hypantrum. Posteriorly, the incision between the zygapophyses widens to form a rounded dorsal opening onto the neural canal in front of the prespinal fossa, as in the theropod *Condorraptor* (Rauhut 2005). The lateral neural arch lamination is well developed, with an almost vertical posterior centrodiapophyseal lamina, a robust prezygodiapophyseal lamina and an almost horizontal paradiapophyseal lamina, which is almost parallel to the prezgodiapophyseal lamina and meets the posterior centrodiapophyseal lamina below the junction of the transverse process and the prezygodiapophyseal lamina. The laminae define deep prezygodiapophyseal and centrodiapophyseal fossae. The neural spine was obviously anteroposteriorly short and slightly thickened transversely.

The specimen MzA NAT15090 is a strongly deformed middle dorsal vertebra (Fig. 14d, e). The vertebral body is amphi- to platycoelous, elongate, higher than wide and strongly constricted. The ventral side is rounded and a shallow depression is present on the lateral side. The neural arch reaches approximately two-thirds of the height of the centrum. The parapophysis is placed on the anterior end of the neural arch; it is high oval in outline and relatively large. The neural arch lamination is similar to that seen in MzA NAT15059, with a vertical pcdl that does not reach the centrum, and parallel prdl and ppdl. A stout podl connects the transverse process with the lateral margin of the postzygapophysis. The prezygapophysis

Table 4 Measurements of vertebrae recovered in a recent excavation at Schleitheim Santierge

Specimen	Centrum length	Anterior height	Anterior width	Posterior height	Posterior width	Minimal width
MzA NAT15090	106	76	63	85	75	14[a]
MzA NAT15095	129	105	–	100	63[a]	19[a]
MzA NAT15100	80	119	95[a]	117	83[a]	42[a]
MzA NAT15091	86	118	86	109	75	48
MzA NAT15098	92	78	66	75	63	46
MzA NAT15089	84	54	59	50	54	45
MzA NAT15097	60	33	38	38	38	29

Measurements are in mm

[a] Indicates deformation

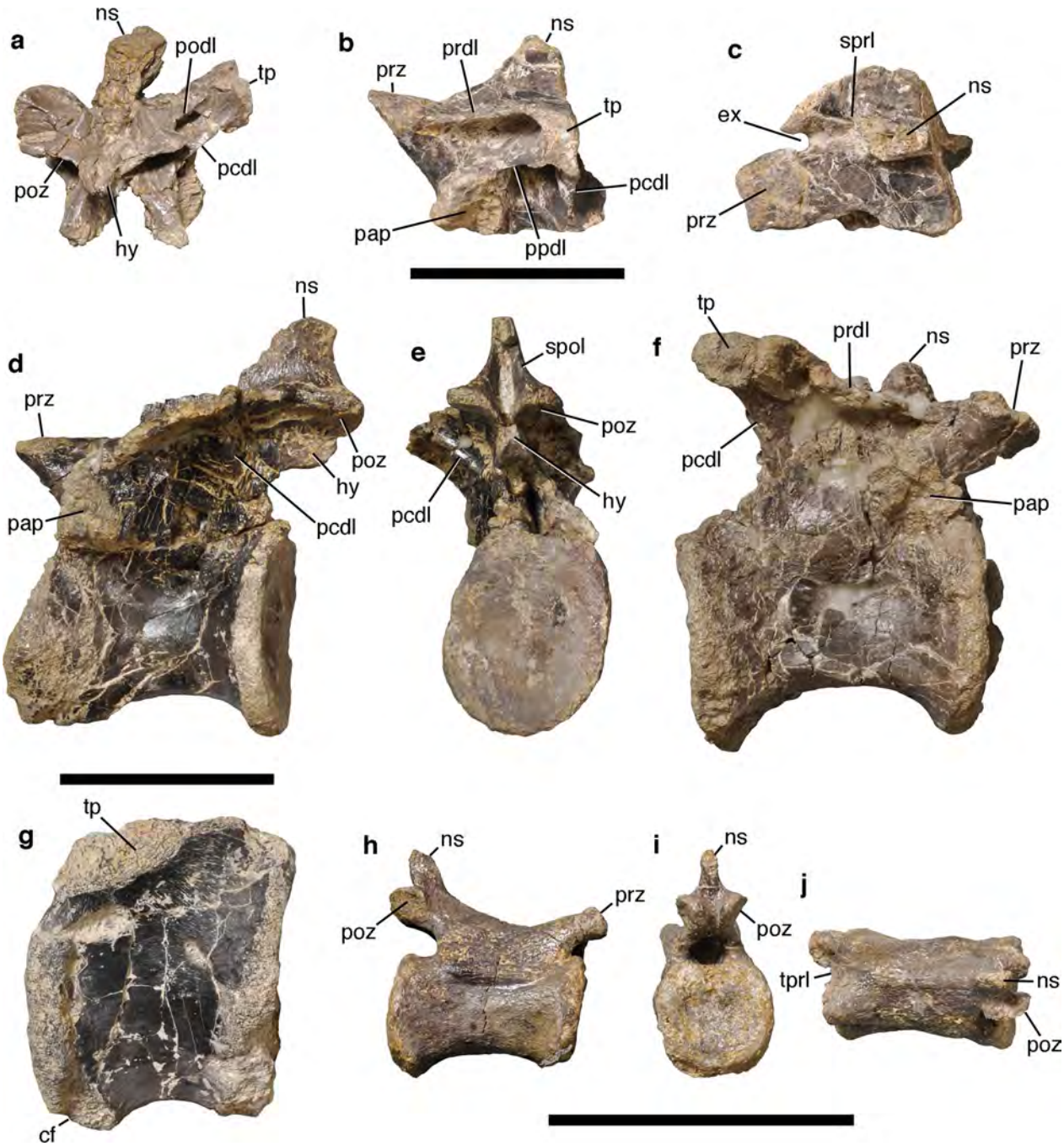

Fig. 14 Sauropodomorph vertebrae resulting from the recent excavation at Schleitheim-Santierge. **a**–**c** Anterior dorsal neural arch, MzA NAT15059, in posterior (**a**), left lateral (**b**) and dorsal (**c**) view; **d**, **e** mid-dorsal vertebra, MzA NAT15090, in left lateral (**d**) and posterior (**e**) view; **f** mid-dorsal vertebra, MzA NAT15095, in right lateral view; **g** anterior caudal vertebral centrum, MzA NAT15091, in right lateral view; **h**–**j** distal caudal vertebra, MzA NAT15097, in right lateral (**h**), posterior (**i**) and dorsal (**j**) view. cf, chevron facet; ex, prespinal expansion of intraprezygapophyseal slit; hy, hyposphene; ns, neural spine; pap, parapophysis; pcdl, posterior centrodiapophyseal lamina; podl, postzygodiapophyseal lamina; poz, postzygapophysis; ppdl, paradiapophyseal lamina; prdl, prezygodiapophyseal lamina; prz, prezygapophysis; spol, spinopostzygapophyseal lamina; sprl, spinoprezygapophyseal lamina; tp, transverse process; tprl, intraprezygapophyseal lamina. Scale bars equal 10 cm

is relatively smaller than in MzA NAT15059, only very slightly medially inclined and forms a well-developed hypantrum medially; as in the specimen described above, the interprezygapophyseal slit widens slightly in front of the neural spine. The postzygapophyses overhang the centrum posteriorly. They are narrowly placed, elongate oval in outline and almost horizontal. A well-developed, ventrally widening hyposphene is present medioventral to them. The neural spine is broken off; it extended over the posterior two-thirds of the neural arch, was almost as long as the centrum, and plate-like. The sprl are short and do not reach the rim of the prezygapophyses, whereas the also short, but stout spol define a narrow, but deep postspinal fossa.

The specimen MzA NAT15095 is a strongly elongated, considerably compressed and thus poorly preserved dorsal vertebra (Fig. 14f). The vertebral centrum is considerably longer (13.5 cm) than high (9.8 cm anteriorly) and slightly flattened ventrally. The parapophysis is placed on the anteroventral end of the neural arch. The prezygapophysis is elongate oval in shape and overhangs the centrum anteriorly. It is connected with the transverse process by a slender prezygodiapophyseal lamina, but the paraprezygapophyseal lamina is only indicated by a broad swelling, and nothing can be said about the possible presence of a paradiapophyseal lamina. The transverse process is placed over the posterior half of the centrum and is directed posterolaterally and slightly dorsally. It is supported ventrally by a stout posterior centrodiapophyseal lamina.

Specimen MzA NAT15100 is an also strongly compressed, large dorsal vertebra with partially preserved neural arch. The vertebral centrum was relatively short and high and strongly constricted between the articular ends. The neural canal is slightly incised into the centrum. The neural arch is too poorly preserved to describe any details. Likewise, specimen MzA NAT15058 is a poorly preserved posterior half of a strongly constricted dorsal vertebra, but does not present much useful information. Interestingly, though, the centrum seems to be hollow ventrally.

Caudal vertebrae Caudal vertebrae include centra (with parts of the neural arch preserved) of an anterior caudal (MzA NAT15091; Fig. 14g) and two mid-caudals (MzA NAT15089 and 15098), as well as a rather well-preserved distal caudal vertebra (MzA NAT15097; Fig. 14h–j).

The most anterior caudal vertebra preserved, MzA NAT15091, has a massive centrum that is slightly higher than long and has high oval articular surfaces (Fig. 14g). The ventral surface is broad and rounded, without a ventral groove, and offset from the lateral sides by rounded ridges. The broken remnant of a stout transverse process is present on the posterior half of the base of the neural arch. The neural canal is narrow and has a level ventral margin, which is not incised into the centrum.

Specimen MzA NAT15098 represents an anterior mid-caudal that seems to be generally similar to the previous element, but is relatively more elongate and has well-developed chevron facets posteriorly. No transverse process is visible, but the dorsal part of the centrum is considerably eroded. Likewise, MzA NAT15089 is an even more elongate caudal vertebra with a centrum that is longer dorsally than ventrally and has a notable lateral swelling at the dorsal margin of the centrum, but the presence of a transverse process is uncertain.

In contrast, the distal caudal vertebra MzA NAT15097 is rather well preserved (Fig. 14h–j). The centrum is elongate, but rather massive, being only slightly constricted and broadly rounded ventrally. Well-developed chevron facets are present posteriorly. A lateral swelling is present at the base of the neural arch, being offset from the lateral side of the centrum by a narrow and shallow longitudinal groove. The neural arch is low and the neural canal is small, being broader than high anteriorly and round posteriorly. The prezygapophyses are broken, but they overhung the centrum anteriorly and are medially connected by a broad intraprezygapophyseal lamina. The postzygapophyses are developed as oval, lateroventrally facing articular facets at the base of the posterior end of the neural spine and overhang the centrum posteriorly for half of their length. The neural spine is anteroposteriorly short and placed over the posteriormost end of the neural arch. It is slightly inclined posteriorly and seems to have been low, although the distal end is missing.

Ribs and chevrons Specimen MzA NAT15105 is a large, probably anterior dorsal rib. The proximal end has a well offset tuberculum that is not connected to the capitulum by a bony webbing, as is the case in some basal sauropods (e.g. Rauhut 2003a). The shaft is only slightly flexed and somewhat transversely flattened, but without the plank-like appearance of dorsal ribs in sauropods. A weakly developed longitudinal anterolateral groove is present.

A slender, rod-like bone, MzA NAT15106, is obviously a gastral rib (Fig. 15a). Although gastralia are rarely reported from sauropodomorphs, they are present in both basal forms (e.g. Fechner and Gößling 2014) as well as sauropods (see e.g. Tschopp and Mateus 2013). The preserved element is 34.5 cm long, but maximally only 1.2 cm wide, and thus very slender, as it is usual for gastralia. The element is slightly bowed and tapers towards both ends. A longitudinal groove is present in one side of the element, probably for the contact with the adjacent medial or lateral element, but extends for less than half of its length.

A large anterior caudal chevron, MzA NAT15081 (Fig. 15b), has a dorsally bridged, triangular hemal

Fig. 15 Sauropodomorph material resulting from the recent excavation at Schleitheim-Santierge. **a** gastral rib, MzA NAT15106, in dorsal or ventral view; **b** chevron, MzA NAT15081, in posterior view; **c**–**e** right metacarpal I, MzA NAT15082, in dorsal (**c**), distal (**d**) and medial (**e**) view. lg, longitudinal groove. Scale bars equal 10 cm

canal and a simple, transversely compressed and distally slightly anteroposteriorly expanded shaft. The proximal facets for the contact with the vertebrae are gently convex anteroposteriorly, but not clearly subdivided. The total length of the element is ca. 22 cm.

Metacarpal A poorly preserved right metacarpal I of a large basal sauropodomorph, MzA NAT15082 (Fig. 15c–e), is present in the newly collected material. The element is strongly compressed and misses the proximal end. However, the proximalmost part of the lateral side expands notably and abruptly, indicating that not much is missing here. Regardless of the compression, the bone was obviously considerably broader transversely than high dorsoventrally, and it was probably only slightly longer proximodistally than broad; as preserved, the bone is 7.3 cm long (missing an estimated 1–1.5 cm) and 6.5 cm wide distally. Two well-developed distal condyles are present and separated by a broad groove. As is usual in saurischian first metacarpals, the condyles are asymmetrical, with the lateral condyle extending notably further distally than the medial condyle. Whereas the former tapers distally, the latter is broad and rounded. A weakly developed extensor groove is present on the dorsal side. The medial condyle flares medially on the ventral side, thus bordering a large, but shallow collateral ligament pit on the medial side. The medial extremity of this medial expansion is eroded.

5.3.3 Dorsal vertebra from Hallau–Bratelen

A rather well-preserved, though slightly deformed dorsal vertebral centrum, MzA NAT 15075, was found in Hallau-Bratelen (Fig. 16). The centrum is massive, but strongly constricted, with a broad, rounded ventral surface. As in the vertebrae of *Schleitheimia*, large, but shallow depressions are present on the lateral sides of the centrum. Only small parts of the neural arch, including a part of the left posterior centrodiapophysial lamina, are preserved. The neural arch was obviously narrow and moderately incised into the centrum. Although the general characteristics of this vertebra are consistent with those seen in the vertebrae of *Schleitheimia*, the element is too incomplete to refer it to any taxon beyond Sauropodomorpha indet.

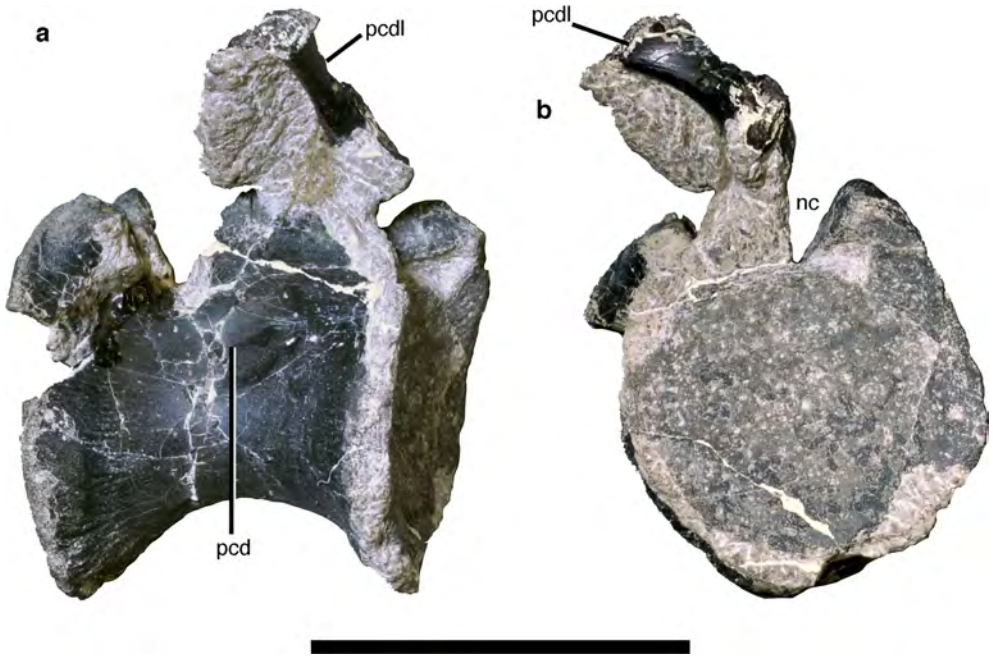

Fig. 16 Sauropodomorph dorsal vertebra from Hallau-Bratelen, MzA NAT 15075. **a** Left lateral view; **b** posterior view. nc, neural canal; pcd, pleurocentral depression; pcdl, posterior centrodiapophyseal lamina. Scale bar equals 10 cm

5.3.4 Material from Hallau-Schwärzibuck

Scapula The left scapula MzA NAT15067 (Fig. 17a, b) from Hallau-Schwärzibuck misses the distal end and large parts of the acromion process. The bone is large and robust, being considerably curved in the preserved, proximal portion. As preserved, the bone is c. 500 mm long, and was originally probably not longer than 700 mm. The minimal height of the shaft is c. 105 mm, c. 240 mm distal to the margin of the glenoid; distal to this point, the shaft expands again, most notably on its anterodorsal border. Proximally, the shaft expands towards the acromion process, which was high and well-developed, so that the anterodorsal margin of the shaft is concave in outline. The posteroventral margin of the shaft is straight to very slightly convex and shows a marked, slightly rugose convexity below the level of the base of the acromion process. The glenoid region expands posteroventrally from the shaft, though less than the acromion process. The glenoid facet is large, semioval in outline and strongly concave transversely and anteroposteriorly, although this might be slightly exaggerated by deformation. A supraglenoid fossa was obviously present on the acromion process and is bordered by a sharp edge posterodorsally in its dorsal part.

Femur The distal end of a large left femur from Hallau-Schwärzibuck, MzA NAT15065 (Fig. 17c, d), is considerably deformed, most notably compressed anteroposteriorly. As preserved, it is c. 220 mm wide mediolaterally and maximally 115 mm deep anteroposteriorly at the lateral condyle. Both distal condyles are well developed, the tibial condyle being wider and more massive than the fibular condyle. The fibular condyle is triangular in distal outline, with a flattened posteromedial side. Both condyles are separated by a wide, subrectangular intercondylar groove. The fibular condyle seems to be offset from the lateral margin of the bone by a wide, rounded shelf, in contrast to the condition in *Schleitheimia*, where such a shelf is apomorphically absent. However, it cannot be completely ruled out that the shelf in this specimen might have at least partially been exaggerated by distortion. On the distal surface, the distal articular surface of the fibular condyle is separated from the strongly convex articular surface on the distal end of the lateral part of the femur by a narrow, oblique groove. Anteriorly, a shallow depression seems to be present on the distal end of the femur, but a deep anterior intercondylar groove is absent.

Pedal phalanges Two pedal phalanges, MzA NAT15068 and NAT15069, were found in the same locality (Fig. 17e–h). Both elements are stout and robust, but whereas MzA NAT15069 is longer proximodistally (73 mm) than wide mediolaterally (61 mm) proximally, MzA NAT15068 is approximately as wide as long (67 mm). The proximal articular surface is broad, semioval in outline and both dorsoventrally and transversely concave in both elements, indicating that they might

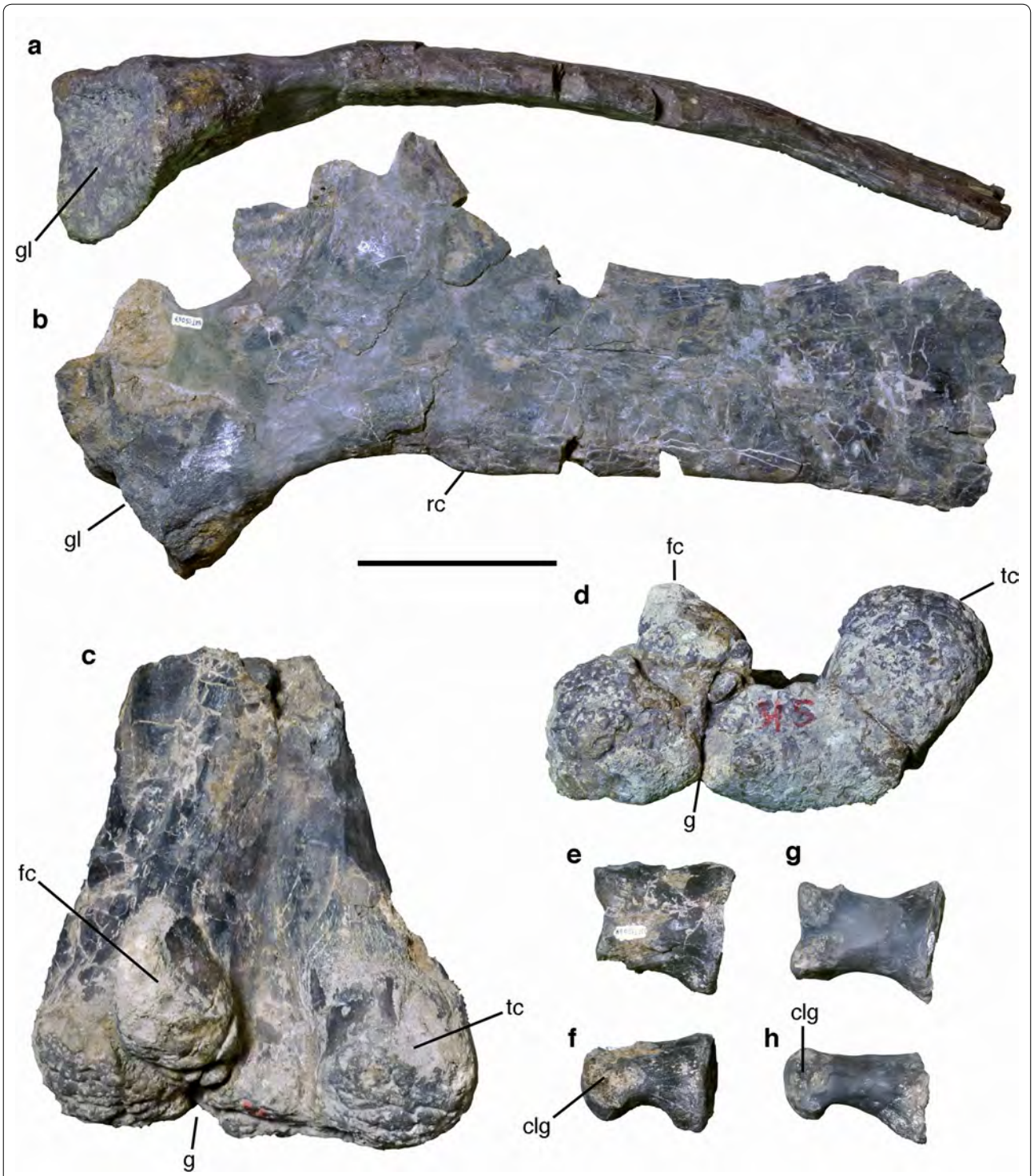

Fig. 17 Sauropodomorph material from Hallau-Schwärzibuck. **a**, **b** Left scapula, MzA NAT15067, in ventral (**a**) and lateral (**b**) view; **c, d** distal end of left femur, MzA NAT15065, in posterior (**c**) and distal (**d**) view; **e**, **f** pedal phalanx, MzA NAT15068, in dorsal (**e**) and lateral (**f**) view; **g**, **h** pedal phalanx, MzA NAT15069, in dorsal (**e**) and lateral (**f**) view. clg, collateral ligament groove; fc, fibular condyle; g, groove; gl, glenoid; rc, rugose convexity; tc, tibial condyle. Scale bar equals 10 cm

represent first phalanges that directly articulated with their respective metatarsal. The distal end is gynglimoidal, with broadly separated condyles and well developed collateral ligament pits.

Identification of material from Hallau-Schwärzibuck As there is no detailed information about the possible association of these remains, it cannot be established if all of these elements might represent the same taxon or even the same individual. However, all of the remains are of fitting size and apparently represent a large, robustly built basal sauropodomorph. The scapula is considerably more robust than scapulae of *Plateosaurus* (e.g. Huene 1926) and also differs from this taxon in the presence of the conspicuous ventral convexity in the shaft below the base of the acromion process. On the other hand, the distal femur differs markedly from the similarly sized femur of *Schleitheimia* in that the crista tibiofibularis is notably more slender than the medial condyle, has a more posteriorly pointed outline in distal view, and is markedly offset from the lateral margin of the distal femoral shaft. Thus, under the assumption that all of this material from Hallau-Schwärzibuck represents the same taxon, a referral to both *Plateosaurus* and *Schleitheimia* seems unlikely. These remains thus most probably indicate the presence of a third, large and robustly built sauropodomorph in the Late Triassic of Schaffhausen. As there is no overlap in material with the also large and robust *Gresslyosaurus ingens* from the Late Triassic (Norian) of Niederschönthal, close to Basel (see Huene 1907-8, 1932; Galton 1986), it cannot be said whether this material might represent the latter taxon.

6 Discussion

6.1 Comparison of *Schleitheimia* with other basal sauropodomorphs

As noted in the introduction, Galton (1986) referred all the material from Canton Schaffhausen to the genus *Plateosaurus*. However, the material from Schleitheim of the excavation of Schutz shows numerous differences from that genus and other sauropodomorphs for which comparable material is known. The posterior cervical vertebra is notably short, with a length/anterior height ratio of approximately 1.3. This is considerably shorter than in most sauropodomorphs. The same ratio is approximately 1.6 in the shortest posterior cervical of *Plateosaurus* (Huene 1926) and a similar ratio is present in a posterior cervical of *Mussaurus* (Otero and Pol 2013). In massospondylids, the cervical vertebrae are even more elongated, and posterior cervicals are typically more than twice as long as high (Martínez 2009; Apaldetti et al. 2013; Barrett et al. 2019). Even in the large and massive *Lessemsaurus*, the probably last cervical vertebral centrum has a length/height ratio of c. 1.5 (Pol and Powell 2007a). Sauropod cervicals tend to be even more elongate. The only other non-sauropodan sauropodomorph which seems to have similarly short posterior cervicals is *Lamplughsaura* (Kutty et al. 2007).

Another noteworthy feature of *Schleitheimia* is the morphology of the anterior dorsal vertebra. As noted in the description, the centrum is strongly constricted, with the constriction being asymmetrical in ventral view, the narrowest portion being placed at approximately one-third of centrum length. This differs from the more symmetrical constriction in *Plateosaurus* (MB Skelett XXV; Huene 1926; Moser 2003), other non-sauropodiform sauropodomorphs (e.g. *Saturnalia*: MCP 3844-PV; *Plateosauravus*: SAM-PK 3342; *Unaysaurus*: UFSM 11069; *Jingshanosaurus*: Zhang and Yang 1994; *Adeopapposaurus*: PVSJ 610), and basal sauropodiforms (e.g. *Xingxiulong*: Wang et al. 2017; in which the narrowest portion of the vertebra is placed more or less at mid-length of the element. A similar condition as in *Schleitheimia* is, however, present in *Lessemsaurus* (Pol and Powell 2007b), the possibly derived sauropodiform *Lamplughasaura* (Kutty et al. 2007) and basal sauropods (e.g. *Tazoudasaurus*: Allain and Aquesbi 2008; *Patagosaurus*: PVL 4170). Thus, the asymmetrical constriction of the anterior dorsal might be another character supporting a derived sauropodiform placement of *Schleitheimia*. A further unusual character of the anterior dorsal, the marked lateroventral ridges on the posterior half of the centrum, have not been described or observed by us in any other non-sauropodan sauropodomorph and might thus also represent an apomorphic character of the new taxon.

A further noteworthy character of the vertebrae of *Schleitheimia* is the shape of the neural canal, which is deeply incised into the dorsal surface of the vertebral centra in its middle course, but becomes shallower towards the anterior and posterior exits of the canal. Unfortunately, the absence or presence of this character is often difficult to evaluate in specimens that are preserved with their neural arches attached, and it is even more rarely described. However, such a deep incision of the neural arch is absent in basal sauropodomorphs such as *Saturnalia* (MCP 3844-PV) and *Plateosaurus* (SMNS and BSPG, numerous specimens). A similar situation to that seen has been described in an anterior caudal of the basal sauropod *Vulcanodon* (Cooper 1984) and the dorsals of the basal sauropod *Amygdalodon* (Rauhut 2003a), and it might also be present in the lessemsaurid *Antetonitrus* (McPhee et al. 2014). Thus, this character might be another feature of sauropodiforms or a subclade thereof, but more data on its distribution is needed. It might be noted, though, that the floor of the neural canal is flat in the dorsal vertebral centra of the basal sauropod *Volkheimeria* (PVL 4077).

A further character shared between *Schleitheimia* and *Lessemsaurus* is the low length/height ratio of the posterior dorsal vertebrae. This ratio is approximately 0.8 in *Schleitheimia* and 0.7 in *Lessemsaurus* (Pol and Powell 2007b), whereas it is around one in *Plateosaurus* (Huene 1926) and even more in taxa such as *Massospondylus* (Barrett et al. 2019) and *Jingchanosaurus* (Zhang and Yang 1994). The basal sauropod *Tazoudasaurus* also has relatively short posterior dorsals, with a length/height ratio of c. 0.74 (Allain and Aquesbi 2008).

The reconstructed ilium of *Schleitheimia* is superficially rather similar to that of other basal sauropodomorphs (Fig. 18). However, one should keep in mind that this partially depends on the reconstruction of the missing portions, and several differences with most other basal sauropodomorphs are found in detailed morphology. One of these characters concerns the articular surface of the ischial peduncle of the ilium. In most basal sauropodomorphs, such as *Ruehleia* (MB.R. 4737, 4718.103), *Plateosaurus* (SMNS 91269), *Adeopapposaurus* (PVSJ 610), or *Lessemsaurus* (Pol and Powell 2007b), the distal end of the peducle is flattened or bluntly convex. In *Schleitheimia* and basal sauropods, such as *Volkheimeria* (PVL 4077), as well as a few non-sauropodan sauropodomorphs, including *Leonerasaurus* (Pol et al. 2011), the peduncle is semicircular in lateral view and transversely widened.

Another character concerns the development of the medial brevis shelf. In basal sauropodomorphs, including *Rhueleia* (MB.R. 4737) and *Plateosaurus* (SMNS 91269), a distinct brevis fossa is present, bound medially by a medial brevis shelf that ascends steeply from the posteromedial side of the ischial peduncle to the posterior end of the postacetabular blade. The third sacral rib attaches to the medial brevis shelf from medially. In other sauropodomorphs, including sauropods, a distinct brevis fossa is absent, and the medial brevis shelf is developed as a medial ridge for the attachment of the sacral rib (the sacricostal ridge of Barrett et al. 2019). In *Schleitheimia*, this ridge is prominent, rounded in cross-section and expands posteriorly into a semicircular expansion, a morphology that seems to be unique to this taxon (Fig. 19).

Finally, the distal femur of *Schleitheimia* is notably robust, with especially the lateral condyle (the crista tibiofibularis) being very wide transversely and massive anteroposteriorly (Fig. 20). One unusual character is the lack of a posteriorly facing shelf lateral to the crista tibiofibularis. A marked lateral expansion of the main femoral body, leading to the formation of such a shelf is present in most saurischians, but only a small, broad, rounded expansion is present in the femur of *Schleitheimia* (Fig. 20d). Although a similar condition is present in some basal saurischians (e.g. *Eoraptor*; Fig. 20a), and a few other basal sauropodomorphs (e.g.

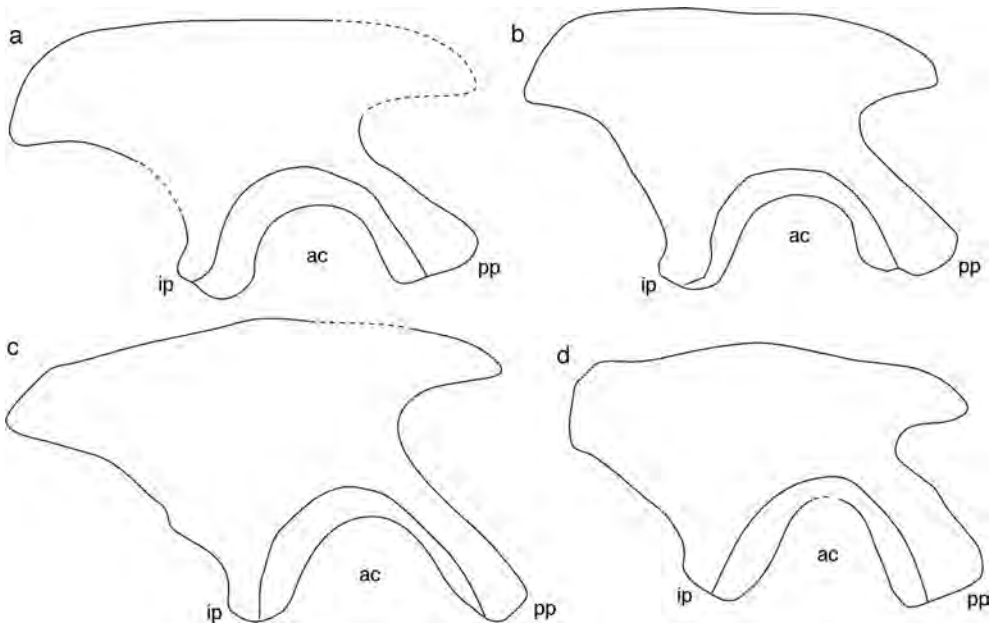

Fig. 18 Comparison of outlines of the right ilia of several non-sauropodan sauropodomorphs. **a** Reconstruction of the ilium of *Schleitheimia*. **b** *Plateosaurus* (based on Galton and Upchurch 2004). **c** *Adeopapposaurus* (left ilium reversed; based on Martínez 2009). **d** *Lessemsaurus* (based on Pol and Powell 2007b). ac, acetabulum; ip, ischial peduncle; pp, pubic peduncle. Not to scale; drawn to the same length over the pubic and ischial peduncles

Fig. 19 Stereophotograph of the medial side of the postacetabular process of the ilium of *Schleitheimia*, PIMUZ A/III 550, showing the unusual development of the medial brevis shelf (mbs). Posterior is to the top

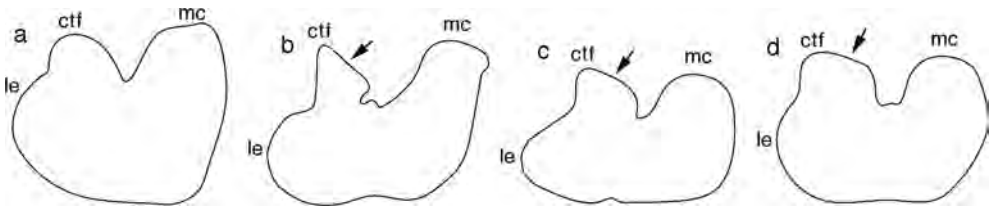

Fig. 20 Comparison of the distal outlines of the left femora of a basal saurischian (**a**) and several non-sauropodan sauropodomorphs (**b**–**d**). **a** *Eoraptor* (right femur reversed; based on Sereno et al. 2013). **b** *Plateosaurus* (right femur reversed; based on Huene 1926). **c** *Coloradisaurus* (based on Apaldetti et al. 2013). **d** *Schleitheimia*. Abbreviations: ctf, crista tibiofibularis; le, lateral expansion, forming a posteriorly facing shelf lateral to the crista tibiofibularis on the distal femur in *Plateosaurus* and *Coloradisaurus*; mc, medial condyle. Arrows point to the flattened posteromedial surface of the crista tibiofibularis in the sauropodomorph taxa. Not to scale; drawn to the same distal width

Ruehleia; MB.R. 4718.99), the vast majority of basal sauropodomorphs and also sauropods (e.g. *Isanosaurus*. Buffetaut et al. 2000; *Volkheimeria*: PVL 4077; *Patagosaurus*: PVL 4170) show this marked expansion and the associated shelf, so that the absence of this feature can be seen as a local autapomorphy of *Schleitheimia*.

6.2 Phylogenetic position of *Schleitheimia*

The phylogenetic analysis resulted in the recovery of 7632 equally parsimonious trees with a length of 1551 steps (CI 0.293, RI 0.655, RC 0.192). The strict consensus tree (Additional file 1: Figure S1) is reasonably well resolved, and in general accordance with the results of McPhee et al. (2015), Otero et al. (2015), and Apaldetti et al. (2018), although with several differences in the placements of individual taxa. A polytomy at the basis of Sauropodomorpha includes the genera *Chromogisaurus*, *Pampadromeus*, *Panphagia*, and *Saturnalia*. Apart from a number of intercalated single taxa, three clades are recognized in basal, non-sauropodan sauropodomorphs: the Plateosauridae (including *Unaysaurus*, *Plateosaurus gracilis*, and *Plateosaurus engelhardti*), a clade comprising *Eucnemesaurus* and *Riojasaurus*, and the Massospondylidae. Interestingly, the latter clade does not only include the genera usually placed in Massospondylidae (*Massospondylus*, *Leyesaurus*, *Adeopapposaurus*, *Lufengosaurus*, *Glacialisaurus* and *Coloradisaurus*; McPhee et al. 2015; Otero et al. 2015; McPhee and Choiniere 2018), but also *Jingshanosaurus*, *Seitaad*, and *Yunnanosaurus*, which form a distinct subclade within massospondylids. Above this clade, *Xingxiulong* was found as the most basal sauropodiform, followed by two large polytomies. The first of these polytomies includes the genera *Aardonyx*, *Anchisaurus*, *Leonerasaurus*, *Meroktenos*, *Mussaurus*, and *Sefapanosaurus*, whereas the second includes *Antetonitrus*, *Blikanasaurus*, *Camelotia*, *Gongxianosaurus*, *Ingentia*, *Lessemsaurus*, *Melanorosaurus*, and *Pulanesaura*. Finally, the new taxon, *Schleitheimia*, and *Isanosaurus* are found in a polytomy as direct outgroups to Sauropoda.

Reduced consensus methods identify several problematic taxa, the a posteriori exclusion of which

considerably improves resolution of the tree (Fig. 21a). Thus, at the basis of Sauropodomorpha, the highly incomplete *Chromogisaurus* (Ezcurra 2010) is identified as problematic taxon, and its exclusion results in the recovery of a monophyletic clade including *Panphagia* and *Pampadromeus* as the most basal sauropodomorphs, followed by *Saturnalia*. At the base of Sauropodiformes, *Leonerasaurus* and *Sefapanosaurus* take several equally parsimonious positions, and exclusion of these two taxa leads to a pectinate arrangement of *Anchisaurus*, *Mussaurus* and a polytomy of *Meroktenos* and *Aardonyx* below the more derived sauropodiforms. The second polytomy in Sauropodiformes is caused by *Blikanasaurus* and *Camelotia*, and excluding these taxa leads to three additional nodes below *Schleitheimia*, with *Melanorosaurus* being the most basal taxon in this pectinate arrangement, followed by a polytomy including *Antetonitrus*, *Ingentia* and *Lessemsaurus*, and a second polytomy including *Pulanesaura* and *Gongxianosaurus*. Thus, in contrast to Apaldetti et al. (2018) we do not recover a monophyletic Lessemsauridae even in the reduced consensus tree, although such an arrangement is found with a frequency of 86% in the majority rule consensus tree.

Characters supporting a position of *Schleitheimia* as a derived, non-sauropodan sauropodiform include the following: Lateral depression on the cervical vertebrae (C 129; shared with sauropods); marked lateral depressions on the dorsal vertebral centra (C 148; shared with sauropods); anteroposteriorly short posterior dorsals (C 152; shared with most sauropods); short posterior caudal vertebrae (C 184; synapomorphy of Sauropodiformes); triangular outline of bases of anterior caudal vertebral transverse processes (C 186; shared with *Pulanesaura* and sauropods); dorsoventrally deep anterior caudal transverse processes (C 190; shared with sauropods); rounded entepicondyle of distal humerus (C 219; reversal to basal saurischian condition; shared with all sauropodiforms that are more derived than *Melanorosaurus*, with the exception of *Pulanesaura*); rounded distal end of the ischial peduncle of the ilium (C 266; shared with sauropods); shortened ischial peduncle of ilium (C 268; shared with sauropods); symmetrical fourth trochanter on the femur (C 309; shared with sauropods); mediolaterally wide crista tibiofibularis on the distal femur (C 315; shared with *Melanorosaurus* and more derived sauropodiforms); pitted surfaces of the articular ends of limb bones (C 279; shared with sauropods).

In order to evaluate the support for the position of *Schleitheimia* as probable outgroup to sauropods, we tested alternative topologies using constrained analyses in TNT. A referral of the material from Schleitheim to *Plateosaurus* or the Plateosauridae, as argued by Galton (1986), requires an additional 12 steps; given that only 45 characters could be coded for *Schleitheimia*, this difference makes it extremely unlikely that *Schleitheimia* represents a plateosaurid or can even be synonymized with *Plateosaurus*. Likewise, a position of *Schleitheimia* outside Sauropodiformes requires 9 additional steps and is thus also rather unlikely. Even a position of the new taxon one node further outside Sauropoda requires four additional steps and is therefore also considerably less parsimonious.

The analysis using all material referred to *Schleitheimia* and implied weights resulted in 5 equally parsimonious trees with a score of 68.58801. The consensus of these trees generally agrees with the results from the unweighted analysis; however, after the a posteriori deletion of the unstable taxon *Ohmdenosaurus* (which is placed in several positions as a derived non-sauropodan sauropodiform), a fully resolved tree was found (Fig. 21b). In this analysis, *Leonerasaurus* and *Anchisaurus* form a clade at the base of sauropodiforms above the basalmost taxon *Xingxiulong*, followed by a pectinate arrangement of *Mussaurus*, *Aardonyx*, *Sefapanosaurus*, *Meroktenos*, *Melanorosaurus*, *Camelotia*, and higher sauropodiforms. The latter include a monophyletic Lessemsauridae, including *Lessemsaurus*, *Antetronitus* and *Ingentia*, at the base and *Blikanasaurus*, *Pulensasaura*, *Gongxianosaurus*, *Schleitheimia*, *Isanosaurus*, and *Tazoudasaurus* as consecutively closer outgroups to Sauropoda. Within sauropods, *Vulcanodon* represents the most basal taxon (by definition of that clade), followed by *Amygdalodon*, *Spinophorosaurus*, *Volkheimeria*, *Cetiosaurus*, a *Patagosaurus* + *Barapasaurus* clade, *Shunosaurus*, *Mamenchisaurus*, and an *Omeisaurus* + Neosauropoda clade. However, as the character list is mainly constructed to resolve non-sauropodan sauropodomorph relationships, results within Sauropoda should be seen with caution.

Our separate analyses of the type ilium or the referred material separately confirm the position of the new taxon and support the association of the remains (Fig. 22). The

(See figure on next page.)

Fig. 21 Reduced consensus cladograms of basal sauropodomorph relationships resulting from a phylogenetic analysis of 382 characters scored for 66 taxa (see text for details), showing the phylogenetic position of *Schleitheimia*. **a** Maximum parsimony analysis using equal weights. **b** Maximum parsimony analysis using implied weights (k = 12). Numbered nodes: 1, Sauropodomorpha; 2, Plateosauridae; 3, Massopoda; 4, Massospondylidae; 5, Sauropodiformes; 6, Sauropoda

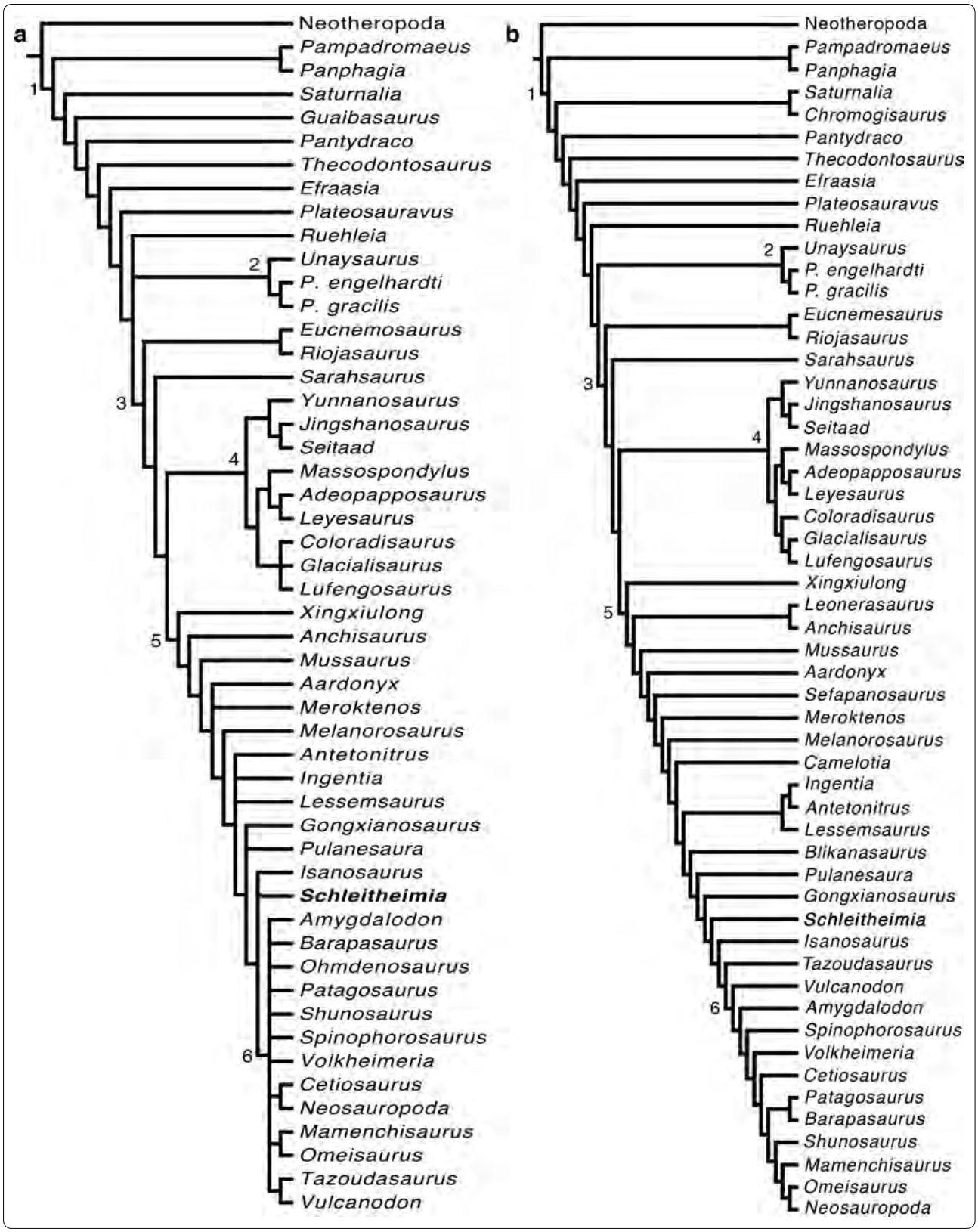
a
Neotheropoda
Pampadromaeus
Panphagia
1
Saturnalia
Guaibasaurus
Pantydraco
Thecodontosaurus
Efraasia
Plateosauravus
Ruehleia
2
Unaysaurus
P. engelhardti
P. gracilis
Eucnemosaurus
Riojasaurus
Sarahsaurus
3
Yunnanosaurus
Jingshanosaurus
Seitaad
4
Massospondylus
Adeopapposaurus
Leyesaurus
Coloradisaurus
Glacialisaurus
Lufengosaurus
Xingxiulong
5
Anchisaurus
Mussaurus
Aardonyx
Meroktenos
Melanorosaurus
Antetonitrus
Ingentia
Lessemsaurus
Gongxianosaurus
Pulanesaura
Isanosaurus
Schleitheimia
Amygdalodon
Barapasaurus
Ohmdenosaurus
Patagosaurus
Shunosaurus
Spinophorosaurus
6
Volkheimeria
Cetiosaurus
Neosauropoda
Mamenchisaurus
Omeisaurus
Tazoudasaurus
Vulcanodon
b
Neotheropoda
Pampadromaeus
Panphagia
1
Saturnalia
Chromogisaurus
Pantydraco
Thecodontosaurus
Efraasia
Plateosauravus
Ruehleia
2
Unaysaurus
P. engelhardti
P. gracilis
Eucnemesaurus
Riojasaurus
Sarahsaurus
3
Yunnanosaurus
Jingshanosaurus
Seitaad
4
Massospondylus
Adeopapposaurus
Leyesaurus
Coloradisaurus
Glacialisaurus
Lufengosaurus
Xingxiulong
5
Leonerasaurus
Anchisaurus
Mussaurus
Aardonyx
Sefapanosaurus
Meroktenos
Melanorosaurus
Camelotia
Ingentia
Antetonitrus
Lessemsaurus
Blikanasaurus
Pulanesaura
Gongxianosaurus
Schleitheimia
Isanosaurus
Tazoudasaurus
Vulcanodon
6
Amygdalodon
Spinophorosaurus
Volkheimeria
Cetiosaurus
Patagosaurus
Barapasaurus
Shunosaurus
Mamenchisaurus
Omeisaurus
Neosauropoda

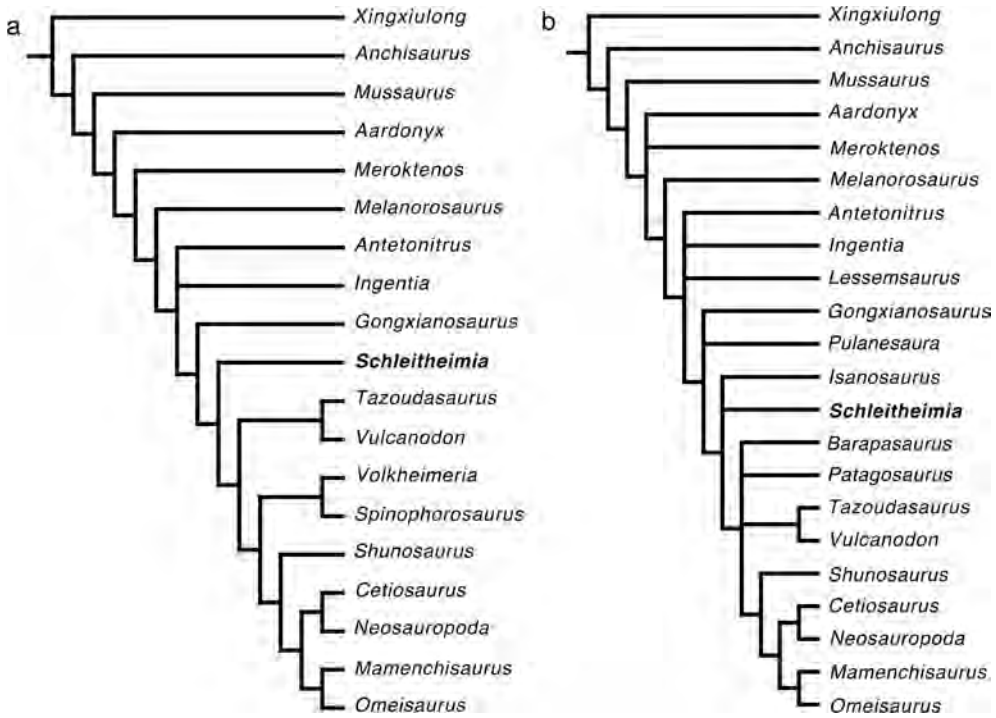

Fig. 22 Separate phylogenetic analysis of the holotype ilium only (**a**) and the referred material of *Schleitheimia*, showing congruent results (**b**). Only simplified sauropodiform interrelationships are shown (see Additional file 2: Figure S2 and Additional file 3: Figure S3 for complete strict consensus trees)

analysis of the type ilium only resulted in the recovery of 5244 equally parsimonious trees with a length of 1546 steps. The strict consensus of this analysis finds the type ilium in a large polytomy outside Sauropoda, together with all other non-sauropodan sauropodiforms more derived than *Meroktenos*. Reduced consensus methods again place the new taxon as sister taxon of Sauropoda (Fig. 22a), though with an uncertain position for *Pulanesaura* (which was removed by reduced consensus methods), for which no ilium is known (McPhee and Choiniere 2018). Likewise, the analysis of the referred material without the type ilium resulted in the recovery of 7632 trees with 1550 steps. This analysis finds the material from Schleitheim in a polytomy with *Isanosaurus* outside Sauropoda already in the strict consensus tree (Fig. 22b), thus mirroring the results of the analysis of all of the material.

6.3 Basal sauropodomorph diversity in the Triassic of Switzerland

With the description of *Schleitheimia*, the Late Triassic (Norian) sauropodomorph fauna from Switzerland includes at least three different taxa of non-neosauropodan sauropodomorphs. The Gruhalde Quarry in Frick, Kanton Aargau, has yielded numerous specimens of the genus *Plateosaurus* (Galton 1986; Sander 1992; Meyer and Thüring 2003; Hofmann and Sander 2014), although it is still somewhat uncertain if these remains represent the same species of this genus as the famous lagerstätten in Baden-Württemberg or other localities in Germany. The astragalus of *Plateosaurus* from Santierge described above provides further evidence that this genus was also widespread in the Norian of Switzerland. *Schleitheimia* represents a considerably larger and more derived sauropodiform sauropodomorph, and the material of Hallau-Schwärzibuck seems to indicate another, large non-sauropodan sauropodomorph, so that at least three medium-sized to large sauropodomorph taxa were present in the Late Triassic of Switzerland.

Another formally named taxon is *Gresslyosaurus ingens* from Niederschönthal in the Canton Basel-Landschaft. This taxon is based on a partial sacrum, some caudal vertebrae, a metacarpal and fragments of the hindlimbs, including partial left and right tibiae, an almost complete fibula, and pedal elements (Huene 1907-8; Galton 1986). Galton (1986) referred this material to *Plateosaurus*, and this assignment was followed by most subsequent authors and has been supported in several recent phylogenetic analyses (e.g. Yates 2007; McPhee et al. 2015; Otero et al. 2015). However, Moser (2003)

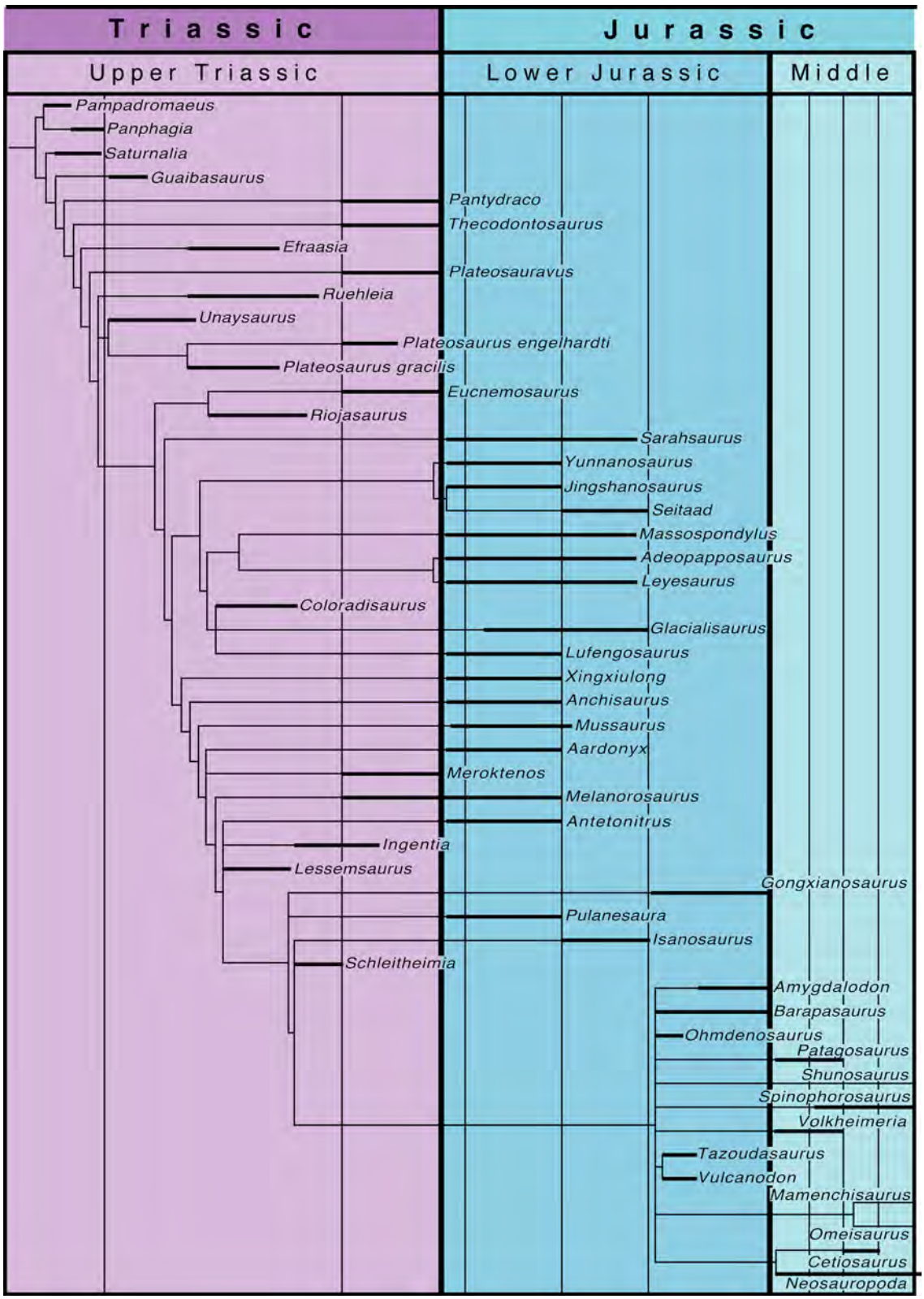

Fig. 23 Time-calibrated cladogram of basal sauropodomorph relationships (based on the unweighted analysis), showing the survival of numerous lineages (including sauropods) across the Triassic-Jurassic boundary

found significant differences in the sacral vertebrae between *Gresslyosaurus* and *Plateosaurus* and questioned the referral of the former to the latter, a conclusion with which we agree (OR, pers. obs, 2017). As noted above, the material is currently being re-prepared, and a detailed revision of all the material from Niederschönthal will certainly help to identify the affinities of this taxon. The material represents an animal of comparable size to both *Schleitheimia* and the remains from Hallau-Schwärzibuck. Unfortunately, however, as there is very limited overlap of remains, it cannot currently be decided with certainty whether it might represent either of these, or a third large basal sauropodomorph taxon from the Late Triassic of Switzerland. *Gresslyosaurus* is similar to *Schleitheimia* in that the neural canal in the sacral vertebrae is deeply incised into the vertebral centra, but, as noted above, this seems to be a more general character found in derived non-sauropodan sauropodiforms and basal sauropods. However, a possible difference between *Gresslyosaurus* and *Schleitheimia* is that the sacral vertebrae of the former are rather elongate (length/height ration of approximately 1.4), whereas both the posterior dorsals and anterior caudals of *Schleitheimia* are short (length/height ratio of 0.8 or less). As the sacral vertebrae tend to be similar in relative length to the last dorsals in sauropodmorphs, this might be an argument against a synonymy of the two taxa. A further difference is found in the caudal vertebrae. The poorly preserved mid-caudals of *Gresslyosaurus* are unusual in being slightly wedge-shaped in lateral view, the ventral side being shorter than the dorsal side (NMB N B 1573, 1577). This character is absent in *Schleitheimia*, in which the mid-caudal vertebrae are rectangular in lateral view. Thus, these—admittedly limited—comparisons indicate that *Schleitheimia* is different from *Gresslyosaurus*.

6.4 Implications for basal sauropodomorph evolution and the origin of sauropods

Disregarding the recent discussion of the definition of Sauropoda (see Peyre de Fabrègues et al. 2015; McPhee and Choiniere 2018), the origin and early evolution of this clade has received considerable attention lately, due to improved resolution of basal sauropodomorph relationships (e.g. Yates 2004, 2007; Upchurch et al. 2007a; Apaldetti et al. 2014, 2018), new discoveries (or interpretations) of close sauropod relatives (e.g. Yates and Kitching 2003; Upchurch et al. 2007b; Yates et al. 2010; Pol et al. 2011; McPhee et al. 2015, 2018; Otero et al. 2015), and several studies on the evolution of the sauropod body plan in relation to their gigantism (e.g. Rauhut et al. 2011; Sander et al. 2011; Sander 2013; Bates et al. 2016; McPhee et al. 2018). As for the timing of sauropod origins, there seems to be a conflict between osteological and ichnological evidence. Whereas the late Early Jurassic (Pliensbachian-Toarcian; McPhee et al. 2017) *Vulcanodon* is generally regarded as the oldest osteological evidence for sauropods, tantalizing trackway evidence from the Late Triassic of Argentina (Marsicano and Barredo 2004) and, especially, Greenland (Lallensack et al. 2017) indicate the existence of sauropods already in the Late Triassic. As the putative Late Triassic sauropod *Isanosaurus* (Buffetaut et al. 2000; here found as one of the immediate outgroups to Sauropoda) has recently been argued to be no older than Pliensbachian in age (Racey and Goodall 2009), the placement of the probably Late Norian *Schleitheimia* as probable sister taxon to Sauropoda lends support to the origin of the latter clade already in the Late Triassic. Interestingly, however, Lallensack et al. (2017) identified several characters in the sauropod tracks of Greenland that indicate a foot morphology more derived than the Early Jurassic *Vulcanodon* and *Tazoudasaurus*. If confirmed, this would signify an early, Triassic split of vulcanodontids from the lineage leading to Eusauropoda and a survival of at least two sauropod lineages of the Triassic/Jurassic boundary. However, pedal anatomy of most sauropodiforms close to the origin of sauropods is still poorly known, and thus there is the possibility that the condition in vulcanodontids represents a reversal, as argued by Yates et al. (2010; see also Wilson 2005), and the Late Triassic sauropod-like tracks might have been made by large, graviportal non-sauropodan sauropodiforms, such as *Schleitheimia*. As argued by McPhee and Choiniere (2018), several pedal morphologies might have evolved in parallel in sauropodiforms on the lineage towards sauropods.

However this may be, the results of our phylogenetic analyses further highlight three aspects in early sauropodomorph evolution: the marked radiation of the clade already in the Late Triassic, the relatively limited effect of the Triassic/Jurassic extinction event on sauropodomorph evolution and diversity, and an apparently delayed ascent of sauropods in the late Early to Middle Jurassic (Fig. 23). Under the phylogenetic hypothesis presented here, all major clades of basal sauropodomorphs, including true sauropods, originated in the Late Triassic, with only the oldest representatives coming from Carnian sediments, while most taxa, including *Schleitheimia* as possible immediate outgroup to Sauropoda appear in the Norian. Furthermore, whereas many of the Carnian taxa for which cranial remains are known still show clear evidence for a carnivorous or at least omnivorous diet (see Cabreira et al. 2016), Norian sauropodomorphs seem to show increasing adaptations towards a herbivorous diet. This is thus in accordance with a rapid radiation of sauropodomorphs in the Late Carnian and early Norian, following an extinction of other large-bodied herbivores

during the Carnian Pluvial Episode in the mid-Carnian, as recently suggested (Bernardi et al. 2018).

On the other hand, the presence of basically all non-eusauropod lineages already in the Triassic [especially if the trackway record from Greenland represents a sauropod more derived than Vulcanodontidae, as argued by Lallensack et al. (2017)] indicates that, apart from single taxa, only few lineages disappeared before the Jurassic, and most seem to have crossed the Triassic-Jurassic boundary (Fig. 23). Apart from the *Panphagia*/*Pampadromeus* clade, which might represent a first small mid-Carnian radiation that disappeared before the main radiation of sauropodomorphs in the latest Carnian and Norian, only the Plateosauridae and the *Riojasaurus*/*Eucnemesaurus* clade did not extend into the Jurassic. On the other hand, given the Late Triassic age of *Schleitheimia,* the nesting of *Coloradisaurus* with *Glacialisaurus* and *Lufengosaurus*, and the relationships among sauropodiforms, at least thirteen lineages of sauropodomorphs survived the end-Triassic extinction. Apart from the three distinct subclades of the Massospondylidae, the Sauropoda and the Lessemsauridae (if this clade is monophyletic and *Antetonitrus* is Early Jurassic in age; see McPhee et al. 2017), these are lineages that lead to single, Early Jurassic taxa, the origin of which must have been in the Norian at the latest. Thus, although the end-Triassic event might have had some effect on sauropodomorph diversity, it neither seems to have had a devastating effect on the early radiation of this clade, nor does it seems to have kick-started their great success in the later Mesozoic.

An interesting consideration in this respect concerns the sauropods. As this clade must have originated by the Late Triassic, if *Schleitheimia* is considered to be its immediate outgroup (and notwithstanding the unresolved position of *Isanosaurus*), sauropods thus remained a seemingly little diverse side lineage of sauropodomorphs over most of the Early Jurassic, as the main dinosaur faunas known from that time (Upper Elliot and Clarens Formations of South Africa, Early Jurassic units in San Juan and Chubut provinces of Argentina, Kayenta Formation of North America, Lufeng Formation of China) were largely dominated by other basal sauropodomorph lineages, usually massospondylids (as recovered in the current analysis), both in terms of taxa represented and number of specimens found. Only after the disappearance of these basal, non-sauropodan forms towards the end of the Jurassic (none of the occurrences of these clades is demonstrably younger than Pliensbachian), sauropods seem to have become more common and then radiated rapidly. Indeed, the recent discoveries of probable neosauropods from the early Middle Jurassic (Carballido et al. 2017; Xu et al. 2018) indicate that this radiation must have been extremely fast in the latest early to early Middle Jurassic. This pattern is consistent with the suggestion by Allain and Aquesbi (2008; see also Allain and Läng 2009) that sauropod radiation and success was associated with and probably triggered by the Pliensbachian/Toarcian extinction event, as it has recently also been suggested for theropod dinosaurs (Pol and Rauhut 2012; Rauhut et al. 2016). What exact ecological changes led to this apparently drastic event, which also affected other clades of terrestrial vertebrates and seemed to have been even more marked in the terrestrial realm than in marine environments, remains unknown and requires further investigation.

7 Conclusions

Fragmentary sauropodomorph remains from the probably Late Norian of Schaffhausen, Switzerland, that were long considered to represent the common central European genus *Plateosaurus* can be shown to represent a separate taxon of non-sauropodan sauropodomorphs, *Schleitheimia schutzi*. The recognition of this new taxon, together with an evaluation of other sauropodomorph material from the Late Triassic of Schaffhausen shows that at least three different basal sauropodomorph taxa were present in the Norian of Switzerland. *Schleitheimia* is a derived sauropodiform and might even represent the immediate outgroup to sauropods. In the context of a phylogenetic analysis, the new taxon indicates that the Triassic/Jurassic extinction event probably only had a minor effect on sauropodomorph evolution, and that the ascent of sauropods was delayed until the late Early Jurassic, when other basal sauropodomorph lineages perished in the Pliensbachian/Toarcian extinction event and gave way to an explosive radiation of that clade.

Supplementary information

Supplementary information accompanies this paper at https://doi.org/10.1186/s00015-020-00360-8.

Additional file 1. Strict consensus tree of the phylogenetic analysis of Schleitheimia.

Additional file 2. Strict consensus tree of the phylogenetic analysis using the type ilium of Schleitheimia only.

Additional file 3. Strict consensus tree of the phylogenetic analysis using the referred material of Schleitheimia only.

Acknowledgements
We are indebted to the late Emil Schutz, who collected much of the material described here, including the type specimen of *Schleitheimia*, and donated it to the PIMUZ. Martin Wäckerlin handed the MzA unpublished documents and additional fossil material from his uncle E. Schutz. Other material was collected and donated by Daniel Egger, Franz Hofmann, Rudolf Schlatter, Bruno Sommerhalder and Bruno Sternegg to the MzA. Willi Bächtold, Urs Oberli, Tobias Reich, Silvan Schaub, Rudolf Schlatter and Iwan Stössel participated in the excavation in 2016, funded by the Naturforschende Gesellschaft Schaffhausen, the Lotteriefonds Kanton Schaffhausen and the Schweizerische Akademie der Naturwissenschaften. The Canton Schaffhausen and the community of Schleitheim granted the permit. The material was prepared by Fritz Buchser, Urs Oberli and Christian Obrist. E. Schneebeli-Hermann studied some test samples on palynomorphs. Sincere thanks go to Urs Weibel for access to the material at MzA, help during collection work, and, together with Iwan Stössel, for providing measurements for the MzA specimens. We also thank Christian Klug for access to the PIMUZ collection. Andrea Villa took photographs of selected elements of *Ruehleia* for us. Chris Takken helped with picking microfossils and Gabriel Aguirre with the design of figures. Last, but not least, Adriana López-Arbarello and Christian Meyer are thanked for discussions, and the critical comments by two anonymous reviewers greatly helped to improve the paper.

Authors' contributions
OR designed the project, OR and FH analysed the data, HF carried out fieldwork, and all authors wrote the manuscript and prepared figures. All authors read and approved the final manuscript.

Funding
Fieldwork was supported by the Naturforschende Gesellschaft Schaffhausen, the Lotteriefonds Kanton Schaffhausen and the Schweizerische Akademie der Naturwissenschaften. No other funding was obtained for this project.

Availability of data and materials
The phylogenetic matrices are deposited on Morphobank (http://www.morphobank.org) under project 2320. The fossil materials described here are permanently deposited in the Palaeontological Institute and Museum of the University of Zurich and the Museum zu Allerheiligen in Schaffhausen, as indicated in the text.

Competing interests
The authors declare no competing interests.

Author details
[1] SNSB, Bayerische Staatssammlung für Paläontologie und Geologie, Richard-Wagner-Str. 10, 80333 Munich, Germany. [2] Sektion Paläontologie und Geobiologie, Department für Geo- und Umweltwissenschaften, Ludwig-Maximilians-Universität, Richard-Wagner-Str. 10, 80333 Munich, Germany. [3] GeoBioCenterLMU, Ludwig-Maximilians-Universität, Munich, Germany. [4] Faculty of Geosciences, Utrecht University, Princetonlaan 8a, 3584 CB Utrecht, The Netherlands. [5] Fachgruppe Paläoumwelt, Friedrich-Alexander Universität Erlangen-Nürnberg, Geozentrum Nordbayern, Loewenichstrasse 28, 91054 Erlangen, Germany. [6] Paläontologisches Institut und Museum, Universität Zürich, Karl Schmid-Strasse 4, 8006 Zurich, Switzerland. [7] Present Address: Royal Tyrrell Museum of Palaeontology, PO Box 7500, Drumheller AB T0J 0Y0, Canada.

Appendix

Character list [based on McPhee et al. (2015), Otero et al. (2015) and Apaldetti et al. (2018) unless otherwise indicated]

1. Skull to femur ratio: greater than 0.6 (0); less than 0.6 (1).
2. Lateral plates appressed to the labial side of the premaxillary, maxillary and dentary teeth: absent (0); present (1).
3. Relative height of the rostrum at the posterior margin of the naris: more than 0.6 the height of the skull at the middle of the orbit (0); less than 0.6 the height of the skull at the middle of the orbit (1).
4. Foramen on the lateral surface of the premaxillary body: absent (0); present (1).
5. Distal end of the dorsal premaxillary process: tapered (0); transversely expanded (1).
6. Profile of premaxilla: convex (0); with an inflection at the base of the dorsal process (1).
7. Size and position of the posterolateral process of premaxilla: large and lateral to the anterior process of the maxilla (0); small and medial to the anterior process of the maxilla (1).
8. Relationship between posterolateral process of the premaxilla and the anteroventral process of the nasal: broad sutured contact (0); point contact (1); separated by maxilla (2). Ordered.
9. Posteromedial process of the premaxilla: absent (0); present (1).
10. Shape of the anteromedial process of the maxilla: narrow, elongated and projecting anterior to lateral premaxilla-maxilla suture (0); short, broad and level with lateral premaxilla-maxilla suture (1).
11. Development of external narial fossa: absent to weak (0); well-developed with sharp posterior and anteroventral rims (1).
12. Development of narial fossa on the anterior ramus of the maxilla: weak and orientated laterally to dorsolaterally (0); well-developed and forming a horizontal shelf (1).
13. Size and position of subnarial foramen: absent (0); small (no larger than adjacent maxillary neurovascular foramina) and positioned outside of narial fossa (1); large and on the rim of, or inside, the narial fossa (2). Ordered.
14. Shape of subnarial foramen: rounded (0); slot-shaped (1).
15. Maxillary contribution to the margin of the narial fossa: absent (0); present (1).
16. Diameter of external naris: less than 0.5 of the orbital diameter (0); greater than 0.5 of the orbital diameter.
17. Shape of the external naris (in adults): rounded (0); subtriangular with an acute posteroventral corner (1).
18. 18. Level of the anterior margin of the external naris: anterior to the midlength of the premaxillary body (0); posterior to the midlength of the premaxillary body (1).
19. Level of the posterior margin of external naris: anterior to, or level with the premaxilla-maxilla suture (0); posterior to the first maxillary alveo-

lus (1); posterior to the midlength of the maxillary tooth row and the anterior margin of the antorbital fenestra (2). Ordered.
20. Dorsal profile of the snout: straight to gently convex (0); with a depression behind the naris (1).
21. Elongate median nasal depression: absent (0); present (1).
22. Width of anteroventral process of nasal at its base: less than the width of the anterodorsal process at its base (0); greater than the width of the anterodorsal process at its base (1).
23. Nasal relationship with dorsal margin of antorbital fossa: not contributing to the margin of the antorbital fossa (0); lateral margin overhangs the antorbital fossa and forms its dorsal margin (1); overhang extensive, obscuring the dorsal lachrymal-maxilla contact in lateral view (2). Ordered.
24. Pointed caudolateral process of the nasal overlapping the lachrymal: absent (0); present (1).
25. Anterior profile of the maxilla: slopes continuously towards the rostral tip (0); with a strong inflection at the base of the ascending ramus, creating a rostral ramus with parallel dorsal and ventral margins (1).
26. Length of rostral ramus of the maxilla: less than its dorsoventral depth (0); greater than its dorsoventral depth (1).
27. Shape of the main body of the maxilla: tapering posteriorly (0); dorsal and ventral margins parallel for most of their length (1).
28. Shape of the ascending ramus of the maxilla in lateral view: tapering dorsally (0); with an anteroposterior expansion at the dorsal end (1).
29. Rostrocaudal length of the antorbital fossa: greater than that of the orbit (0); less than that of the orbit (1).
30. Posteroventral extent of medial wall of antorbital fossa: reaching the anterior tip of the jugal (0); terminating anterior to the anterior tip of the jugal (1).
31. Development of the antorbital fossa on the ascending ramus of the maxilla: deeply impressed and delimited by a sharp, scarp-like rim (0); weakly impressed and delimited by a rounded rim or a change in slope (1).
32. Shape of the antorbital fossa: crescentic with a strongly concave posterior margin that is roughly parallel to the anterior margin of the antorbital fossa (0); subtriangular with a straight to gently concave posterior margin (1); antorbital fossa absent (2).
33. Size of the neurovascular foramen at the posterior end of the lateral maxillary row: not larger than the others (0); distinctly larger than the others in the row (1).
34. Direction that the neurovascular foramen at the posterior end of the lateral maxillary row opens: posteriorly (0); anteriorly, ventrally, or laterally (1).
35. Arrangement of lateral maxillary neurovascular foramina: linear (0); irregular (1).
36. Longitudinal ridge on the posterior lateral surface of the maxilla: absent (0); present (1).
37. Dorsal exposure of the lachrymal: present (0); absent (1).
38. Shape of the lachrymal: dorsoventrally short and blockshaped (0); dorsoventrally elongate and shaped like an inverted L (1).
39. Orientation of the lachrymal orbital margin: strongly sloping anterodorsally (0); erect and close to vertical (1).
40. Length of the anterior ramus of the lachrymal: greater than half the length of the ventral ramus (0); less than half the length of the ventral ramus (1); absent altogether (2). Ordered.
41. Web of bone spanning junction between anterior and ventral rami of lachrymal: absent and antorbital fossa laterally exposed (0); present, obscuring posterodorsal corner of antorbital fossa (1).
42. Extension of the antorbital fossa onto the ventral end of the lachrymal: present (0); absent (1).
43. Length of the posterior process of the prefrontal: short (0); elongated, so that total prefrontal length is equal to the anteroposterior diameter of the orbit (1).
44. Ventral process of prefrontal extending down the posteromedial side of the lachrymal: present (0); absent (1).
45. Maximum transverse width of the prefrontal: less than 0.25 of the skull width at that level (0); more than 0.25 of the skull width at that level (1).
46. Shape of the orbit: subcircular (0); ventrally constricted making the orbit subtriangular (1).
47. Slender anterior process of the frontal intruding between the prefrontal and the nasal: absent (0); present (1).
48. Jugal-lachrymal relationship: lachrymal overlapping lateral surface of jugal or abutting it dorsally (0); jugal overlapping lachrymal laterally (1).
49. Shape of the suborbital region of the jugal: an anteroposteriorly elongate bar (0); an anteroposteriorly shortened plate (1).
50. Jugal contribution to the antorbital fenestra: absent (0); present (1).
51. Dorsal process of the anterior jugal: present (0); absent (1).

52. Ratio of the minimum depth of the jugal below the orbit to the distance between the anterior end of the jugal and the anteroventral corner of the infratemporal fenestra: less than 0.2 (0); greater than 0.2 (1).
53. Transverse width of the ventral ramus of the postorbital: less than its anteroposterior width at midshaft (0); greater than its anteroposterior width at midshaft (1).
54. Shape of the dorsal margin of postorbital in lateral view: straight to gently curved (0); with a distinct embayment between the anterior and posterior dorsal processes (1).
55. Height of the postorbital rim of the orbit: flush with the posterior lateral process of the postorbital (0); raised so that it projects laterally to the posterior dorsal process (1).
56. Postfrontal bone: present (0); absent (1).
57. Position of the anterior margin of the infratemporal fenestra: behind the orbit (0); extends under the rear half of the orbit (1); extends as far forward as the midlength of the orbit (2). Ordered.
58. Frontal contribution to the supratemporal fenestra: present (0); absent (1).
59. Orientation of the long axis of the supratemporal fenestra: longitudinal (0); transverse (1).
60. Medial margin of supratemporal fossa: simple smooth curve (0); with a projection at the frontal/postorbital-parietal suture producing a scalloped margin (1).
61. Length of the quadratojugal ramus of the squamosal relative to the width at its base: less than four times its width (0); greater than four times its width (1).
62. Proportion of infratemporal fenestra bordered by squamosal: more than 0.5 of the depth of the infratemporal fenestra (0); less than 0.5 of the depth of the infratemporal fenestra (1).
63. Squamosal-quadratojugal contact: present (0); absent (1).
64. Angle of divergence between jugal and squamosal rami of quadratojugal: close to 90° (0); close to parallel (1).
65. Length of jugal ramus of quadratojugal: no longer than the squamosal ramus (0); longer than the squamosal ramus (1).
66. Shape of the rostral end of the jugal ramus of the quadratojugal: tapered (0); dorsoventrally expanded (1).
67. Relationship of quadratojugal to jugal: jugal overlaps the lateral surface of the quadratojugal (0); quadratojugal overlaps the lateral surface of the jugal (1); quadratojugal sutures along the ventrolateral margin of the jugal (2).
68. Position of the quadrate foramen: on the quadrate-quadratojugal suture (0); deeply incised into, and partly encircled by, the quadrate (1); on the quadrate-squamosal suture, just below the quadrate head (2).
69. Shape of posterolateral margin of quadrate: sloping anterolaterally from posteromedial ridge (0); everted posteriorly creating a posteriorly facing fossa (1); posterior fossa deeply excavated, invading quadrate body (2). Ordered.
70. Exposure of the lateral surface of the quadrate head: absent, covered by lateral sheet of the squamosal (0); present (1).
71. Proportion of the length of the quadrate that is occupied by the pterygoid wing: at least 70% (0); greater than 70% (1).
72. Depth of the occipital wing of the parietal: less than 1.5 times the depth of the foramen magnum (0); more than 1.5 times the depth of the foramen magnum (1).
73. Position of foramina for mid-cerebral vein on occiput: between supraoccipital and parietal (0); on the supraoccipital (1).
74. Postparietal fenestra between supraoccipital and parietals: absent (0); present (1).
75. Shape of the supraoccipital: diamond-shaped, at least as high as wide (0); semilunate and wider than high (1).
76. Orientation of the supraoccipital plate: erect to gently sloping (0); strongly sloping forward so that the dorsal tip lies level with the basipterygoid processes (1).
77. Orientation of the paroccipital processes in occipital view: slightly dorsolaterally directed to horizontal (0); ventrolaterally directed (1).
78. Orientation of the paroccipital processes in dorsal view: posterolateral forming a V-shaped occiput (0); lateral forming a flat occiput (1).
79. Size of the post-temporal fenestra: large fenestra (0); a small hole that is much less than half the depth of the paroccipital process (1).
80. Exit of the mid-cerebral vein: through trigeminal foramen (0); through a separate foramen anterodorsal to trigeminal foramen (1).
81. Shape of the floor of the braincase in lateral view: relatively straight with the basal tuberae, basipterygoid processes and parasphenoid rostrum roughly aligned (0); bent with the basipterygoid processes and the parasphenoid rostrum below the level of the basioccipital condyle and the basal tuberae (1);

bent with the basal tuberae lowered below the level of the basioccipital and the parasphenoid rostrum raised above it (2).

82. Shape of basal tuberae: knob-like, with basisphenoidal component rostral to basioccipital component (0); forming a transverse ridge with the basisphenoidal component lateral to the basioccipital component (1).
83. Length of the basipterygoid processes (from the top of the parasphenoid to the tip of the process): less than the height of the braincase (from the top of the parasphenoid to the top of the supraoccipital) (0); greater than the height of the braincase (from the top of the parasphenoid to the top of the supraoccipital) (1).
84. Ridge formed along the junction of the parabasisphenoid and the basioccipital, between the basal tuberae: present with a smooth anterior face (0); present with a median fossa on the anterior face (1); absent with the basal tuberae being separated by a deep posteriorly opening U-shaped fossa (2).
85. Deep septum spanning the interbasipterygoid space: absent (0); present (1).
86. Dorsoventral depth of the parasphenoid rostrum: much less than the transverse width (0); about equal to the transverse width (1).
87. Shape of jugal process of ectopterygoid: gently curved (0); strongly recurved and hook-like (1).
88. Pneumatic fossa on the ventral surface of the ectopterygoid: present (0); absent (1).
89. Relationship of the ectopterygoid to the pterygoid: ectopterygoid overlapping the ventral surface of the pterygoid (0); ectopterygoid overlapping the dorsal surface of the pterygoid (1).
90. Position of the maxillary articular surface of the palatine: along the lateral margin of the bone (0); at the end of a narrow anterolateral process due to the absence of the posterolateral process (1).
91. Centrally located tubercle on the ventral surface of palatine: absent (0); present (1).
92. Medial process of the pterygoid forming a hook around the basipterygoid process: absent (0); flat and blunt-ended (1); bent upward and pointed (2). Ordered.
93. Length of the vomers: less than 0.25 of the total skull length (0); more than 0.25 of the total skull length (1).
94. Position of jaw joint: no lower than the level of the dorsal margin of the dentary (0); depressed, well below this level (1).
95. Shape of upper jaws in ventral view: narrow with an acute rostral apex (0); broad and U-shaped (1).
96. Length of the external mandibular fenestra: more than 0.1 of the length of the mandible (0); less than 0.1 of the length of the mandible (1).
97. Caudal end of dentary tooth row medially inset with a thick lateral ridge on the dentary forming a buccal emargination: absent (0); present (1).
98. Height: length ratio of the dentary: less than 0.2; greater than 0.2 (1).
99. Orientation of the symphyseal end of the dentary: in line with the long axis of the dentary (0); strongly curved ventrally (1).
100. Position of first dentary tooth: adjacent to symphysis (0); inset one tooth's width from the symphysis (1).
101. Dorsoventral expansion at the symphyseal end of the dentary: absent (0); present (1).
102. Splenial foramen: absent (0); present and enclosed (1); present and open anteriorly (2). Ordered.
103. Splenial-angular joint: flattened sutured contact (0); synovial joint surface between tongue-like process of angular fitting in groove of the splenial (1).
104. A stout, triangular, medial process of the articular, behind the glenoid: present (0); absent (1).
105. Length of the retroarticular process: less than the depth of the mandible below the glenoid (0); greater than the depth of the mandible below the glenoid (1).
106. Strong medial embayment behind glenoid of the articular in dorsal view: absent (0); present (1).
107. Number of premaxillary teeth: four (0); more than four (1).
108. Number of dentary teeth (in adults): less than 18 (0); 18 or more (1).
109. Arrangement of teeth within the jaws: linearly placed, crowns not overlapping (0); imbricated with distal side of tooth overlapping mesial side of the succeeding tooth (1).
110. Orientation of the maxillary tooth crowns: erect (0); procumbent (1).
111. Orientation of the dentary tooth crowns: erect (0); procumbent (1).
112. Teeth with basally constricted crowns: absent (0); present (1).
113. Tooth-tooth occlusal wear facets: absent (0); present (1).
114. Mesial and distal serrations of the teeth: fine and set at right angles to the margin of the tooth (0); coarse and angled upwards at an angle of 45° to the margin of the tooth (1).
115. Distribution of serrations on the maxillary and dentary teeth: present on both the mesial and distal carinae (0); absent on the posterior carinae (1); absent on both carinae (2).

116. Long axis of the tooth crowns distally recurved: present (0); absent (1).
117. Texture of the enamel surface: entirely smooth (0); finely wrinkled in some patches (1); extensively and coarsely wrinkled (2). Ordered.
118. Lingual concavities of the teeth: absent (0); present (1).
119. Longitudinal labial grooves on the teeth: absent (0); present (1).
120. Distribution of the serrations along the mesial and distal carinae of the tooth: extend along most of the length of the crown (0); restricted to the upper half of the crown (1).
121. Number of cervical vertebrae: eight or fewer (0); 9–10 (1); 12–13 (2); more than 13 (3). Ordered.
122. Shallow, dorsally facing fossa on the atlantal neurapophysis bordered by a dorsally everted lateral margin: absent (0); present (1).
123. Width of axial intercentrum: less than width of axial centrum (0); greater than width of axial centrum (1).
124. Position of axial prezygapophyses: on the anterolateral surface of the neural arch (0); mounted on anteriorly projecting pedicels (1).
125. Posterior margin of the axial postzygapophyses: overhang the axial centrum (0); flush with the caudal face of the axial centrum (1).
126. Length of the axial centrum: less than three times the height of the centrum (0); at least three times the height of the centrum (1).
127. Length of the anterior cervical centra (cervicals 3–5): no more than the length of the axial centrum (0); greater than the length of the axial centrum (1).
128. Length of middle to posterior cervical centra (cervical 6–8): no more than the length of the axial centrum (0); greater than the length of the axial centrum (1).
129. Lateral depression in the cervical vertebral centra: absent, lateral side straight or dorsoventrally convex (0), present, shallow to moderately deep and fades out anteriorly and posteriorly (1), present, deep, with marked anterior margin, fades out posteriorly (2), present, with sharply defined anterior and posterior margins (3). Ordered. (modified from Upchurch 1998, Wilson & Sereno 1998).
130. Dorsal excavation of the cervical parapophyses: absent (0); present (1).
131. Lateral compression of the anterior cervical vertebrae: centra are no higher than they are wide (0); are approximately 1.25 times higher than wide (1).
132. Relative elongation of the anterior cervical centra (cervical 3–5): lengths of the centra are less than 2.5 times the height of their anterior faces (0); lengths are 2.5–4 times the height of their anterior faces (1); the length of at least cervical 4 or 5 exceeds 4 times the anterior centrum height (2). Ordered.
133. Ventral keels on cranial cervical centra: present (0); absent (1).
134. Height of the mid cervical neural arches: no more than the height of the posterior centrum face (0); greater than the height of the posterior centrum face (1).
135. Cervical epipophyses on the dorsal surface of the postzygapophyses: absent (0); present on at least some cervical vertebrae (1).
136. Posterior ends of the anterior, postaxial epipophyses: with a free pointed tip (0); joined to the postzygapophysis along their entire length (1).
137. Shape of the epipophyses: tall ridges (0); flattened, horizontal plates (1).
138. Epipophyses overhanging the rear margin of the postzygapophyses: absent (0); present in at least some postaxial cervical vertebrae (1).
139. Anterior spur-like projections on mid-cervical neural spines: absent (0); present (1).
140. Shape of mid-cervical neural spines: less than twice as long as high (0); at least twice as long as high (1).
141. Shape of cervical rib shafts: short and posteroventrally directed (0); longer than the length of their centra and extending parallel to cervical column (1).
142. Position of the base of the cervical rib shaft: level with, or higher than the ventral margin of the cervical centrum (0); located below the ventral margin due to a ventrally extended parapophysis (1).
143. Postzygodiapophyseal lamina in cervical neural arches 4-8: present (0); absent (1).
144. Laminae of the cervical neural arches 4-8: well-developed tall laminae (0); weakly developed low ridges (1).
145. Shape of anterior centrum face in cervical centra: concave (0); flat (1); convex (2). Ordered.
146. Ventral surface of the centra in the cervicodorsal transition: transversely rounded (0); with longitudinal keels (1).
147. Number of vertebrae between cervicodorsal transition and primordial sacral vertebrae: 15–16 (0); no more than 14 (1).
148. Lateral surfaces of the dorsal centra: with at most vague, shallow depressions (0); with deep fossae that approach the midline (1); with invasive, sharp-rimmed pleurocoels (2). Ordered.
149. Oblique ridge dividing pleural fossa of cervical vertebrae: absent (0); present (1).
150. Laterally expanded tables at the midlength of the dorsal surface of the neural spines: absent in all

vertebrae (0); present on the pectoral vertebrae (1); present on the pectoral and cervical vertebrae (2). Ordered.

151. Dorsal centra: entirely amphicoelous to amphiplatyan (1); first two dorsals are opisthocoelous (1); cranial half of dorsal column is opisthocoelous (2). Ordered.
152. Shape of the posterior dorsal centra: relatively elongated for their size (0); strongly axially compressed for their size (1).
153. Laminae bounding triangular infradiapophyseal fossae (chonae) on dorsal neural arches: absent (0); present (1).
154. Location of parapophysis in first two dorsals: at the anterior end of the centrum (0); located at the mid-length of the centrum, within the middle chonos (1).
155. Parapophyses of the dorsal column completely shift from the centrum to the neural arch: anterior to the thirteenth presacral vertebra (0); posterior to the thirteenth presacral vertebra (1).
156. Orientation of the transverse processes of the dorsal vertebrae: most horizontally directed (0); all upwardly directed (1).
157. Contribution of the paradiapophyseal lamina to the margin of the anterior chonos in mid-dorsal vertebrae: present (0); prevented by high placement of parapophysis (1).
158. Hyposphenes in the dorsal vertebrae: absent (0); present but less than the height of the neural canal (1); present and equal to the height of the neural canal (2). Ordered.
159. Prezygodiapophyseal lamina and associated anterior triangular fossa (anterior infradiapophyseal fossa): present on all dorsals (0); absent in mid-dorsals (1).
160. Anterior centroparapophyseal lamina in dorsal vertebrae: absent (0); present (1).
161. Prezygoparapophyseal lamina in dorsal vertebrae: absent (0); present (1).
162. Accessory lamina dividing posterior chonos from postzygapophysis: absent (0); present (1).
163. Lateral pneumatic fenestra in centrodiapophyseal fossa in middle and posterior dorsal vertebrae, opening into neural cavity: absent (0), present (1).
164. Separation of lateral surfaces of anterior dorsal neural arches under transverse processes: widely spaced (0); only separated by a thin midline septum (1).
165. Height of dorsal neural arches, from neurocentral suture to level of zygapophyseal facets: much less than height of centrum (0); subequal to or greater than height of centrum (1).
166. Form of anterior surface of neural arch: simple centroprezygopophyseal ridge (0); broad anteriorly facing surface bounded laterally by centroprezygopophyseal lamina (1).
167. Shape of posterior dorsal neural canal: subcircular (0); slit-shaped (1).
168. Height of middle dorsal neural spines: less than the length of the base (0); higher than the length of the base but less than 1.5 times the length of the base (1); greater than 1.5 times the length of the base (2). Ordered.
169. Shape of anterior dorsal neural spines: lateral margins parallel in anterior view (0); transversely expanding towards dorsal end (1).
170. Cross-sectional shape of dorsal neural spines: transversely compressed (0); broad and triangular (1); square-shaped in posterior vertebrae (2). Ordered.
171. Spinodiapophyseal lamina on dorsal vertebrae: absent (0); present and separated from spinopostzygapophyseal lamina (1); present and joining spinopostzygapophyseal lamina to create a composite posterolateral spinal lamina (2). Ordered.
172. Well-developed, sheet-like suprapostzygapophyseal laminae: absent (0); present on at least the caudal dorsal vertebrae (1).
173. Shape of the spinopostzygapophyseal lamina in middle and posterior dorsal vertebrae: singular (0); bifurcated at its distal end (1).
174. Shape of posterior margin of middle dorsal neural spines in lateral view: approximately straight (0); concave with a projecting posterodorsal corner (1).
175. Transversely expanded plate-like summits of posterior dorsal neural spines: absent (0); present (1).
176. Last presacral rib: free (0); fused to vertebra (1).
177. Sacral rib much narrower than the transverse process of the first primordial sacral vertebra (and dorsosacral if present) in dorsal view: absent (0); present (1).
178. Number of dorsosacral vertebrae: none (0); one (1); two (2). Ordered.
179. Caudosacral vertebra: absent (0); present (1).
180. Shape of the iliac articular facets of the first primordial sacral rib: singular (0); divided into dorsal and ventral facets separated by a non-articulating gap (1).
181. Depth of the iliac articular surface of the primordial sacrals: less than 0.75 of the depth of the ilium (0); greater than 0.75 of the depth of the ilium (1).
182. Sacral ribs contributing to the rim of the acetabulum: absent (0); present (1).
183. Posterior and anterior expansion of the transverse processes of the first and second primordial sacral

vertebrae, respectively, partly roofing the intercostal space: absent (0); present (1).
184. Length of first caudal centrum: greater than its height (0); less than its height (1).
185. Length of base of the proximal caudal neural spines: less than (0), or greater than (1), half the length of the neural arch (Otero et al. 2015: c. 184).
186. Outline of basis of anterior caudal transverse processes in lateral view: oval to round (0), triangular, becoming higher anteriorly (1) (new character).
187. Position of postzygapophyses in proximal caudal vertebrae: protruding with an interpostzygapophyseal notch visible in dorsal view (0); placed on either side of the caudal end of the base of the neural spine without any interpostzygapophyseal notch (1).
188. A hyposphenal ridge on caudal vertebrae: absent (0); present (1).
189. Prezygadiapophyseal laminae on anterior caudals: absent (0); present (1).
190. Depth of the bases of the proximal caudal transverse processes: shallow, restricted to the neural arches (0); deep, extending from the centrum to the neural arch (1).
191. Position of last caudal vertebra with a protruding transverse process: distal to caudal 16 (0); proximal to caudal 16 (1).
192. Orientation of posterior margin of proximal caudal neural spines: sloping posterodorsally (0); vertical (1).
193. Longitudinal ventral sulcus on proximal and middle caudal vertebrae: present (0); absent (1).
194. Length of midcaudal centra: greater than twice the height of their anterior faces (0); less than twice the height of their anterior faces (1).
195. Cross-sectional shape of the distal caudal centra: oval with rounded lateral and ventral sides (0); square-shaped with flattened lateral and ventral sides (1).
196. Length of distal caudal prezygapophyses: short, not overlapping the preceding centrum by more than a quarter (0); long and overlapping the preceding the centrum by more than a quarter (1).
197. Shape of the terminal caudal vertebrae: unfused, size decreasing toward tip (0); expanded and fused to form a club-shaped tail (1).
198. 'Weaponized' dermal spikes on tail: absent (0); present (1).
199. Length of the longest chevron: less than twice the length of the preceding centrum (0); greater than twice the length of the preceding centrum (1).
200. Anteroventral process on distal chevrons: absent (0); present (1).
201. Mid-caudal chevrons with a ventral slit: absent (0); present (1).
202. Longitudinal ridge on the dorsal surface of the sternal plate: absent (0); present (1).
203. Craniocaudal length of the acromion process of the scapula: less than 1.5 times the minimum width of the scapula blade (0); greater than 1.5 times the minimum width of the scapula blade (1).
204. Minimum width of the scapula: greater than 20% of its length (0); less than 20% of its length (1).
205. Caudal margin of the acromion process of the scapula: rises from the blade at angle that is less than 65° from the long axis of the scapula, at its steepest point (0); rises from the blade at angle that is greater than 65° from the long axis of the scapula, at its steepest point (1).
206. Ventromedial ridge of scapula: absent (0) or present (1).
207. Width of dorsal expansion of the scapula: less than the width of the ventral end of the scapula (0); equal to the width of the ventral end of the scapula (1).
208. Flat caudoventrally facing surface on the coracoids between glenoid and coracoid tubercle: absent (0); present (1).
209. Coracoid tubercle: present (0); absent (1).
210. Length of the humerus: less than 55% of the length of the femur (0); 55–65% of the length of the femur (1); 65–70% of the length of the femur (2); more than 70% of the length of the femur (3). Ordered.
211. Shape of the humeral head: weakly developed, rounded in anterior–posterior view but minimally expanded perpendicular to the latter axis (0); flat in anterior–posterior view with only a slightly expanded lateral component (1); domed, being convex/hemispherical in anterior–posterior view with a strong lateral incursion onto the humeral shaft (2) (Unordered).
212. Shape of the deltopectoral crest: subtriangular (0); subrectangular (1).
213. Length of the deltopectoral crest of the humerus: less than 30% of the length of the humerus (0); 30–50% of the length of the humerus (1); greater than 50% of the length of the humerus (2). Ordered.
214. Shape of the anterolateral margin of the deltopectoral crest of the humerus: straight (0); strongly sinuous (1).
215. Rugose pit centrally located on the lateral surface of the deltopectoral crest: absent (0); present (1).
216. Well-defined fossa on the distal flexor surface of the humerus: present (0); absent (1).
217. Posterior side of the distal end of the humerus: with large, shallow, triangular depression that cov-

ers more or less all of the posterior side (0), with only narrow median depression, bounded by transversely convex lateral and medial Sects. (1) (new character).
218. Transverse width of the distal humerus: less than 33% of the length of the humerus (0); greater than 33% of the length of the humerus (1).
219. Shape of the entepicondyle of the distal humerus: rounded process (0): with a flat distomedially facing surface bounded by a sharp proximal margin (1).
220. Length of the radius: greater than 80% of the humerus (0); less than 80% of the humerus (1).
221. Caudodistal tubercle of the radius: absent (0) or present (1).
222. 368.Biceps tubercle of the radius: absent (0) or present (1).
223. Deep radial fossa, bounded by an anterolateral process, on proximal ulna: absent (0); present (1).
224. Medial expansion of posterior part of proximal end of the ulna: present, proximal surface T-shaped or irregularly club-shaped (0), absent, proximal end hook-shaped (1) (new character).
225. Olecranon process on proximal ulna: present (0); absent (1).
226. Maximum linear dimensions of the ulnare and radiale: exceed that of at least one of the first three distal carpals (0); less than any of the distal carpals (1).
227. Transverse width of the first distal carpal: less than 120% of the transverse width of the second distal carpal (0); greater than 120% of the transverse width of the second distal carpal (1).
228. Sulcus across the medial end of the first distal carpal:absent (0); present (1).
229. Lateral end of first distal carpal: abuts second distal carpal (0); overlaps second distal carpal (1).
230. Second distal carpal: completely covers the proximal end of the second metacarpal (0); does not completely cover the proximal end of the second metacarpal (1).
231. Ossification of the fifth distal carpal: present (0); absent (1).
232. Length of the manus: less than 38% of the humerus + radius (0); 38–45% of the humerus + radius (1); greater than 45% of the humerus + radius (2). Ordered.
233. Shape of metacarpus: flattened to gently curved and spreading (0); a colonnade of subparallel metacarpals tightly curved into a U-shape (1).
234. Proximal width of first metacarpal: less than the proximal width of the second metacarpal (0); greater than the proximal width of the second metacarpal (1).
235. Minimum transverse shaft width of first metacarpal: less than twice the minimum transverse shaft width of second metacarpal (0); greater than twice the minimum transverse shaft width of second metacarpal (1).
236. Proximal end of first metacarpal: flush with other metacarpals (0); inset into the carpus (1).
237. Shape of the first metacarpal: proximal width less than 65% of its length (0); proximal width 65–80% of its length (1); proximal width 80–100% of its length (2); greater than 100% of its length (3). Ordered.
238. Ventromedial margin of first metacarpal: straight or slightly concave (0) or deeply concave (1).
239. Strong asymmetry in the lateral and medial distal condyles of the first metacarpal: absent (0); present (1).
240. Deep distal extensor pits on the second and third metacarpals: absent (0); present (1).
241. Shape of the distal ends of second and third metacarpals: subrectangular in distal view (0); trapezoidal with flexor rims of distal collateral ligament pits flaring beyond extensor rims (1).
242. Shape of the fifth metacarpal: longer than wide at the proximal end with a flat proximal surface (0); almost as wide as it is long with a strongly convex proximal articulation surface (1).
243. Length of the fifth metacarpal: less than 75% of the length of the third metacarpal (0); greater than 75% of the length of the third metacarpal (1).
244. Length of manual digit one: less than the length of manual digit two (0); greater than the length of manual digit two (1).
245. Ventrolateral twisting of the transverse axis of the distal end of the first phalanx of manual digit one relative to its proximal end: absent (0); present but much less than 60° (1); 60° (2). Ordered.
246. Length of the first phalanx of manual digit one: less than the length of the first metacarpal (0); greater than the length of the first metacarpal (1).
247. Shape of the proximal articular surface of the first phalanx of manual digit one: rounded (0); with an embayment on the medial side (1).
248. Shape of the first phalanx of manual digit one: elongate and subcylindrical (0); strongly proximodistally compressed and wedge-shaped (1).
249. Length of first phalanx of manual digit 1: much greater than (0), subequal or equal to (1), or much less than (2), its mediolateral width at proximal end.

250. Length of the penultimate phalanx of manual digit two: less than the length of the second metacarpal (0); greater than the length of the second metacarpal (1).
251. Length of the penultimate phalanx of manual digit three: less than the length of the third metacarpal (0); greater than the length of the third metacarpal (1).
252. Shape of non-terminal phalanges of manual digits two and three: longer than wide (0); as long as wide (1).
253. Shape of the unguals of manual digits two and three: straight (0); strongly curved with tips projecting well below flexor margin of proximal articular surface (1).
254. Length of the ungual of manual digit two: greater than the length of the ungual of manual digit one (0); 75-100% of the ungual of manual digit one (1); less than 75% of the ungual of manual digit one (2); the ungual of manual digit two is absent (3). Ordered.
255. Phalangeal formula of manual digits two and three: three and four, respectively (0); with at least one phalanx missing from each digit (1).
256. Phalangeal formula of manual digits four and five: greater than 2–0, respectively (0); less than 2–0, respectively (1).
257. Strongly convex dorsal margin of the ilium: absent (0); present (1).
258. Cranial extent of preacetabular process of ilium: does not project further anterior than the anterior margin of the pubic peduncle (0); projects anterior to the cranial margin of the pubic peduncle (1).
259. Shape of the preacetabular process: blunt and rectangular (0); with a pointed, projecting anteroventral corner and a rounded dorsum (1).
260. Depth of the preacetabular process of the ilium: much less than the depth of the ilium above the acetabulum (0); subequal to the depth of the ilium above the acetabulum (1).
261. Length of preacetabular process of the ilium: less than twice its depth (0); greater than twice its depth (1).
262. Supraacetabular crest on the anterodorsal margin of the acetabulum: absent (0), present (1) (modified from Gauthier 1986).
263. Medial wall of acetabulum: fully closing acetabulum with a triangular ventral process between the pubic and ischial peduncles (0); partially open acetabulum with a straight ventral margin between the peduncles (1); partially open acetabulum with a concave ventral margin between the peduncles (2); fully open acetabulum with medial ventral margin closely approximating lateral rim of acetabulum (3). Ordered.
264. Length of the pubic peduncle of the ilium: less than twice the anteroposterior width of its distal end (0); greater than twice the anteroposterior width of its distal end (1).
265. Distal articular surface of the pubic peduncle of the ilium: undivided, facing mainly ventrally or anteroventrally (0), divided into a more anteriorly facing and a more ventrally facing facet by a notable kink (1) (Rauhut 2003b).
266. Articular surface of the ischial peduncle of the ilium: flat to slightly convex (0), strongly convex anteroposteriorly, semicircular in lateral view (1) (new character). In most non-sauropodan sauropodomorphs, the articular facet for the ischium on the ischia peduncle of the ilium is flat or bluntly convex anteroposteriorly. In *Schleitheimia*, sauropods, and a few other sauropodomorph taxa, such as *Leonerasaurus* and *Panphagia*, the articular surface of the ischial peduncle is pronouncedly convex anteroposteriorly, being semicircular in lateral view (Fig. 18).
267. Caudally projecting 'heel' at the distal end of the ischial peduncle: absent (0); present (1).
268. Length of the ischial peduncle of the ilium: similar to pubic peduncle (0); much shorter than pubic peduncle (1); virtually absent so that the chord connecting the distal end of the pubic peduncle with the ischial articular surface contacts the postacetabular process (2). Ordered.
269. Length of the postacetabular process of the ilium: between 40 and 100% of the distance between the pubic and ischial peduncles (0); less than 40% of the distance between the pubic and ischial peduncles (1); more than 100% of the distance between the pubic and ischial peduncles (2).
270. Well-developed brevis fossa with sharp margins on the ventral surface of the postacetabular process of the ilium: absent (0); present, ventrally facing (1); present, lateroventrally facing (2).
271. Anterior end of ventrolateral ridge bounding brevis fossa: not connected to supracetabular crest (0); joining supracetabular crest (1).
272. Shape of the caudal margin of the postacetabular process of the ilium: rounded to bluntly pointed (0); square ended (1); with a pointed ventral corner and a rounded caudodorsal margin (2).
273. Width of the conjoined pubes: less than 75% of their length (0); greater than 75% of their length (1).
274. Pubic tubercle on the lateral surface of the proximal pubis: present (0); absent (1).

275. Proximal anterior profile of pubis: anterior margin of pubic apron smoothly confluent with anterior margin of iliac pedicel (0); iliac pedicel set anterior to the pubic apron creating a prominent inflection in the proximal anterior profile of the pubis (1).
276. Minimum transverse width of the pubic apron: much more than 40% of the width across the iliac peduncles of the ilium (0); less than 40% of the width across the iliac peduncles of the ilium (1).
277. Position of the obturator foramen of the pubis: at least partially occluded by the iliac pedicel in anterior view (0); completely visible in anterior view (1).
278. Lateral margins of the pubic apron in anterior view: straight (0); concave (1).
279. Anterior fossa on the proximal region of the pubic apron: absent (0) or present (1).
280. Orientation of distal third of the blades of the pubic apron: confluent with the proximal part of the pubic apron (0); twisted posterolaterally relative to proximal section so that the anterior surface turns to face laterally (1).
281. Orientation of the entire blades of the pubic apron: transverse (0); twisted posteromedially (1).
282. Craniocaudal expansion of the distal pubis: absent (0); less than 15% of the length of the pubis (1); greater than 15% of the length of the pubis (2). Ordered.
283. Notch separating posteroventral end of the ischial obturator plate from the ischial shaft: present (0); absent (1).
284. Elongate interischial fenestra: absent (0); present (1).
285. Longitudinal dorsolateral sulcus on proximal ischium: absent (0); present (1).
286. Shape of distal ischium: broad and plate-like, not distinct from obturator region (0); with a discrete rod-like distal shaft (1).
287. Length of ischium: less than that of the pubis (0); greater than that of the pubis (1).
288. Ischial component of acetabular rim: larger than the pubic component (0); equal to the pubic component (1).
289. Shape of the transverse section of the ischial shaft: ovoid to subrectangular (0); triangular (1).
290. Orientation of the long axes of the transverse section of the distal ischia: meet at an angle (0); are coplanar (1).
291. Depth of the transverse section of the ischial shaft: much less than the transverse width of the Sect. (0); at least as great as the transverse width of the Sect. (1).
292. Distal ischial expansion: absent (0); present (1).
293. Transverse width of the conjoined distal ischial expansions: greater than their sagittal depth (0); less than their sagittal depth (1).
294. Length of the hindlimb: greater than the length of the trunk (0); less than the length of the trunk (1).
295. Longitudinal axis of the femur in lateral view: strongly bent with an offset between the proximal and distal axes greater than 15° (0); weakly bent with an offset of less than 10° (1); straight (2). Ordered.
296. Shape of the cross-section of the mid-shaft of the femur: subcircular (0); strongly elliptical with the long axis orientated mediolaterally (1).
297. Angle between the long axis of the femoral head and the transverse axis of the distal femur: about 30° (0); close to 0° (1).
298. Shape of femoral head: roughly rectangular in profile with a sharp medial distal corner (0); roughly hemispherical with no sharp medial distal corner (1).
299. Posterior proximal tubercle on femur: well-developed (0); indistinct to absent (1).
300. Shape of the lesser trochanter: small rounded tubercle (0); proximodistally orientated, elongate ridge (1); absent (2).
301. Position of proximal tip of lesser trochanter: level with the femoral head (0); distal to the femoral head (1).
302. Projection of the lesser trochanter: just a scar upon the femoral surface (0); a raised process (1).
303. Transverse ridge extending laterally from the lesser trochanter: absent (0); present (1).
304. Height of the lesser trochanter in cross section: less than its basal width (0); at least as high as its basal width (1).
305. Position of the lesser trochanter in anterior view: near the centre of the anterior face of the femoral shaft (0); close to the lateral margin of the femoral shaft (1).
306. Visibility of the lesser trochanter in posterior view: not visible (0); visible (1).
307. Height of the fourth trochanter: a tall crest (0); a low rugose ridge(1).
308. Position of the fourth trochanter along the length of the femur: in the proximal half (0); straddling the midpoint (1).
309. Symmetry of the profile of the fourth trochanter of the femur: subsymmetrical without a sharp distal corner (0); asymmetrical with a steeper distal slope than the proximal slope and a distinct distal corner (1); symmetrical, with sharp proximal and distal corner (2).

310. Shape of the profile of the fourth trochanter of the femur: rounded (0); subrectangular (1).
311. Position of fourth trochanter along the mediolateral axis of the femur: centrally located (0); on the medial margin (1).
312. Extensor depression on anterior surface of the distal end of the femur: absent (0); present (1).
313. Size of the medial condyle of the distal femur: subequal to the fibular + lateral condyles (0); larger than the fibular + lateral condyles (1).
314. Posterior surface of the crista tibiofemoralis: rounded transversely (0), with flattened, posteromedially facing surface (1) (new character). In sauropodomorph outgroups, sauropods, and several non-sauropodan sauropodomorphs, the posteriorly expanded condyle of the crista tibiofemoralis is rounded transversely. In many other non-sauropodan sauropodomorphs, including *Schleitheimia*, there is a flattened, posteromedially inclined plateau on the posterior side of the crista, the inclination of which can vary between taxa. In distal view, this plateau is visible as a straight, posteromedially inclined edge of the crista tibiofemoralis (see Fig. 20).
315. Distal surface of tibiofibular crest: as deep anteroposteriorly as wide mediolaterally or deeper (0); wider mediolaterally than deep anteroposteriorly (1).
316. Tibia:femur length ratio: greater than 1.0 (0); between 0.6 and 1.0 (1); less than 0.6 (2). Ordered.
317. Orientation of cnemial crest: projects anteriorly to anterolaterally (0); projecting laterally (1).
318. Paramarginal ridge on lateral surface of cnemial crest: absent (0); present (1).
319. Position of the tallest point of the cnemial crest: close to the proximal end of the crest (0); about half-way along the length of the crest, creating an anterodorsally sloping proximal margin of the crest (1).
320. Proximal end of tibia with a flange of bone that contacts the fibula: absent (0): present (1).
321. Position of the posterior end of the fibular condyle on the proximal articular surface tibia: anterior to the posterior margin of the proximal articular surface (0); level with the posterior margin of the proximal articular surface (1).
322. Shape of the proximal articular surface of the tibia: transverse width subequal to anteroposterior length (0); transverse width between 0.6 and 0.9 times anteroposterior length (1); anteroposterior length twice the transverse width or higher (2). Ordered.
323. Transverse width of the distal tibia: subequal to its craniocaudal length (0); greater than its craniocaudal length (1).
324. Anteroposterior width of the lateral side of the distal articular surface of the tibia: as wide as the anteroposterior width of the medial side (0); narrower than the anteroposterior width of the medial side (1).
325. Relationship of the posterolateral process of the distal end of the tibia with the fibula: not flaring laterally and not making significant contact with the fibula (0); flaring laterally and backing the fibula (1).
326. Shape of the distal articular end of the tibia in distal view: ovoid (0); subrectangular (1).
327. Shape of the anteromedial corner of the distal articular surface of the tibia: forming a right angle (0); forming an acute angle (1).
328. Position of the lateral margin of descending caudoventral process of the distal end of the tibia: protrudes laterally at least as far as the anterolateral corner of the distal tibia (0); set well back from the anterolateral corner of the distal tibia (1).
329. A triangular rugose area on the medial side of the fibula: absent (0); present (1).
330. Transverse width of the midshaft of the fibula: greater than 0.75 of the transverse width of the midshaft of the tibia (0); between 0.5 and 0.75 of the transverse width of the midshaft of the tibia (1); less than 0.5 of the transverse width of the midshaft of the tibia (2). Ordered.
331. Position of fibula trochanter: on anterior surface of fibula (0); laterally facing (1); anteriorly facing but with strong lateral bulge (2).
332. Depth of the medial end of the astragalar body in cranial view: roughly equal to the lateral end (0); much shallower creating a wedge-shaped astragalar body (1).
333. Shape of the posteromedial margin of the astragalus in dorsal view: forming a moderately sharp corner of a subrectangular astragalus (0); evenly rounded without formation of a caudomedial corner (1).
334. Dorsally facing horizontal shelf forming part of the fibular facet of the astragalus: present (0); absent with a largely vertical fibular facet (1).
335. Pyramidal dorsal process on the posteromedial corner of the astragalus: absent (0); present (1).
336. Shape of the ascending process of the astragalus: anteroposteriorly deeper than transversely wide (0); transversely wider than anteroposteriorly deep (1).

337. Posterior extent of ascending process of the astragalus: positioned anteriorly upon the astragalus (0); close to the posterior margin of the astragalus (1).
338. Sharp medial margin around the depression posterior to the ascending process of the astragalus: absent (0); present (1).
339. Buttress dividing posterior fossa of astragalus and supporting ascending process: absent (0); present (1).
340. Vascular foramina set in a fossa at the base of the ascending process of the astragalus: present (0); absent (1).
341. Mediolateral surface of distal astragalus straight (0), concave (1), or convex (2).
342. Posterior margin of astragalus: straight (0) or convex (1).
343. Distal articular surface of astragalus: relatively flat or weakly convex (0); extremely convex and roller-shaped (1).
344. Transverse width of the calcaneum: greater than 30% of the transverse width of the astragalus (0); less than 30% of the transverse width of the astragalus (1).
345. Lateral surface of calcaneum: simple (0); with a fossa (1).
346. Medial peg of calcaneum fitting into astragalus: present, even if rudimentary (0); absent (1).
347. Calcaneal tuber: large and well developed (0); highly reduced to absent (1).
348. Shape of posteromedial heel of distal tarsal four (lateral distal tarsal): proximodistally deepest part of the bone (0); no deeper than the rest of the bone (1).
349. Shape of posteromedial process of distal tarsal four in proximal view: rounded (0); pointed (1).
350. Ossified distal tarsals: present (0); absent (1).
351. Proximal width of the first metatarsal: less than the proximal width of the second metatarsal (0); at least as great as the proximal width of the second metatarsal (1).
352. Size of first metatarsal: maximum proximal breadth less than 0.4 times its proximodistal length (0); maximum proximal breadth between 0.4 and 0.7 times its proximodistal length (1); maximum proximal breadth greater than 0.7times its proximodistal length (2). Ordered.
353. Orientation of proximal articular surface of metatarsal one: horizontal (0); sloping proximolaterally relative to the long axis of the bone (1).
354. Shaft of metatarsal I: closely appressed to metatarsal II throughout its length (0); only closely appressed proximally, with a space between metatarsals I and II distally (1).
355. Orientation of the transverse axis of the distal end of metatarsal one: horizontal (0); angled proximomedially (1).
356. Shape of the medial margin of the proximal surface of the second metatarsal: straight (0); concave (1).
357. Shape of the lateral margin of the proximal surface of the second metatarsal: straight (0); concave (1).
358. Projection of ventral flange on proximal surface of second metatarsal: neither corner appreciably more developed than the other (0); laterally flaring (1); medially flaring (2).
359. Well-developed facet on proximolateral corner of plantar ventrolateral flange of mt II for articulation with medial distal tarsal: absent (0); present (1).
360. Length of the third metatarsal: greater than 40% of the length of the tibia (0); less than 40% of the length of the tibia (1).
361. Proximal outline of metatarsal III: subtriangular with acute or rounded posterior border (0); subtrapezoidal, with posterior border broadly exposed in plantar view (1).
362. Minimum transverse shaft diameters of third and fourth metatarsals: greater than 60% of the minimum transverse shaft diameter of the second metatarsal (0); less than 60% of the minimum transverse shaft diameter of the second metatarsal (1).
363. Transverse width of the proximal end of the fourth metatarsal: less than twice the anteroposterior depth of the proximal end (0); at least twice the anteroposterior depth of the proximal end (1).
364. Angle formed by the anterior and anteromedial borders of metatarsal IV: obtuse (0); right angle, or acute (1).
365. Transverse width of the proximal end of the fifth metatarsal: less than 25 percent of the length of the fifth metatarsal (0); between 30 and 49 percent of the length of the fifth metatarsal (1); greater than 50 percent of the length of the fifth metatarsal (2). Ordered.
366. Transverse width of distal articular surface of metatarsal four in distal view: greater than the anteroposterior depth (0); less than the anteroposterior depth (1).
367. Pedal digit five: reduced, non-weight bearing (0); large (fifth metatarsal at least 70% of fourth metatarsal), robust and weight bearing (1).
368. Length of non-terminal pedal phalanges: all longer than wide (0); proximalmost phalanges longer than wide while more distal phalanges are as wide as long (1); all non-terminal phalanges are as wide, if not wider, than long(2).Ordered.
369. Length of the first phalanx of pedal digit one: greater than the length of the ungual of pedal digit

one (0); less than the length of the ungual of pedal digit one (1).

370. Length of the ungual of pedal digit one: less than at least some non-terminal phalanges (0); longer than all non-terminal phalanges but shorter than first metatarsal (1); longer than the first metatarsal (2). Ordered.
371. Shape of the ungual of pedal digit one: shallow, pointed, with convex sides and a broad ventral surface (0); deep, abruptly tapering, with flattened sides and a narrow ventral surface (1).
372. Shape of proximal articular surface of pedal unguals: proximally facing, visible on medial and lateral sides (0); proximomedially facing and visible only in medial view, causing medial deflection of pedal unguals in articulation (1).
373. Penultimate phalanges of pedal digits two and three: well-developed (0); reduced disc-shaped elements if they are ossified at all (1).
374. Shape of the unguals of pedal digits two and three: dorsoventrally deep with a proximal articulating surface that is at least as deep as it is wide (0); dorsoventrally flattened with a proximal articulating surface that iswider than deep (1).
375. Length of the ungual of pedal digit two: greater than the length of the ungual of pedal digit one (0); between 90 and 100% of the length of the ungual of pedal digit one (1); less than 90% of the length of the ungual of pedal digit one (2). Ordered.
376. Size of the ungual of pedal digit three: greater than 85% of the ungual of pedal digit two in all linear dimensions (0); less than 85% of the ungual of pedal digit two in all linear dimensions (1).
377. Number of phalanges in pedal digit four: four (0); fewer than four (1).
378. Phalanges of pedal digit five: present (0); absent (1).
379. Articular surface of the long bones of the limbs: smooth or with some irregularly distributed grooves and ridges (0), intensely rugosely pitted (1) (new character). Strongly pitted articular surfaces, probably indicating an extensive cartilage cap, have long been recognized as a typical character of sauropod limb bones (see Holliday et al. 2010; Sander et al. 2011). Although this structure is probably at least somewhat related to their large size, such an extensive pitting is not seen in large-bodied basal sauropodomorphs, such as *Lessemsaurus* (Pol and Powell 2007a) or *Ledumahadi* (McPhee et al. 2018), which have only a few pits and grooves on the articular surfaces of the long bones.
380. Femoral length: less than 200 mm (0); between 200 and 399 mm (1); between 400 and 599 mm (2); between 600 and 799 mm (3); between 800 and 1000 mm (4); greater than 1000 mm (5). Ordered.
381. Growth marks (LAGs or annuli) in the cortex: present (0); absent or only present in the outer cortex (1).
382. Relative abundance of parallel-fibered bone (PFB) and woven fibered bone (WFB): PFB > WFB (0), WFB > PFB (1).

Received: 14 January 2020 Accepted: 11 April 2020
Published online: 01 July 2020

References

Achilles, H., & Schlatter, R. (1986). Palynostratigraphische Untersuchungen im 'Rhät-Bonebed' von Hallau (Kt. Schaffhausen) mit einem Beitrag zur Ammonitenfauna im basalen Lias. *Eclogae Geologicae Helvetiae, 79,* 149–179.

Allain, R., & Aquesbi, N. (2008). *Tazoudasaurus naimi* (Dinosauria, Sauropoda) from the late Early Jurassic of Morocco. *Geodiversitas, 30,* 345–424.

Allain, R., & Läng, É. (2009). Origine et évolution des saurischiens. *Comptes Rendus Palevol, 8,* 243–256.

Apaldetti, C., Martínez, R. N., Cerda, I. A., Pol, D., & Alcober, O. (2018). An early trend towards gigantism in Triassic sauropodomorph dinosaurs. *Nature Ecology and Evolution, 2,* 1227–1232.

Apaldetti, C., Martínez, R. N., Pol, D., & Souter, T. (2014). Redescription of the skull of *Coloradisaurus brevis* (Dinosauria, Sauropodomorpha) from the Late Triassic Los Colorados Formation of the Ischigualasto-Villa Union Basin, northwestern Argentina. *Journal of Vertebrate Paleontology, 34,* 1113–1132.

Apaldetti, C., Pol, D., & Yates, A. M. (2013). The postcranial anatomy of *Coloradisaurus brevis* (Dinosauria: Sauropodomorpha) from the Late Triassic of Argentina and its phylogenetic implications. *Palaeontology, 56,* 277–301.

Barrett, P. M., Chapelle, K. E. J., Staunton, C. K., Botha, J., & Choiniere, J. N. (2019). Postcranial osteology of the neotype specimen of *Massospondylus carinatus* Owen, 1854 (Dinosauria: Sauropodomorpha) from the upper Elliot Formation of South Africa. *Palaeontologia Africana, 53,* 114–178.

Bates, K. T., Mannion, P. D., Falkingham, P. L., Brusatte, S. L., Hutchinson, J. R., Otero, A., et al. (2016). Temporal and phylogenetic evolution of the sauropod dinosaur body plan. *Royal Society Open Science, 3,* 150636.

Bernardi, M., Gianolla, P., Petti, F., Mietto, P., & Benton, M. (2018). Dinosaur diversification linked with the Carnian Pluvial Episode. *Nature Communications, 9,* 1499.

Bonaparte, J. F. (1979). Dinosaurs: a Jurassic assemblage from Patagonia. *Science, 205,* 1377–1379.

Bonaparte, J. F. (1986). Les Dinosaures (Carnosaures, Allosauridés, Sauropodes, Cétiosauridés) du Jurassique moyen de Cerro Cóndor (Chubut, Argentine). *Annales de Paléontologie, 72*(247–289), 326–386.

Bonaparte, J. F. (1999). Evolución de las vértebras presacras en Sauropodomorpha. *Ameghiniana, 36,* 115–187.

Bonaparte, J. F., & Vince, M. (1979). El hallazgo del primer nido de Dinosaurios Triasicos, (Saurischia, Prosauropoda), Triasico Superior de Patagonia, Argentina. *Ameghiniana, 16,* 173–182.

Buffetaut, E., Suteethorn, V., Cuny, G., Tong, H., Le Loeuff, J., Khansubha, S., et al. (2000). The earliest known sauropod dinosaur. *Nature, 407,* 72–74.

Butler, R. J., Porro, L. B., & Heckert, A. B. (2006). A supposed heterodontosaurid tooth from the Rhaetian of Switzerland and a reassessment of the European Late Triassic record of Ornithischia (Dinosauria). *Neues Jahrbuch für Geologie und Paläontologie Monatshefte, 2006,* 613–633.

Cabreira, S., Kellner, A., Dias-Da-Silva, S., Da Silva, L., Bronzati, M., Marsola, J., et al. (2016). A unique Late Triassic dinosauromorph assemblage reveals dinosaur ancestral anatomy and diet. *Current Biology, 26,* 3090–3095.

Cabrera, A. (1947). Un saurópodo nuevo del Jurásico de Patagonia. *Notas del Museo de La Plata, Paleontología, 12,* 1–17.
Carballido, J. L., Holwerda, F. M., Pol, D., & Rauhut, O. W. M. (2017). An Early Jurassic sauropod tooth from Patagonia (Cañadón Asfalto Formation): implications for sauropod diversity. *Publicación Electrónica de la Asociación Paleontológica Argentina, 17,* 50–57.
Carballido, J. L., & Sander, P. M. (2014). Postcranial axial skeleton of *Europasaurus holgeri* (Dinosauria, Sauropoda) from the Upper Jurassic of Germany: implications for sauropod ontogeny and phylogenetic relationships of basal Macronaria. *Journal of Systematic Palaeontology, 12,* 335–387.
Casamiquela, R. M. (1963). Consideraciones acerca de *Amygdalodon* Cabrera (Sauropoda, Cetiosauridae) del Jurásico Medio de la Patagonia. *Ameghiniana, 3,* 79–95.
Clemens, W. A. (1980). Rhaeto-Liassic mammals from Switzerland and West Germany. *Abhandlungen der Bayerischen Staatssammlung für Paläontologie und historischen Geologie, 5,* 51–92.
Cooper, M. R. (1984). A reassessment of *Vulcanodon karibaensis* Raath (Dinosauria: Saurischia) and the origin of the Sauropoda. *Palaeontologia africana, 25,* 203–231.
Etzold, A., & Schweitzer, V. (2005). Der Keuper in Baden-Württemberg. Deutsche Stratigraphische Kommission, 2005: Stratigraphie von Deutschland IV: Keuper. *Courier Forschungsinsitut Senckenberg, 253,* 214–258.
Ezcurra, M. D. (2010). A new early dinosaur (Saurischia: Sauropodomorpha) from the Late Triassic of Argentina: a reassessment of dinosaur origin and phylogeny. *Journal of Systematic Palaeontology, 8,* 371–425.
Fechner, R., & Gössling, R. (2014). The gastralial apparatus of *Plateosaurus engelhardti*: morphological description and soft-tissue reconstruction. *Palaeontologia Electronica, 17.1.13,* 1–11.
Foster, J. R. (2003). Paleoecological analysis of the vertebrate fauna of the Morrison Formation (Upper Jurassic), Rocky Mountain Region, USA. *Bulletin of the New Mexico Museum of Natural History & Science, 23,* 1–95.
Galton, P. M. (1985). Notes on the Melanorosauridae, a family of large prosauropod dinosaurs (Saurischia: Sauropodomorpha). *Geobios, 18,* 671–676.
Galton, P. M. (1986). Prosauropod dinosaur *Plateosaurus* (= *Gresslyosaurus*) (Saurischia: Sauropodomorpha) from the Upper Triassic of Switzerland. *Geologica et Palaeontologica, 20,* 167–183.
Galton, P. M. (1998). Saurischian dinosaurs from the Upper Triassic of England: *Camelotia* (Prosauropoda, Melanorosauridae) and *Avalonianus* (Theropoda,?Carnosauria). *Palaeontgraphica A, 250,* 155–172.
Galton, P. M. (2001a). Prosauropod dinosaurs from the Upper Triassic of Germany. *Actas de las I Jornadas internacionales sobre Paleontología de Dinosaurios y su entorno* (pp. 25–92). Burgos: Colectivo Arqueológico-Paleontológico de Salas.
Galton, P. M. (2001b). The prosauropod dinosaur *Plateosaurus* Meyer, 1837 (Saurischia: Sauropodomorpha; Upper Triassic). II. Notes on the referred species. *Revue de Paléobiologie, 20,* 435–502.
Galton, P. M., & Heerden, J. V. (1985). Partial hindlimb of *Blikanasaurus cromptoni* n. gen. and n. sp., representing a new family of prosauropod dinosaurs from the Upper Triassic of South Africa. *Geobios, 18,* 509–516.
Galton, P. M., & Upchurch, P. (2004). Prosauropoda. In D. B. Weishampel, P. Dodson, & H. Osmólska (Eds.), *The Dinosauria* (2nd ed., pp. 232–258). Berkeley: University of California Press.
Gauthier, J. (1986). Saurischian monophyly and the origin of birds. *Memoirs of the Californian Academy of Science, 8,* 1–55.
Goloboff, P. A., Farris, J. S., & Nixon, K. C. (2008). TNT, a free program for phylogenetic analysis. *Cladistics, 24,* 774–786.
Goloboff, P. A., Torres, A., & Arias, J. S. (2018). Weighted parsimony outperforms other methods of phylogenetic inference under models appropriate for morphology. *Cladistics, 34,* 407–437.
Hofmann, F. (1981). *Erläuterungen zu Blatt 74: Neunkirch (LK 1031) des Geologischen Atlas der Schweiz 1:25 000.* Schweizerische Geologische Kommission. 49 pp.
Hofmann, R., & Sander, P. (2014). The first juvenile specimens of *Plateosaurus engelhardti* from Frick, Switzerland: isolated neural arches and their implications for developmental plasticity in a basal sauropodomorph. *Peerj, 2,* e458.
Holliday, C. M., Ridgely, R. C., Sedlmayr, J. C., & Witmer, L. M. (2010). Cartilaginous epiphyses in extant archosaurs and their implications for reconstructing limb function in dinosaurs. *PLoS ONE, 5,* e13120.
Huene, F. V. (1907). Die Dinosaurier der europäischen Triasformation mit Berücksichtigung der aussereuropäischen Vorkommnisse. *Geologische und Paläontologische Abhandlungen, 1,* 1–419.
Huene, F. V. (1926). Vollständige Osteologie eines Plateosauriden aus dem schwäbischen Keuper. *Geologische und Palaeontologische Abhandlungen, Neue Folge, 15,* 139–179.
Huene, F. V. (1932). Die fossile Reptil-Ordnung Saurischia, ihre Entwicklung und Geschichte. *Monographien zur Geologie und Palaeontologie (Serie 1)* 4, 1-361.
Jordan, P., Pietsch, J., Blasi, H., Furrer, H., Kundig, N., Looser, N., et al. (2016). The middle to late Triassic Bankerjoch and Klettgau formations of northern Switzerland. *Swiss Journal of Geosciences, 109,* 257–284.
Kutty, T. S., Chatterjee, S., Galton, P. M., & Upchurch, P. (2007). Basal sauropodomorphs (Dinosauria: Saurischia) from the Lower Jurassic of India: their anatomy and relationships. *Journal of Paleontology, 81,* 1218–1240.
Lallensack, J., Klein, H., Milan, J., Wings, O., Mateus, O., & Clemmensen, L. (2017). Sauropodomorph dinosaur trackways from the Fleming Fjord Formation of East Greenland: evidence for Late Triassic sauropods. *Acta Palaeontologica Polonica, 62,* 833–843.
Langer, M. C. (2003). The pelvic and hind limb anatomy of the stem-sauropodomorph *Saturnalia tupiniquim* (Late Triassic, Brazil). *PaleoBios, 23,* 1–40.
Looser, N., Schneebeli-Hermann, E., Furrer, H., Blattmann, T., & Bernasconi, S. M. (2018). Environmental Changes and Carbon Cycle Perturbations at the Triassic-Jurassic Boundary in Northern Switzerland. *Swiss Journal of Geosciences, 111,* 445–460.
Maddison, W. P., Maddison, D. R. (2018). Mesquite: a modular system for evolutionary analysis. Version 3.5. http://mesquiteproject.org.
Marsicano, C. A., & Barredo, S. P. (2004). A Triassic tetrapod footprint assemblage from southern South America: palaeobiogeographical and evolutionary implications. *Palaeogeography, Palaeoclimatology, Palaeoecology, 203,* 313–335.
Martínez, R. N. (2009). *Adeopapposaurus mognai*, gen. et sp. nov. (Dinosauria: Sauropodomorpha), with comments on adaptations of basal Sauropodomorpha. *Journal of Vertebrate Paleontology, 29,* 142–164.
McPhee, B. W., Benson, R. B. J., Botha-Brink, J., Bordy, E. M., & Choiniere, J. M. (2018). A giant dinosaur from the Earliest Jurassic of South Africa and the transition to quadrupedality in early sauropodomorphs. *Current Biology, 28,* 1–9.
McPhee, B. W., Bonnan, M., Yates, A., Neveling, J., & Choiniere, J. (2015). A new basal sauropod from the pre-Toarcian Jurassic of South Africa: evidence of niche-partitioning at the sauropodomorph-sauropod boundary? *Scientific Reports, 5,* 13224.
McPhee, B. W., Bordy, E., Sciscio, L., & Choiniere, J. (2017). The sauropodomorph biostratigraphy of the Elliot Formation of southern Africa: tracking the evolution of Sauropodomorpha across the Triassic-Jurassic boundary. *Acta Palaeontologica Polonica, 62,* 441–465.
McPhee, B. W., & Choiniere, J. (2018). The osteology of *Pulanesaura eocollum*: implications for the inclusivity of Sauropoda (Dinosauria). *Zoological Journal of the Linnean Society, 182,* 830–861.
McPhee, B. W., Yates, A., Choiniere, J., & Abdala, F. (2014). The complete anatomy and phylogenetic relationships of *Antetonitrus ingenipes* (Sauropodiformes, Dinosauria): implications for the origins of Sauropoda. *Zoological Journal of the Linnean Society, 171,* 151–205.
Meyer, H. V. (1837). Brief an Prof. Bronn vom 4. April 1837. *Neues Jahrbuch für Mineralogie, Geognosie, Geologie und Petrefaktenkunde, 1837,* 314–316.
Meyer, C., & Thuring, B. (2003). Dinosaurs of Switzerland. *Comptes Rendus Palevol, 2,* 103–117.
Moser, M. (2003). *Plateosaurus engelhardti* Meyer, 1837 (Dinosauria: Sauropodomorpha) aus dem Feuerletten (Mittelkeuper; Obertrias) von Bayern. *Zitteliana B, 24,* 1–188.
Otero, A., Krupandan, E., Pol, D., Chinsamy, A., & Choiniere, J. (2015). A new basal sauropodiform from South Africa and the phylogenetic relationships of basal sauropodomorphs. *Zoological Journal of the Linnean Society, 174,* 589–634.
Otero, A., & Pol, D. (2013). Postcranial anatomy and phylogenetic relationships of *Mussaurus patagonicus* (Dinosauria, Sauropodomorpha). *Journal of Vertebrate Paleontology, 33,* 1138–1168.

Owen, R. (1842). Report on British fossil reptiles. Part II. *Reports of the British Association for the Advancement of Sciences, 11*, 60–204.
Peyer, B. (1943a). Beiträge zur Kenntnis von Rhät und Lias. *Eclogae Geologicae Helvetiae, 36,* 303–326.
Peyer, B. (1943b). Über Wirbeltierfunde aus dem Rhät von Hallau (Kt. Schaffhausen). *Eclogae Geologicae Helvetiae, 36,* 260–263.
Peyer, B. (1956). Über Zähne von Haramyiden, von Triconodonten und von wahrscheinlich synapsiden Reptilien aus dem Rhät von Hallau, Kt. Schaffhausen, Schweiz. *Schweizerische paläontologische Abhandlungen, 72,* 1–72.
Peyre de Fabrègues, C., & Allain, R. (2016). New material and revision of *Melanorosaurus thabanensis*, a basal sauropodomorph from the Upper Triassic of Lesotho. *Peerj, 4,* e1639.
Peyre de Fabrègues, C., Allain, R., & Barriel, V. (2015). Root causes of phylogenetic incongruence observed within basal sauropodomorph interrelationships. *Zoological Journal of the Linnean Society, 175,* 569–586.
Pol, D., Garrido, A., & Cerda, I. A. (2011). A new sauropodomorph dinosaur from the Early Jurassic of Patagonia and the origin and evolution of the sauropod-type sacrum. *PLoS ONE, 6,* e14572.
Pol, D., & Powell, J. E. (2007a). New information on *Lessemsaurus sauropoides* (Dinosauria: Sauropodomorpha) from the Upper Triassic of Argentina. *Special Papers in Palaeontology, 77,* 223–243.
Pol, D., & Powell, J. E. (2007b). Skull anatomy of *Mussaurus patagonicus* (Dinosauria: Sauropodomorpha) from the Late Triassic of Patagonia. *Historical Biology, 19,* 125–144.
Pol, D., & Rauhut, O. W. M. (2012). A Middle Jurassic abelisaurid from Patagonia and the early diversification of theropod dinosaurs. *Proceedings of the Royal Society London B, 279,* 3170–3175.
Prieto-Marquez, A., & Norell, M. A. (2011). Redescription of a nearly complete skull of *Plateosaurus* (Dinosauria: Sauropodomorpha) from the Late Triassic of Trossingen (Germany). *American Museum Novitas, 3727,* 1–58.
Racey, A., & Goodall, J. G. S. (2009). Palynology and stratigraphy of the Mesozoic Khorat Group red bed sequences from Thailand. *Geological Society of London Special Publications, 315,* 69–83.
Rauhut, O. W. M. (2003a). Revision of *Amygdalodon patagonicus* Cabrera, 1947 (Dinosauria: Sauropoda). *Mitteilungen aus dem Museum für Naturkunde in Berlin, Geowissenschaftliche Reihe, 6,* 173–181.
Rauhut, O. W. M. (2003b). The interrelationships and evolution of basal theropod dinosaurs. *Special Papers in Palaeontology, 69,* 1–213.
Rauhut, O. W. M. (2005). Osteology and relationships of a new theropod dinosaur from the Middle Jurassic of Patagonia. *Palaeontology, 48,* 87–110.
Rauhut, O. W. M., Fechner, R., Remes, K., & Reis, K. (2011). How to get big in the Mesozoic: the evolution of the sauropodomorph body plan. In N. Klein, K. Remes, C. T. Gee, & P. M. Sander (Eds.), *Biology of the sauropod dinosaurs: Understanding the life of giants* (pp. 119–149). Bloomington and Indianapolis: Indiana University Press.
Rauhut, O. W. M., Hübner, T. R., & Lanser, K.-P. (2016). A new megalosaurid theropod dinosaur from the late Middle Jurassic (Callovian) of northwestern Germany: implications for theropod evolution and faunal turnover in the Jurassic. *Palaeontologia Electronica, 19,* 1–65.
Reisdorf, A., Wetzel, A., Schlatter, R., & Jordan, P. (2011). The Staffelegg Formation: a new stratigraphic scheme for the Early Jurassic of northern Switzerland. *Swiss Journal of Geosciences, 104,* 97–146.
Remes, K., Ortega, F., Fierro, I., Joger, U., Kosma, R., Ferrer, J. M. M., et al. (2009). A new basal sauropod dinosaur from the Middle Jurassic of Niger and the early evolution of Sauropoda. *PLoS ONE, 4,* 1–13.
Riley, H., & Stutchbury, S. (1836). A description of various fossil remains of three distinct saurian animals discovered in the autumn of 1834, in the Magnesian Conglomerate on Durdham Down, near Bristol. *Proceedings of the Geological Society of London, 2,* 397–399.
Romer, A. S. (1966). *Vertebrate paleontology* (3rd ed.). Chicago: University of Chicago Press.
Rütimeyer, L. (1856a). Herr Rütimeyer legt der Versammlung fossile Reptilknochen aus dem Keuper vor, welche von Herrn Gressly in der Nähe von Liestal gefunden worden sind. *Verhandlungen der schweizerischen naturforschenden Gesellschaft, 41,* 62–64.
Rütimeyer, L. (1856b). [Rutimeyer présente à la Société des ossements gigantesques de reptiles que M. Gressly… a trouvé dans les marnes keupériennes des environs de Bâle]. *Archives des Sciences Physiques et Naturelles, 33,* 53.
Rütimeyer, L. (1857). Über die im Keuper zu Liestal bei Basel aufgefundenen Reptilien-Reste von *Belodon*. *Neues Jahrbuch für Mineralogie, Geognosie, Geologie und Petrefakten-Kunde, 1857,* 141–152.
Salgado, L., Coria, R. A., & Calvo, J. O. (1997). Evolution of titanosaurid sauropods. I: Phylogenetic analysis based on the postcranial evidence. *Ameghiniana*, *34*, 3–32.
Sander, P. M. (2013). An evolutionary cascade model for sauropod dinosaur gigantism - overview, update and tests. *PLoS ONE, 8,* e78573.
Sander, P. M., Christian, A., Clauss, M., Fechner, R., Gee, C. T., Griebeler, E.-M., et al. (2011). Biology of the sauropod dinosaurs: the evolution of gigantism. *Biological Reviews, 86,* 117–155.
Sander, P. M., & Gee, C. T. (1992). A volunteer-powered dinosaur excavation in the Upper Triassic of Switzerland. *Journal of Geological Education, 40,* 194–203.
Schalch, F., & Peyer, B. (1919). Über ein neues Rhätvorkommen im Keuper des Donau-Rheinzuges. *Mitteilungen der Badischen Geologischen Landesanstalt, 8,* 263–298.
Schlatter, R. (1983). Erstnachweis des tiefsten Hettangium im Klettgau (Kanton Schaffhausen, Schweiz). *Mitteilungen der naturforschenden Gesellschaft Schaffhausen, 32,* 159–175.
Schneebeli-Hermann, E., Looser, N., Hochuli, P. A., Furrer, H., Reisdorf, A. G., Wetzel, A., et al. (2018). Palynology of Triassic-Jurassic boundary sections in northern Switzerland. *Swiss Journal of Geosciences, 111,* 99–115.
Sereno, P. C. (2007). Basal Sauropodomorpha: historical and recent phylogenetic hypotheses, with comments on *Ammosaurus major* (Marsh, 1889). *Special Papers in Palaeontology, 77,* 261–289.
Sereno, P. C., Martínez, R. N., & Alcober, O. A. (2013). Osteology of *Eoraptor lunensis* (Dinosauria, Sauropodomorpha). *Society of Vertebrate Paleontology Memoir, 12,* 83–179.
Tschopp, E., & Mateus, O. (2013). Clavicles, interclavicles, gastralia, and sternal ribs in sauropod dinosaurs: new reports from Diplodocidae and their morphological, functional and evolutionary implications. *Journal of Anatomy, 222,* 321–340.
Upchurch, P., Barrett, P. M., & Dodson, P. (2004). Sauropoda. In D. B. Weishampel, P. Dodson, & H. Osmólska (Eds.), *The Dinosauria* (2nd ed., pp. 259–322). Berkeley: University of California Press.
Upchurch, P., Barrett, P. M., & Galton, P. M. (2007a). A phylogenetic analysis of basal sauropodomorph relationships: implications for the origin of sauropod dinosaurs. *Special Papers in Palaeontology, 77,* 57–90.
Upchurch, P., Barrett, P. M., Zhao, X., & Xu, X. (2007b). A re-evaluation of *Chinshakiangosaurus chunghoensis* Ye vide Dong 1992 (Dinosauria, Sauropodomorpha): implications for cranial evolution in basal sauropod dinosaurs. *Geological Magazine, 144,* 247–262.
Wang, Y., You, H., & Wang, T. (2017). A new basal sauropodiform dinosaur from the Lower Jurassic of Yunnan Province. *China. Scientific Reports, 7,* 41881.
Wellnhofer, P. (1993). Prosauropod dinosaurs from the Feuerletten (Middle Norian) of Ellingen near Weissenburg in Bavaria. *Revue de Palebiologie, 7,* 263–271.
Whiteside, D. I., Duffin, C. J., & Furrer, H. (2017). The Late Triassic lepidosaur fauna from Hallau, North-Eastern Switzerland, and a new 'basal' rhynchocephalian *Deltadectes elvetica* gen. et sp. nov. *Neues Jahrbuch für Geologie und Paläontologie Abhandlungen, 285,* 53–74.
Wild, R. (1978). Ein Sauropoden-Rest (Reptilia, Saurischia) aus dem Posidonienschiefer (Lias, Toarcium) von Holzmaden. *Stuttgarter Beiträge zur Naturkunde, Serie B, 41,* 1–15.
Wilson, J. A. (2005). Integrating ichnofossil and body fossil records to estimate locomotor posture and spatiotemporal distibution of early sauropod dinosaurs: a stratocladistic approach. *Paleobiology, 31,* 400–423.
Wilson, J. A. (2012). New vertebral laminae and patterns of serial variation in vertebral laminae of sauropod dinosaurs. *Contributions from the Museum of Paleontology, UNiversity of Michigan, 32,* 91–110.
Xu, X., Upchurch, P., Mannion, P., Barrett, P., Regalado-Fernandez, O., Mo, J., et al. (2018). A new Middle Jurassic diplodocoid suggests an earlier dispersal and diversification of sauropod dinosaurs. *Nature Communications, 9,* 2700.
Yates, A. M. (2003). The species taxonomy of the sauropodomorph dinosaurs from the Löwenstein Formation (Norian, Late Triassic) of Germany. *Palaeontology, 46,* 317–337.
Yates, A. M. (2004). *Anchisaurus polyzelus* (Hitchcock): the smallest known sauropod dinosaur and the evolution of gigantism among sauropodomorph dinosaurs. *Postilla, 230,* 1–58.

Yates, A. M. (2007). The first complete skull of the Triassic dinosaur *Melanorosaurus* Haughton (Sauropodomorpha: Anchisauria). *Special Papers in Palaeontology, 77,* 9–55.
Yates, A. M., Bonnan, M. F., Neveling, J., Chinsamy, A., & Blackbeard, M. G. (2010). A new transitional sauropodomorph dinosaur from the Early Jurassic of South Africa and the evolution of sauropod feeding and quadrupedalism. *Proceedings of the Royal Society London B, 277,* 787–794.
Yates, A. M., & Kitching, J. W. (2003). The earliest known sauropod dinosaur and the first steps towards sauropod locomotion. *Proceedings of the Royal Society of London B, 270,* 1753–1758.
Zhang, Y., & Yang, Z. (1994). *A new complete osteology of Prosauropoda in Lufeng Basin Yunnon China*. Jingshanosaurus: Yunnan Publishing Houe of Science and Technology, Kunming.

Publisher's Note